MISCELLANEOUS PAPER CERC-92-5

(2)

US Army Corps of Engineers

DIFFRACTION OF DIRECTIONAL WAVE SPECTRA AROUND A SEMI-INFINITE BREAKWATER

by

Matthew T. Walsh

DEPARTMENT OF THE ARMY
US Army Engineer District, Buffalo
1776 Niagara Street
Buffalo, New York 14207-3199

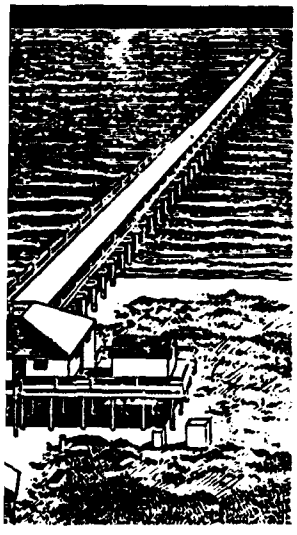

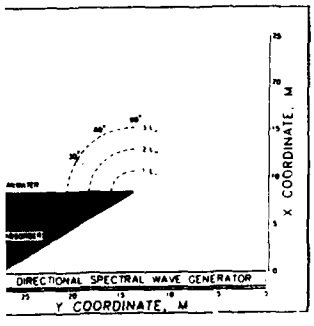

August 1992
Final Report

Prepared for DEPARTMENT OF THE ARMY
US Army Corps of Engineers
Washington, DC 20314-1000

Monitored by Coastal Engineering Research Center
US Army Engineer Waterways Experiment Station
3909 Halls Ferry Road, Vicksburg, Mississippi 39180-6199

Destroy this report when no longer needed. Do not return it to the originator.

The findings in this report are not to be construed as an official Department of the Army position unless so designated by other authorized documents.

The contents of this report are not to be used for advertising, publication, or promotional purposes. Citation of trade names does not constitute an official endorsement or approval of the use of such commercial products.

REPORT DOCUMENTATION PAGE

Form Approved
OMB No. 0704-0188

1. AGENCY USE ONLY (Leave blank)	2. REPORT DATE	3. REPORT TYPE AND DATES COVERED
	August 1992	Final report

4. TITLE AND SUBTITLE
Diffraction of Directional Wave Spectra Around a Semi-Infinite Breakwater

5. FUNDING NUMBERS

6. AUTHOR(S)
Matthew T. Walsh

7. PERFORMING ORGANIZATION NAME(S) AND ADDRESS(ES)
USAED, Buffalo
1776 Niagara Street
Buffalo, NY 14207-3199

8. PERFORMING ORGANIZATION REPORT NUMBER

9. SPONSORING/MONITORING AGENCY NAME(S) AND ADDRESS(ES)
US Army Corps of Engineers
Washington, DC 20314-1000;
USAE Waterways Experiment Station, Coastal Engineering Research Center, 3909 Halls Ferry Road
Vicksburg, MS 39180-6199

10. SPONSORING/MONITORING AGENCY REPORT NUMBER
Miscellaneous Paper CERC-92-5

11. SUPPLEMENTARY NOTES
Available from National Technical Information Service, 5285 Port Royal Road, Springfield, VA 22161.

12a. DISTRIBUTION/AVAILABILITY STATEMENT
Approved for public release; distribution is unlimited.

12b. DISTRIBUTION CODE

13. ABSTRACT *(Maximum 200 words)*

A numerical model was developed for this study to predict the diffraction of incident directional wave spectra by a semi-infinite breakwater. The model was validated against a set of laboratory data from a physical model test that included incident spectra with narrow and broad frequency distributions and narrow and broad directional spread. The best agreement between measured and predicted diffraction was achieved for the incident spectra with a narrow directional spread, independent of frequency distribution. The numerical model predicted higher diffraction coefficients than were measured for the incident spectra with a broad directional spread. The difference was not unreasonable, and was probably due to the problems encountered in attempting to generate a spectrum of waves with a broad directional spread in a small-scale physical model. The numerical model also predicted larger diffraction coefficients than were measured for the monochromatic incident wave condition, but the difference was small in the shadow zone, away from the region of high gradients in wave height.

14. SUBJECT TERMS
Laboratory experiments
Numerical modeling
Spectral wave diffraction
Spectral wave modeling
Spectral wave transformation

15. NUMBER OF PAGES
85

16. PRICE CODE

17. SECURITY CLASSIFICATION OF REPORT	18. SECURITY CLASSIFICATION OF THIS PAGE	19. SECURITY CLASSIFICATION OF ABSTRACT	20. LIMITATION OF ABSTRACT
UNCLASSIFIED	UNCLASSIFIED		

PREFACE

This study was performed in accordance with the requirements of the Coastal Engineering Education Program (CEEP), which is a part of the Corps of Engineers Long-Term Training Program. This one-year program is offered through the Graduate Institute at the US Army Engineer Waterways Experiment Station (WES), the WES Coastal Engineering Research Center (CERC), and Texas A&M University.

This study was conducted by Mr. Matthew T. Walsh of the Coastal/ Geotechnical Section (CENCB-PE-TC), US Army Engineer District, Buffalo, in partial fulfillment of the requirements for the Master of Engineering degree in Ocean Engineering from Texas A&M University. Work was performed at Texas A&M University, College Station, TX, and at CERC.

Work performed at CERC was under the general administrative supervision of Dr. James R. Houston, Director, CERC, and Mr. Charles C. Calhoun, Assistant Director, CERC. Mr. Michael J. Briggs and Mses. Debbie R. Green, J. Holley Messing, and Ann R. Sherlock, all of CERC, greatly assisted in the preparation of this report.

Work was performed under the supervision of Dr. Edward F. Thompson, visiting Associate Professor at Texas A&M University and Research Engineer at CERC, Dr. Francis C. K. Ting, Assistant Professor at Texas A&M University, and Distinguished Professor Robert O. Reid of Texas A&M University.

At the time of publication of this report, Director of WES was Dr. Robert W. Whalin. Commander and Deputy Director was COL Leonard G. Hassell, EN.

CONTENTS

DIFFRACTION OF DIRECTIONAL WAVE SPECTRA AROUND A SEMI-INFINITE BREAKWATER

PART I: INTRODUCTION

Background

1. When waves encounter an obstacle such as a breakwater, island, or headland, wave energy can flow along the wave crest and move into the shadow zone. This phenomenon is known as wave diffraction. Consideration of wave diffraction is important in the design of detached and shore-connected breakwaters, which provide protection for commercial harbors, small craft marinas, and harbors of refuge. The ability to predict the diffraction of incident waves by protective structures is essential in the evaluation of design alternatives.

2. Diffraction theory has been extensively validated with laboratory tests for the diffraction of monochromatic waves, that is, long-crested waves with one period from one direction. However, real seas often consist of short-crested waves with different directions. Energy in the wave field is distributed over a range of frequencies and directions, as defined by the directional wave spectrum.

3. It is known that directional and monochromatic incident waves give quite different diffracted wave heights within a harbor. Mobarek and Wiegel (1966) recognized this. They were the first to propose the application of monochromatic diffraction theory to the components of an incident directional spectrum, and linear superposition of the diffracted components to obtain the diffracted frequency spectrum in the lee of a breakwater. Water depth was assumed constant. This approach to directional wave diffraction has been accepted by a number of researchers, using a variety of forms of the incident directional spectrum, but has received little validation.

4. Mobarek and Wiegel conducted a physical model test with a semi-infinite breakwater to validate their predictions. The test was conducted in a 18.3-m-long by 3.7-m-wide wind-wave flume with a constant water depth of 34 cm. The plywood breakwater was 0.61 m high and 1.27 cm thick.

Measurements of diffracted spectra were taken at four locations in the lee of the breakwater for one wind-generated incident wave condition. They concluded that diffraction theory could be applied to the components of an incident directional spectrum to predict diffracted spectra within acceptable engineering accuracy.

5. Goda et al. (1985) and Irie (1975) compared predictions from directional wave diffraction theory to field measurements in Japan. Goda examined diffraction through a breakwater gap at Nagoya Port, and Irie examined diffraction around a long breakwater at Akita Port. In both cases, wave measurements were taken at one location seaward of and one location in the lee of the breakwaters. There was some uncertainty in the incident wave measurement at Nagoya Port. Because the caisson-type breakwater was highly reflective, Goda assumed that one-half of the measured wave energy seaward of the breakwater was due to the incident waves. Wave direction was inferred from the observed wind direction. Irie obtained wave direction from radar installed on shore. Goda and Irie applied a directional spreading function to the incident frequency spectra to obtain an incident directional spectrum. At both locations, the spectrum of diffracted waves was calculated from the incident directional spectrum, and was found to be in good agreement with the measured diffracted spectrum.

6. Takayama and Kamiyama (1977) formulated the diffraction of a particular directional spectrum for a variety of breakwater types, but conducted model tests to validate only unidirectional irregular waves.

7. Sand et al. (1983) reported physical and numerical model tests with one incident directional wave condition for diffraction around a semi-infinite breakwater and through a breakwater gap. Sand obtained reasonably good agreement based on measurements made at nine locations in the lee of the semi-infinite breakwater.

8. The theory of directional wave diffraction is widely applied in Japan in harbor planning studies (Goda 1985). Despite the lack of definitive validation, the theory is known to give better predictions of diffracted wave heights within harbors than those obtained through monochromatic diffraction analysis.

Objectives

9. A numerical model to predict the diffraction of incident directional wave spectra by a semi-infinite breakwater was developed for this study. The objectives were two-fold. First, the model was used to validate directional diffraction theory against a relatively complete set of laboratory data obtained from a physical model test conducted at the US Army Engineer Waterways Experiment Station's Coastal Engineering Research Center (CERC) in 1986 (Briggs et al. 1991).

10. The second objective was to determine how the numerical model could be expanded in the future to predict directional wave diffraction under conditions which could be expected in the field. These conditions include oblique as well as normal wave incidence, incident directional spectra representative of different sites, and breakwater gaps as well as semi-infinite breakwaters.

Scope

11. The physical model test was conducted in CERC's flat-bottom 35 m by 29 m directional wave basin in a water depth of 46 cm. One monochromatic and four directional spectral wave conditions were generated. The four directional spectra represent the four combinations of narrow and broad frequency distributions with narrow and broad directional spread. Waves were normally incident to the semi-infinite breakwater. Incident spectra were measured with a linear array of nine wave gages prior to installation of the breakwater. Diffracted spectra were measured at 27 locations in the lee of the breakwater within three nominal wave lengths of the breakwater tip (Figure 1).

12. For the numerical model, the incident directional spectra were discretized into energy components. A diffraction coefficient was computed for each component frequency and direction from monochromatic diffraction theory at 27 points corresponding to the locations of measurement in the physical model test. Incident energy components were then diffracted individually to produce the components of the diffracted spectrum.

13. Incident spectra $S_i(f)$, measured diffracted spectra $S_{dm}(f)$, and diffracted spectra predicted by the numerical model $S_{dp}(f)$, were plotted for comparison. The spectral significant wave height H_{mo} was calculated for

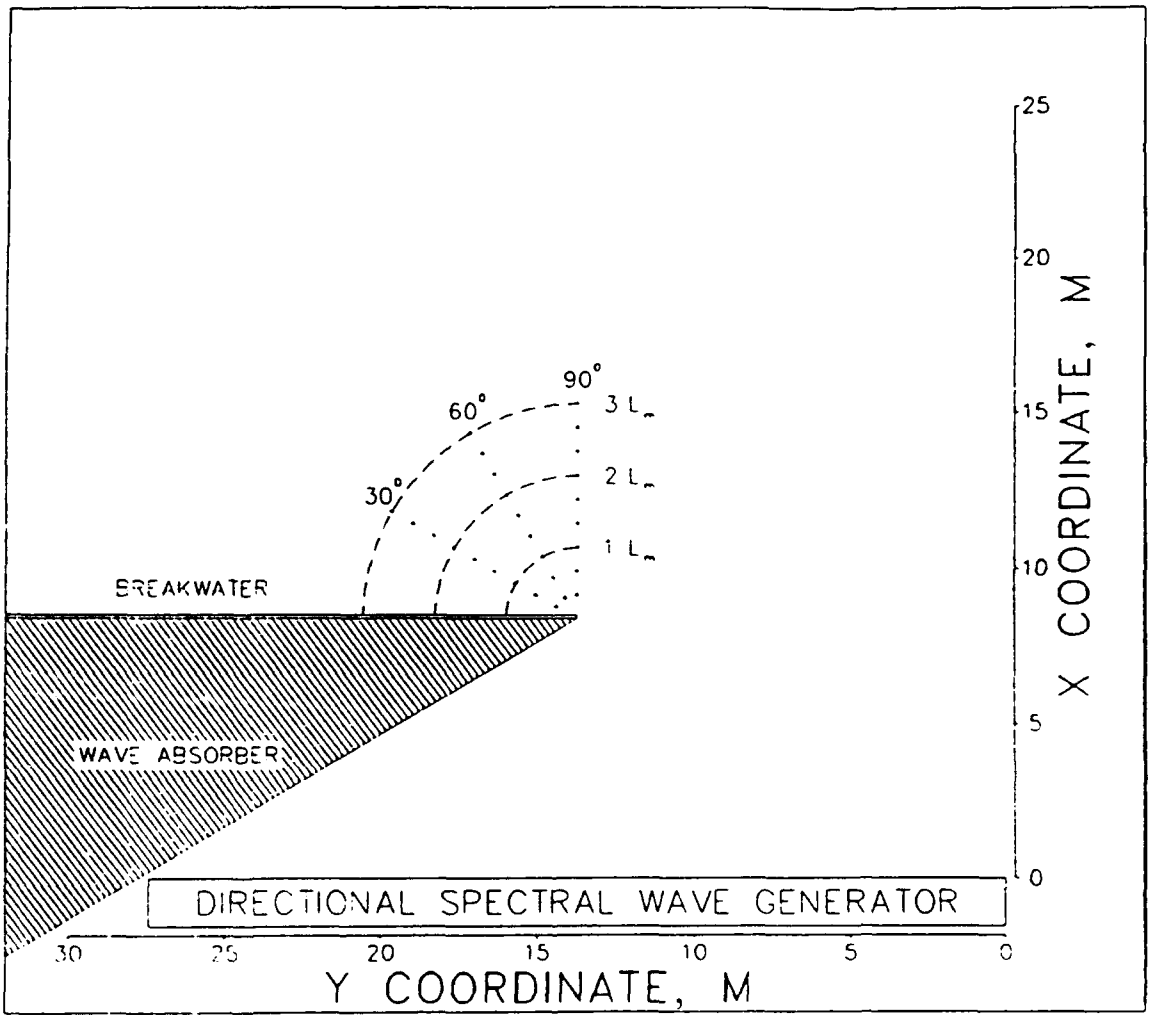

Figure 1. Layout of physical model test

each spectrum, and a spectral diffraction coefficient was calculated from:

$$K_{ds} = \frac{H_{mod}}{H_{moi}} \qquad (1)$$

where

K_{ds} = spectral diffraction coefficient

H_{moi} = H_{mo} of incident spectrum

H_{mod} = H_{mo} of diffracted spectrum

Spectral diffraction coefficients were calculated for the measured diffracted and the predicted diffracted spectra and contoured for comparison.

PART II: EXISTING METHODS OF DIFFRACTION ANALYSIS

Monochromatic

14. Penney and Price (1944) stated that the diffraction of long-crested water waves by a rigid obstacle is similar to the diffraction of a beam of light that is partially cut off by an opaque screen. Hence, by making use of Sommerfeld's (1896) solution for the diffraction of light waves at the edge of a semi-infinite screen, they were able to obtain the solution for the diffraction of water waves around the end of a long, straight breakwater. The solution is obtained by solving for the velocity potential which satisfies the two-dimensional Laplace equation with appropriate boundary conditions and simplifying assumptions. Assumptions include linear waves; a flat bottom; and a thin, rigid, vertical structure.

15. The theory has been validated extensively using laboratory data for the diffraction of monochromatic waves with a single period from a single direction. The results are presented as diagrams showing the distribution of the ratio of diffracted to incident wave heights, and are called diffraction diagrams. Several sets of diffraction diagrams have been published based on this theory. Chapter 2 of the Shore Protection Manual (SPM 1984) provides diffraction diagrams developed by Wiegel (1962) for the diffraction of monochromatic waves around a semi-infinite breakwater or through a breakwater gap. Diffraction coefficients in the lee of the breakwater are contoured in terms of relative radial distance from the breakwater tip R/L, where R is the absolute radial distance from the breakwater tip, and L is the wavelength of the incident wave.

16. Chen (1987) and Kaihatu and Chen (1988) developed mainframe- and PC-based programs, respectively, to numerically solve the boundary value problem of linear wave reflection and diffraction by a vertical wedge of arbitrary wedge angle, which had been formulated and presented by Stoker (1957).

Directional Spectra

17. Diffraction diagrams for monochromatic waves do not accurately represent the diffraction of directional wave spectra. Nagai (1972) cites the

wind tunnel experiments done by Mobarek and Wiegel and field studies by Goda (originally published in Japanese in 1971, and later presented in Goda 1985) in stating that directional wave diffraction, in the absence of nonlinear effects, is physically accounted for by the theory of linear superposition of the spectral components.

18. Based on that theory, Nagai constructed diffraction diagrams for directional spectra expressed by the Pierson-Moskowitz frequency spectrum and the directional spreading function obtained from the Stereo Wave Observation Project (SWOP). Diagrams were presented for diffraction around a semi-infinite breakwater and through a breakwater gap. For the case of a semi-infinite breakwater and waves of normal incidence, the diffraction coefficients on the line extending from the breakwater tip in the direction of incident wave propagation were approximately 0.5 for monochromatic waves and 0.7 for directional waves.

19. Goda et al. (1978) constructed diffraction diagrams for a directional spectrum composed of the Bretschneider-Mitsuyasu frequency spectrum and the Mitsuyasu spreading function. Diagrams were constructed for diffraction of normally incident directional wave spectra around a semi-infinite breakwater or through a breakwater gap. For the case of a semi-infinite breakwater, diffraction coefficients in the lee of the breakwater are contoured in terms of relative distance from the breakwater tip X/L_p and Y/L_p, where X and Y are the absolute distances in rectangular coordinates from the breakwater tip, and L_p is the wavelength corresponding to the peak period T_p of the incident spectrum. Two sets of diagrams are provided, one each for sea and swell incident wave conditions. Although directional wave diffraction analysis has been conducted by several researchers as previously discussed, the diffraction diagrams developed by Goda et al., which have been incorporated into Chapter 7 of the SPM, are the only tool currently available for general use in engineering studies.

PART III: PHYSICAL MODEL

Experimental Setup

20. The physical model tests were conducted in CERC's directional wave basin (Figure 1). Incident waves were generated using CERC's 27.43-m-long directional spectral wave generator (DSWG). A 0.61 m high by 18.22-m-long vertical-faced breakwater was located 8.38 m in front of and parallel to the DSWG, and extended from the DSWG centerline to the basin side wall. The breakwater was constructed of 1.27-cm-thick plywood backed by 2X4 lumber, and was therefore a reasonably thin, rigid, vertical structure. Incident and diffracted wave heights were measured using nine parallel-wire resistance-type wave sensors mounted on a frame. Briggs et al. (1991) give more details concerning the physical model.

Generated Incident Spectra

21. The incident directional spectrum is represented by the product of a frequency spectrum $S_i(f)$ and a directional spreading function $D(f,\theta)$ as:

$$S_I(f,\theta) = S_I(f) \cdot D(f,\theta) \tag{2}$$

where

f = frequency

θ = wave direction

The frequency spectrum and spreading function are subject to the following constraints:

$$S_I(f) = \int_0^{2\pi} S(f,\theta)\, d\theta \tag{3}$$

$$\int_0^{2\pi} D(f,\theta)\, d\theta = 1 \tag{4}$$

22. Briggs et al. (1991) used the TMA shallow-water frequency distribution (Bouws, et al. 1985) and the wrapped normal directional spreading function (Borgman 1990) in the physical model tests. The TMA spectrum is a

function of five parameters: peak period T_p , constant α , peak enhancement factor γ , right and left spectral width parameters $\sigma_a = 0.07$ and $\sigma_b = 0.09$, and water depth h .

23. The wrapped normal spreading function is a function of the principle direction θ_m and the circular standard deviation σ_m in radians. Both are linear functions of f , consisting of a constant and slope component (Briggs 1988). The Fourier series representation is given by:

$$D(f,\theta) = \frac{1}{2\pi} + \frac{1}{\pi} \sum_{\ell=1}^{L} \exp - \frac{(\ell \sigma_m)^2}{2} \cos \ell(\theta - \theta_m) \qquad (5)$$

where

$$\theta_m = \theta_0 + \theta_1 (f - f_p)$$
$$\sigma_m = \sigma_0 + \sigma_1 (f - f_p)$$

In the physical model, both θ_1 and σ_1 were set to zero, which removed the frequency dependence in the directional spreading function. Therefore, the generated incident directional spectrum is given by:

$$S_I(f,\theta) = S_I(f) \cdot D(\theta) \qquad (6)$$

One monochromatic and four directional spectral incident wave conditions were generated, as listed in Table 1.

Table 1

Incident Wave Conditions

Case	Description
M4	Monochromatic
N1	Broad Frequency Distribution, Narrow Directional Spread
N2	Narrow Frequency Distribution, Narrow Directional Spread
B1	Broad Frequency Distribution, Broad Directional Spread
B2	Narrow Frequency Distribution, Broad Directional Spread

The target incident spectral parameters in the TMA frequency distribution and the wrapped normal directional spreading function are listed in Table 2. The values of $\gamma = 2$ and $\gamma = 20$ used in the physical model test represent

extremes of sea and swell conditions, respectively. The target incident directional spectra are shown in Appendix A.

Table 2

Target Incident Spectral Parameters

	TMA Frequency Distribution				Wrapped Normal Directional Spreading Function	
Case	H_s[1] cm	T_p sec	α	γ	θ_m deg	σ_m deg
M4	7.75	1.30	-	-	-	-
N1	7.75	1.30	0.0144	2	0	10
N2	7.75	1.30	0.0044	20	0	10
B1	7.75	1.30	0.0144	2	0	30
B2	7.75	1.30	0.0044	20	0	30

(1) $H_s = H_{1/3}$ for monochromatic or H_{mo} for incident wave spectra

24. Prior to installation of the breakwater, test series were conducted to calibrate the control signal to the DSWG. Incident spectra were measured using the linear array and a Maximum Likelihood Method (MLM) analysis of the time series. The linear array was placed 3.05 m, 9.15 m, and 15.25 m in front of and parallel to the DSWG during the test series. This was done to determine the distance required between the DSWG and the breakwater to ensure that the incident directional spectra were fully formed at the breakwater. For some incident wave conditions, the gages on the ends of the array were excluded from the MLM analysis of the time series, since they were not exposed to the fully formed wave field. The MLM analysis computes the frequency spectrum and directional spreading function of the incident directional spectrum based on the time series from the linear array. For incident spectra with a broad directional spread, the MLM analysis is sensitive to the frequency and directional bandwidths, Δf and $\Delta\theta$, respectively, used in the analysis. Briggs et al. (1991) used 30 frequency bands of variable bandwidth centered around the peak, and 91 directional bands of constant bandwidth $\Delta\theta$ =

2 deg,* and showed good to excellent agreement between target and generated wave parameters.

Diffracted Spectra

25. Diffracted waves were measured at 27 locations in the lee of the breakwater within three nominal wavelengths of the breakwater tip. Measurements were made for each of the five incident wave conditions. Nine resistance-type wave sensors were mounted on a long frame at a nominal spacing of 77 cm. The frame was positioned on three radial transects from the breakwater tip covering a 60-deg sector of the shadow zone. The transects were 30, 60, and 90 deg from the breakwater, as shown in Figure 1.

26. Diffracted spectra were computed from the measured time series using a single channel frequency analysis (SCFA). Spectral energy densities were printed from the SCFA analysis in 22 frequency bands of 0.05 Hz from 0.47 to 1.52 Hz. It was determined that energy outside of that range was negligible.

---

* To convert degrees (angle) to metric units (radians), multiply times a factor of 0.01745329.

PART IV: NUMERICAL MODEL

Discretized Incident Spectra

27. Each incident directional spectrum $S_i(f,\theta)$ used in the numerical model was constructed as the product of the measured incident frequency spectrum $S_i(f)$, obtained from the MLM analysis, and the directional spreading function $D(\theta)$, as shown by Equation 6. Although the wrapped normal spreading function used in this analysis did not have a frequency dependence, the MLM analysis of the linear array measurements computes a value for the spreading function in each (f,θ) band. As previously stated, Briggs et al. used 30 frequency bands and 91 directional bands in the MLM analysis of the incident directional spectrum. This results in $30 \cdot 91 = 2,730$ values for the spreading function. From Equation 6, this results in 2,730 energy components to be diffracted, which would require a great deal of computer run time. An attempt was made to reduce the number of (f,θ) bands used in the MLM analysis while still maintaining reasonable agreement with the target incident wave parameters listed in Table 2. Various combinations of Δf and $\Delta\theta$ were analyzed. Table 3 shows the results obtained using 22 frequency bands of 0.05 Hz from 0.47-1.52 Hz, and 37 directional bands of 5 deg from 0-180 deg, resulting in $22 \cdot 37 = 814$ (f,θ) bands. Comparing the target spectral parameters listed in Table 2 with the spectral parameters of the discretized spectra, it seems that cases M4, N1, and N2 closely matched the target parameters, but that the spreading σ_m of cases B1 and B2 was not in good agreement.

28. Rather than increase the number of (f,θ) bands, which would increase computation time, it was decided to use the calculated values from the wrapped normal spreading function instead of the measured values from the MLM analysis of the linear array. It was believed that this was acceptable as Briggs et al. had shown that the generated spectra closely matched the target. The discretized incident directional spectra were plotted and are shown in Appendix B.

29. Previous field studies have used somewhat coarser resolution. Nagai (1972) stated that ten frequency bands and eight directional bands ($\Delta\theta$ = 22.5 deg) were adequate to compute diffraction coefficients in his numerical

model with a relative error of less than 5 percent. Goda (1985) used ten frequency bands and from 20 to 36 directional bands ($\Delta\theta$ = 9 deg to 5 deg).

30. The measured incident frequency spectra and the calculated directional spreading function were read using the computer program FILEMGMT, which was written for the study. The program FILEMGMT then computes the incident directional spectral energy density for each case by Equation 6, and writes them in the format shown in Appendix C. The program FILEMGMT is included in Appendix E.

Table 3

Discretized Incident Spectral Parameters

Case	H_s (1) cm	T_p sec	θ_m deg	σ_m deg
M4	8.98	1.30	0	3
N1	7.18	1.30	-5	8
N2	7.29	1.30	-5	11
B1	7.29	1.22	5	44
B2	7.34	1.30	0	48

(1) $H_s = H_{1/3}$ for monochromatic or H_{mo} for incident wave spectra

Diffracted Spectra

31. The diffracted spectrum predicted by the numerical model $S_{dp}(f,x,y)$ is computed as:

$$S_{dp}(f,x,y) = \sum_{j=1}^{37} S_i(f,\theta_j)\ K_d^2(f,\theta_j,x,y)\ \Delta\theta \qquad (7)$$

where

$S_i(f,\theta_j)$ = discretized incident directional spectrum

$K_d(f,\theta_j,x,y)$ = diffraction coefficient

$\Delta\theta$ = directional bandwidth

x,y = horizontal spatial coordinates

The spatial dependence is omitted from subsequent equations for brevity. Consistent with directional diffraction theory, a diffraction coefficient was computed for each component of the discretized incident spectrum.

32. In calculating the diffraction coefficients, each spectral component, with frequency f and incident direction θ, was treated as a monochromatic wave of period T, where $T = 1/f$, and incident direction θ. Diffraction coefficients were then computed from monochromatic diffraction theory.

33. As the incident spectrum was discretized into 22 frequency bands and 37 directional bands, a matrix containing $22 \cdot 37 = 814$ diffraction coefficients was computed. The diffraction coefficients are also a function of position, so each matrix was unique to a particular location of interest in the lee of the breakwater. Twenty-seven locations were chosen to coincide with the 27 locations of wave measurement in the physical model test. The locations were labeled according to the angle of the array of gages (30, 60, or 90 deg from the breakwater) and by the gage number. Gages were numbered 1-9, with gage 1 being closest to the breakwater. Table 4 shows diffraction coefficients for gage 6 along array angle 60 deg for illustration.

34. The computer program KD GENeration (KDGEN) was written for this study to compute and construct the matrices of diffraction coefficient. The KDGEN calls subroutine PADES (Chen and Thompson 1985) to compute the wavelength L of a component wave of frequency f from the linear dispersion relation. The KDGEN then calls subroutine DRWEDGE (original coding by Chen 1987, adapted to ACES by Leenknecht et al. 1989) to compute the diffraction coefficient of each of the component waves with that frequency (wavelength) for each of the 37 directional components. The KDGEN then increments the frequency by Δf, and again loops through subroutines PADES and DRWEDGE. This process is continued over the 22 frequency bands. The KDGEN then reads a new location of interest, and goes through the above procedure to compute and construct a matrix of diffraction coefficients at that point. This procedure continues until matrices of diffraction coefficient have been computed at each of the 27 locations.

35. Subroutines PADES was hardwired with a constant water depth of 46 cm corresponding to the water depth used in the physical model, and subroutine DRWEDGE was hardwired with an incident wave angle of 90 deg, and

TABLE 4
DIFFRACTION COEFFICIENTS

GAGE NUMBER 6, ARRAY ANGLE = 60°, |X/Lp| = 1.02, |Y/Lp| = 1.76

KD(f,THETA)

WAVE DIRECTION (DEG CCW FROM POSITIVE X-AXIS)	FREQUENCY (Hz)										
	0.47	0.52	0.57	0.62	0.67	0.72	0.77	0.82	0.87	0.92	0.97
0	0.087	0.082	0.078	0.074	0.071	0.067	0.064	0.061	0.059	0.056	0.054
5	0.175	0.165	0.156	0.149	0.141	0.135	0.129	0.123	0.117	0.112	0.108
10	0.176	0.166	0.157	0.149	0.142	0.135	0.129	0.123	0.118	0.113	0.108
15	0.177	0.167	0.158	0.150	0.143	0.136	0.130	0.124	0.119	0.114	0.109
20	0.179	0.169	0.160	0.152	0.145	0.138	0.132	0.126	0.120	0.115	0.110
25	0.182	0.171	0.162	0.154	0.147	0.140	0.134	0.128	0.122	0.117	0.112
30	0.185	0.174	0.165	0.157	0.149	0.143	0.136	0.130	0.124	0.119	0.114
35	0.189	0.178	0.169	0.160	0.153	0.146	0.139	0.133	0.127	0.122	0.116
40	0.193	0.183	0.173	0.165	0.157	0.149	0.143	0.136	0.130	0.125	0.120
45	0.199	0.188	0.178	0.169	0.161	0.154	0.147	0.140	0.134	0.129	0.123
50	0.205	0.194	0.184	0.175	0.167	0.159	0.152	0.145	0.139	0.133	0.128
55	0.213	0.202	0.191	0.182	0.174	0.166	0.158	0.151	0.145	0.139	0.133
60	0.222	0.210	0.200	0.190	0.181	0.173	0.165	0.158	0.152	0.145	0.139
65	0.233	0.221	0.210	0.200	0.191	0.182	0.174	0.167	0.160	0.153	0.146
70	0.245	0.233	0.222	0.211	0.202	0.193	0.184	0.177	0.169	0.162	0.155
75	0.260	0.247	0.235	0.225	0.215	0.206	0.197	0.189	0.181	0.173	0.166
80	0.277	0.264	0.252	0.241	0.231	0.221	0.212	0.203	0.195	0.187	0.180
85	0.297	0.284	0.271	0.260	0.250	0.240	0.230	0.221	0.213	0.204	0.196
90	0.320	0.307	0.295	0.283	0.273	0.262	0.253	0.243	0.234	0.226	0.217
95	0.348	0.335	0.323	0.311	0.300	0.290	0.280	0.271	0.261	0.253	0.244
100	0.380	0.368	0.356	0.345	0.334	0.324	0.314	0.305	0.296	0.287	0.278
105	0.418	0.406	0.396	0.385	0.375	0.366	0.357	0.348	0.339	0.330	0.322
110	0.461	0.452	0.442	0.433	0.425	0.417	0.409	0.401	0.393	0.386	0.378
115	0.511	0.504	0.497	0.490	0.484	0.478	0.472	0.467	0.461	0.456	0.450
120	0.567	0.563	0.560	0.556	0.553	0.551	0.548	0.546	0.544	0.542	0.540
125	0.630	0.630	0.630	0.631	0.632	0.634	0.636	0.638	0.641	0.644	0.647
130	0.697	0.702	0.707	0.713	0.720	0.727	0.734	0.742	0.751	0.760	0.770
135	0.768	0.778	0.788	0.799	0.811	0.824	0.837	0.851	0.865	0.880	0.896
140	0.838	0.853	0.869	0.885	0.901	0.918	0.936	0.954	0.972	0.991	1.009
145	0.906	0.924	0.943	0.962	0.981	1.000	1.019	1.037	1.055	1.071	1.086
150	0.965	0.985	1.005	1.024	1.042	1.059	1.073	1.086	1.096	1.102	1.104
155	1.011	1.030	1.047	1.062	1.074	1.083	1.089	1.090	1.086	1.076	1.061
160	1.039	1.054	1.065	1.072	1.075	1.073	1.065	1.053	1.036	1.014	0.991
165	1.049	1.056	1.058	1.056	1.049	1.037	1.021	1.003	0.984	0.968	0.958
170	1.040	1.039	1.035	1.026	1.014	1.000	0.987	0.976	0.970	0.972	0.983
175	1.020	1.016	1.010	1.002	0.994	0.988	0.984	0.985	0.991	0.999	1.008
180	1.000	1.000	1.000	1.000	1.000	1.000	1.000	1.000	1.000	1.000	1.000

TABLE 4 (CONCLUDED)

GAGE NUMBER 6, ARRAY ANGLE = 60°, |X/Lp| = 1.02, |Y/Lp| = 1.76

KD(f,THETA)

WAVE DIRECTION (DEG CCW FROM POSITIVE X-AXIS)	FREQUENCY (Hz)										
	1.02	1.07	1.12	1.17	1.22	1.27	1.32	1.37	1.42	1.47	1.52
0	0.051	0.049	0.047	0.045	0.044	0.042	0.040	0.039	0.038	0.036	0.035
5	0.103	0.099	0.095	0.091	0.088	0.084	0.081	0.078	0.075	0.073	0.071
10	0.104	0.099	0.095	0.092	0.088	0.085	0.081	0.079	0.076	0.073	0.071
15	0.104	0.100	0.096	0.092	0.089	0.085	0.082	0.079	0.076	0.074	0.071
20	0.106	0.101	0.097	0.093	0.090	0.086	0.083	0.080	0.077	0.075	0.072
25	0.107	0.103	0.099	0.095	0.091	0.088	0.084	0.081	0.078	0.076	0.073
30	0.109	0.105	0.100	0.096	0.093	0.089	0.086	0.083	0.080	0.077	0.075
35	0.112	0.107	0.103	0.099	0.095	0.091	0.088	0.085	0.082	0.079	0.076
40	0.115	0.110	0.105	0.101	0.097	0.094	0.090	0.087	0.084	0.081	0.078
45	0.118	0.113	0.109	0.104	0.100	0.096	0.093	0.090	0.086	0.084	0.081
50	0.122	0.117	0.113	0.108	0.104	0.100	0.096	0.093	0.090	0.087	0.084
55	0.127	0.122	0.117	0.113	0.108	0.104	0.100	0.097	0.093	0.090	0.087
60	0.133	0.128	0.123	0.118	0.113	0.109	0.105	0.101	0.098	0.094	0.091
65	0.140	0.135	0.129	0.124	0.119	0.115	0.111	0.107	0.103	0.100	0.096
70	0.149	0.143	0.137	0.132	0.127	0.122	0.118	0.114	0.110	0.106	0.103
75	0.160	0.153	0.147	0.142	0.136	0.131	0.126	0.122	0.118	0.114	0.110
80	0.173	0.166	0.159	0.153	0.148	0.142	0.137	0.132	0.128	0.124	0.120
85	0.189	0.182	0.175	0.168	0.162	0.156	0.151	0.145	0.141	0.136	0.132
90	0.209	0.202	0.194	0.187	0.181	0.174	0.168	0.163	0.157	0.152	0.147
95	0.235	0.227	0.220	0.212	0.205	0.198	0.192	0.185	0.180	0.174	0.169
100	0.269	0.261	0.253	0.245	0.237	0.230	0.223	0.216	0.210	0.204	0.198
105	0.313	0.305	0.297	0.289	0.281	0.274	0.267	0.260	0.253	0.247	0.241
110	0.371	0.363	0.356	0.349	0.342	0.335	0.328	0.321	0.315	0.309	0.303
115	0.445	0.439	0.434	0.429	0.423	0.418	0.413	0.408	0.403	0.399	0.394
120	0.538	0.536	0.535	0.533	0.532	0.531	0.529	0.528	0.527	0.526	0.525
125	0.651	0.655	0.659	0.664	0.668	0.673	0.679	0.684	0.689	0.695	0.701
130	0.780	0.791	0.802	0.814	0.826	0.838	0.851	0.864	0.877	0.891	0.904
135	0.912	0.929	0.946	0.964	0.981	0.999	1.016	1.032	1.048	1.063	1.077
140	1.028	1.046	1.063	1.079	1.093	1.106	1.116	1.123	1.128	1.129	1.127
145	1.098	1.108	1.114	1.117	1.115	1.108	1.097	1.081	1.061	1.037	1.012
150	1.101	1.093	1.079	1.060	1.037	1.010	0.983	0.958	0.939	0.928	0.927
155	1.041	1.016	0.990	0.965	0.946	0.936	0.938	0.953	0.977	1.005	1.031
160	0.970	0.953	0.946	0.951	0.968	0.993	1.018	1.038	1.044	1.035	1.013
165	0.959	0.970	0.990	1.012	1.029	1.035	1.025	1.004	0.982	0.970	0.977
170	0.998	1.014	1.024	1.022	1.009	0.992	0.980	0.982	0.998	1.015	1.018
175	1.013	1.011	1.003	0.993	0.989	0.993	1.004	1.010	1.006	0.996	0.991
180	1.000	1.000	1.000	1.000	1.000	1.000	1.000	1.000	1.000	1.000	1.000

a wedge angle of 0 deg corresponding to the case of a semi-infinite breakwater. Since the diffraction coefficients are independent of the amplitude of the component waves, the matrices of diffraction coefficient were applicable to all of the incident spectra.

36. As shown in Equation 7, the predicted diffracted frequency spectrum $S_{dp}(f)$ at each point was computed by applying the square of the diffraction coefficient ($K_d^2(f,\theta)$) to the incident energy component $S_i(f,\theta)$ in the corresponding (f,θ) band, and then summing over θ to obtain the total diffracted energy in that frequency band. This was done for each frequency to obtain the distribution of diffracted wave energy in frequency space.

37. The computer program DIRectional SPectral DIFraction (DIRSPDIF) was written for this study to construct the diffracted frequency spectra according to Equation 7. The DIRSPDIF is included in Appendix E. As previously stated, the discretized incident spectra were written in the format shown in Appendix C by the program FILEMGMT, and the matrices of diffraction coefficient were written in the format shown in Table 4 by the program KDGEN. The DIRSPDIF read those files and constructed the diffracted frequency spectra for each of the 27 locations for each of the five incident wave conditions.

PART V: RESULTS AND ANALYSIS

38. For each incident wave condition, the discretized incident directional spectrum $S_i(f,\theta)$ was converted to a nondirectional frequency spectrum $S_i(f)$ by summing energy densities over direction in each frequency band as:

$$S_i(f) = \sum_{j=1}^{37} S_i(f,\theta_j)\,\Delta\theta \qquad (8)$$

39. For each of the five incident wave conditions, the incident frequency spectrum $S_i(f)$, the measured diffracted spectrum $S_{dm}(f)$, and the predicted diffracted spectrum $S_{dp}(f)$ were tabulated at the 27 locations in the lee of the breakwater. The measured and predicted diffracted frequency spectra were also plotted at representative locations. Figures 2, 3, and 4 show the diffracted spectra at locations corresponding to gages 3, 6, and 9, respectively, along the 30-deg array angle. Figures 5, 6, and 7 show the diffracted spectra from the same gages for the 60-deg array angle. Figure 8 shows the diffracted as well as the incident spectra at the location corresponding to gage 6 for the 90-deg array angle. The incident spectra were included at this location because they could be clearly presented on the same plot at a reasonable scale.

40. The variance m_0 of each incident, measured diffracted, and predicted diffracted frequency spectrum was computed from:

$$m_0 = \sum_{j=1}^{22} S(f_j)\,\Delta f \qquad (9)$$

and the spectral significant wave height corresponding to each spectrum was computed from:

$$H_{mo} = 4\sqrt{m_o} \qquad (10)$$

Spectral diffraction coefficients K_{ds} were then calculated from Equation 1 for both the measured and predicted diffracted spectra at each of the 27 locations for each of the five incident wave conditions. Note that K_{ds} is defined by Equation 1 as the ratio of the H_{mo} of the diffracted spectrum to the H_{mo} of the incident spectrum. This is to be distinguished from the

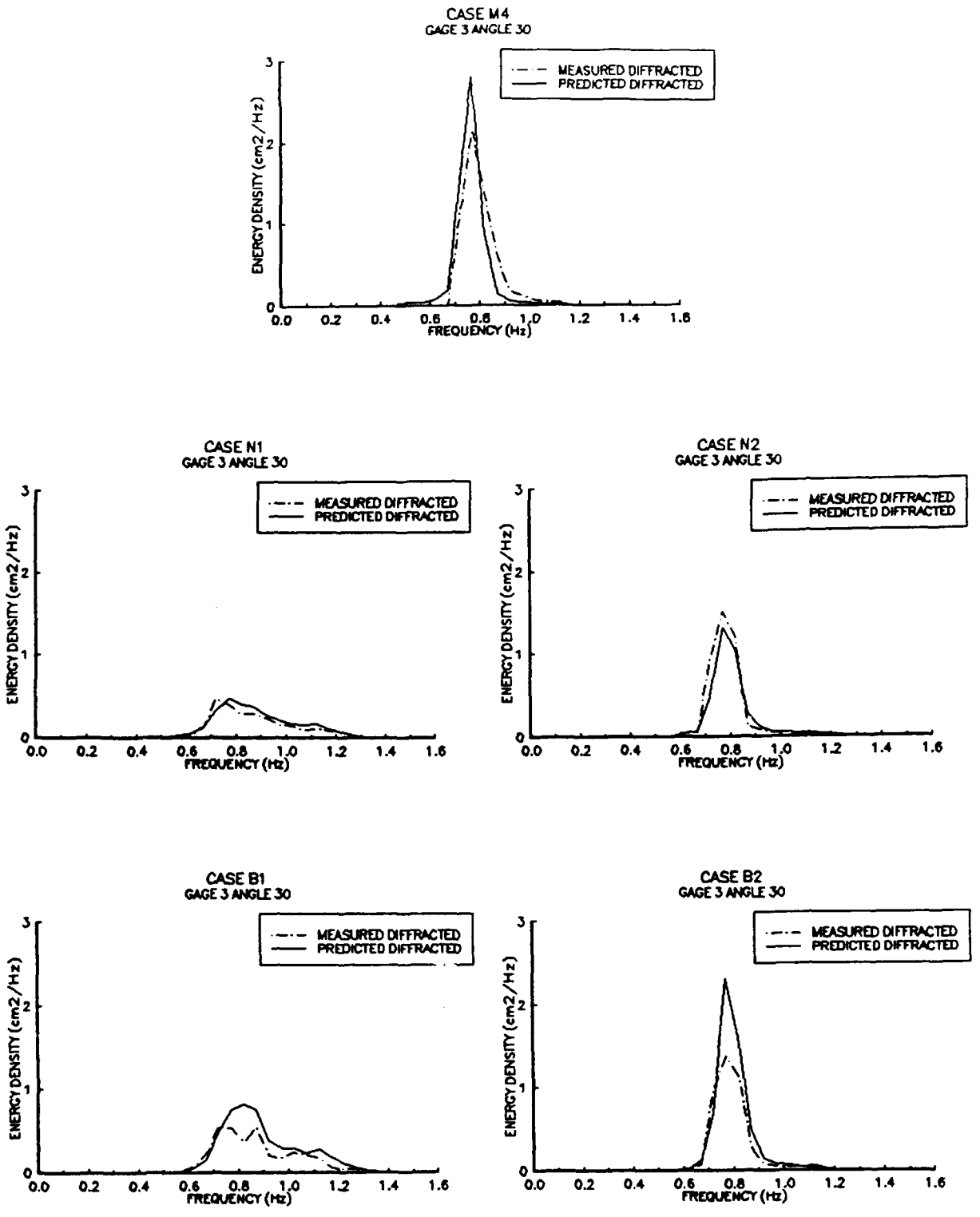

Figure 2. Frequency spectra - gage 3 angle 30 deg

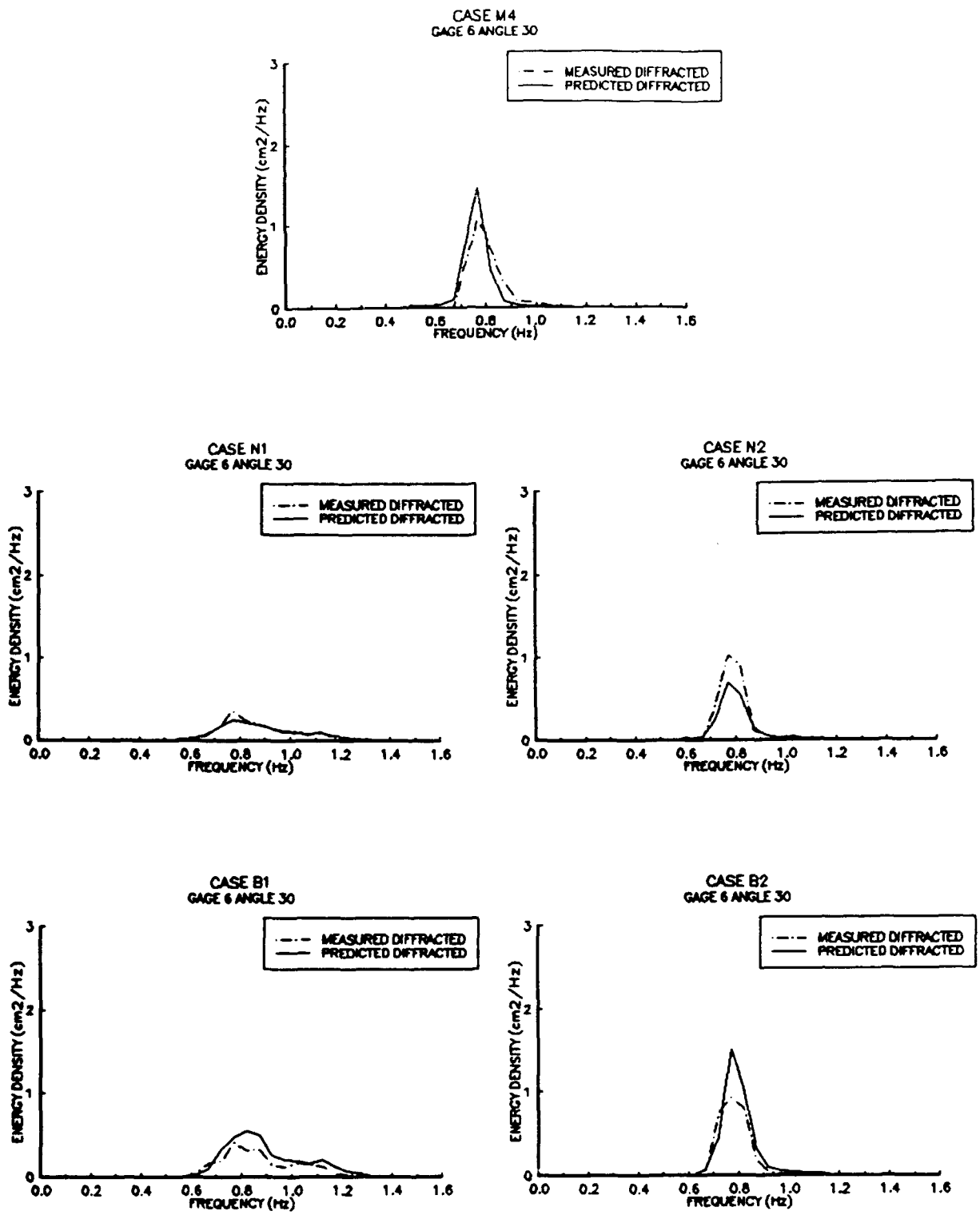

Figure 3. Frequency spectra - gage 6 angle 30 deg

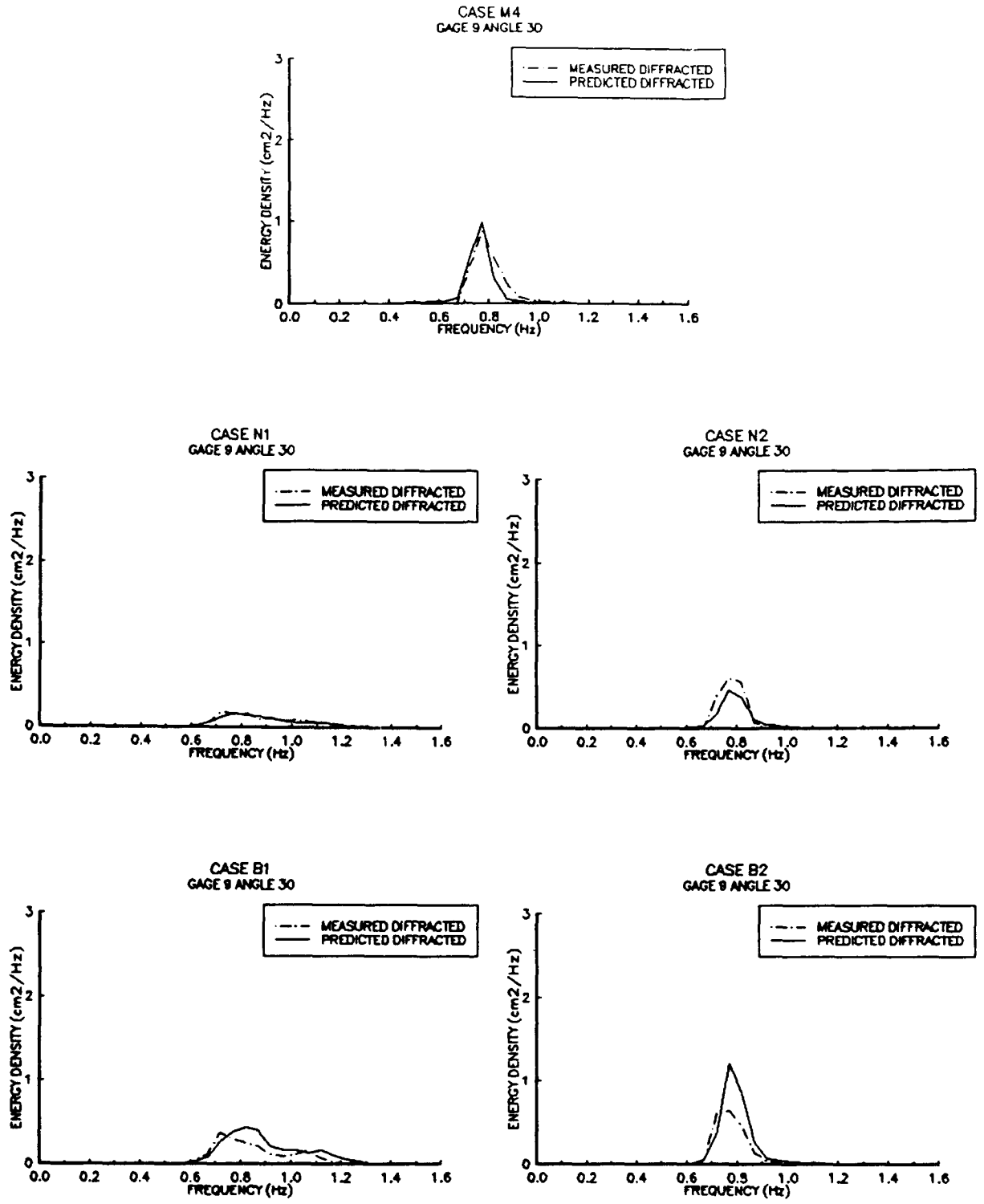

Figure 4. Frequency spectra - gage 9 angle 30 deg

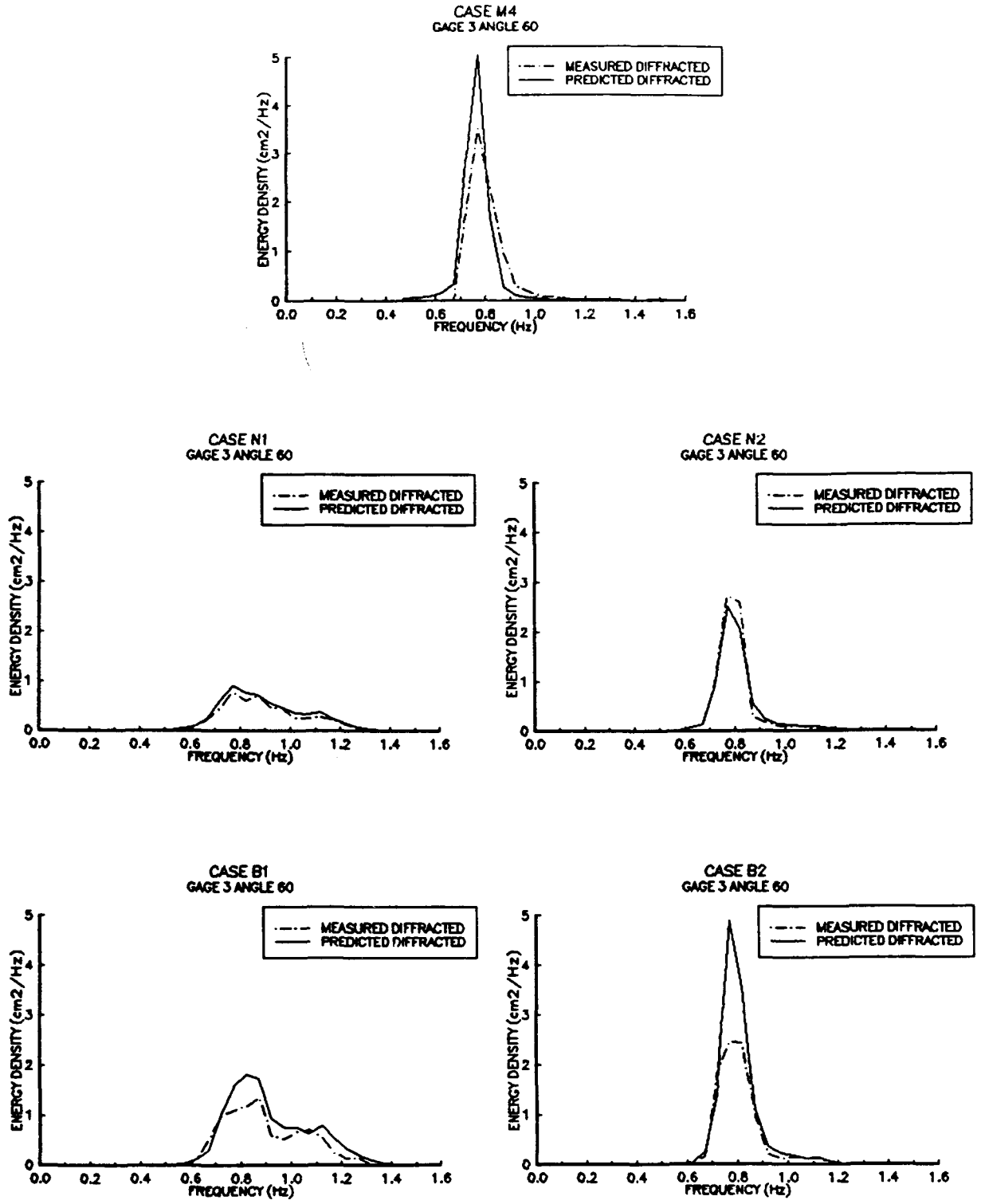

Figure 5. Frequency spectra - gage 3 angle 60 deg

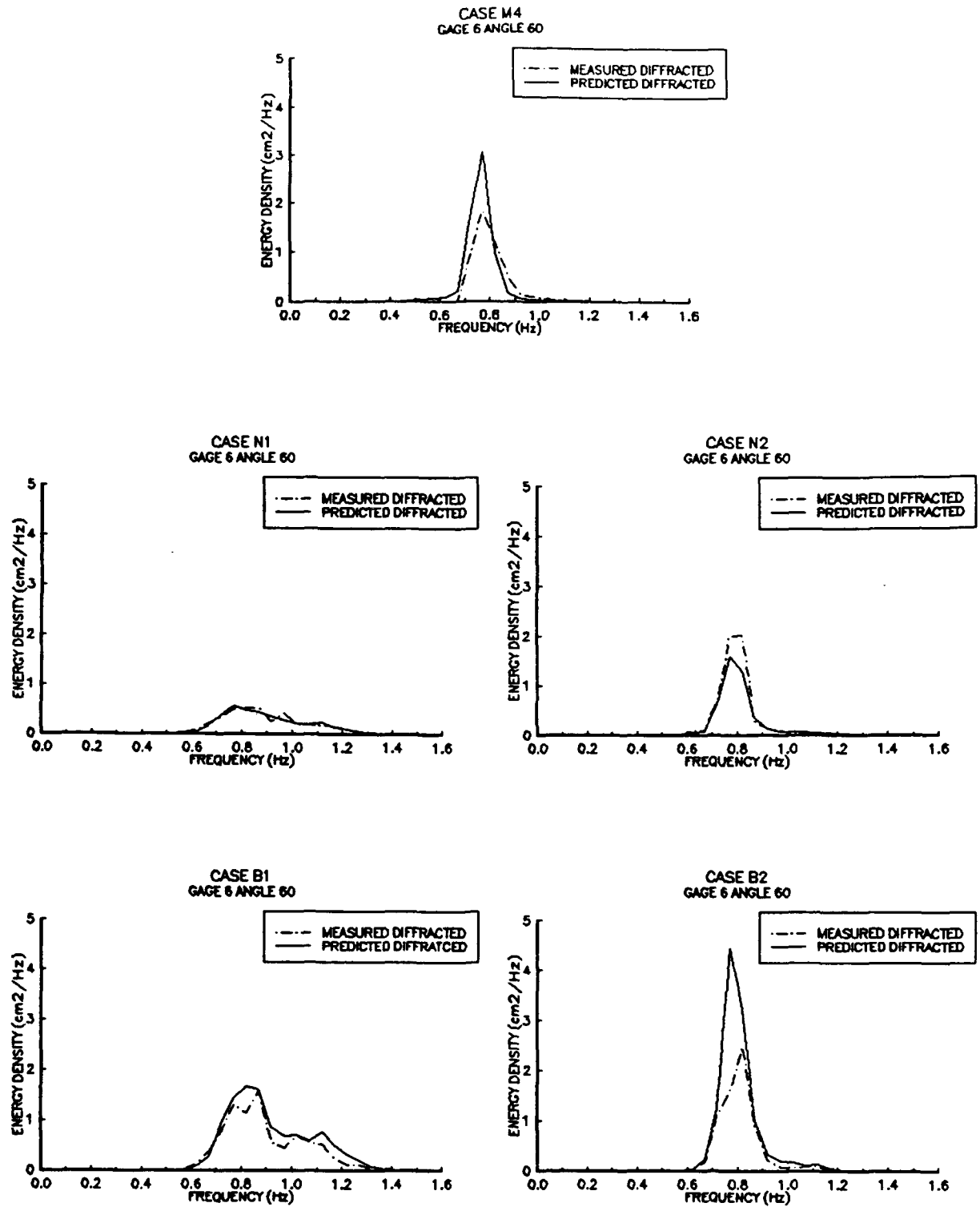

Figure 6. Frequency spectra - gage 6 angle 60 deg

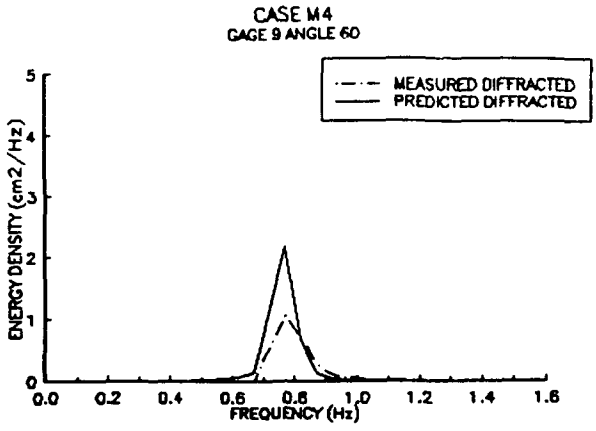

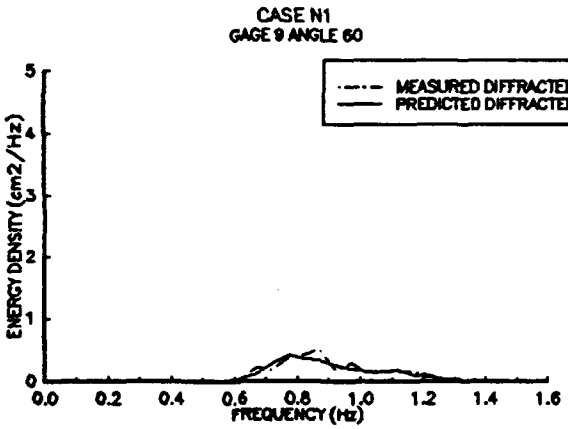

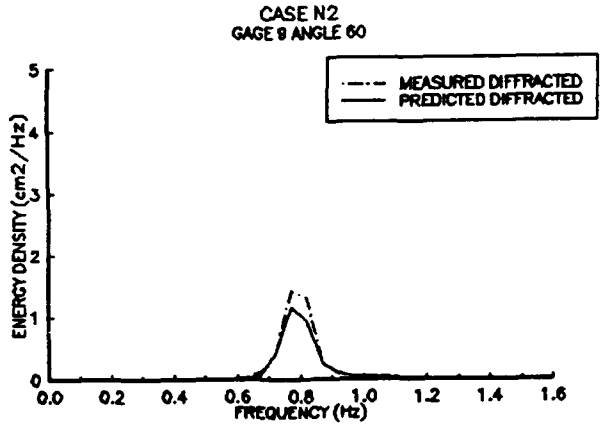

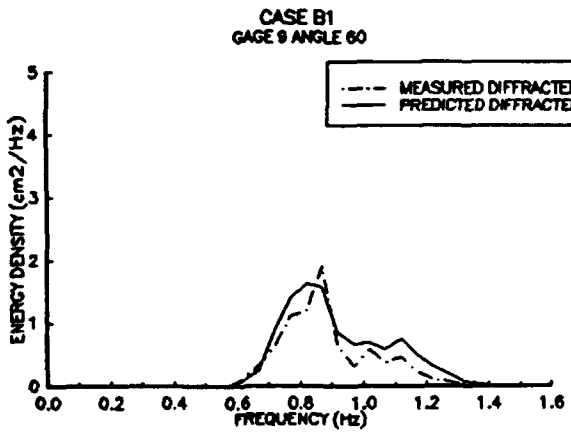

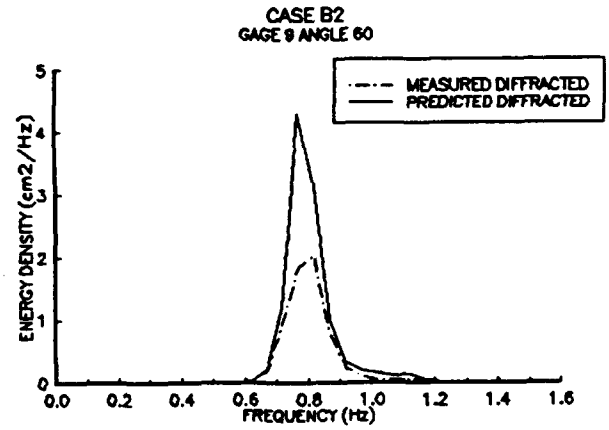

Figure 7. Frequency spectra - gage 9 angle 60 deg

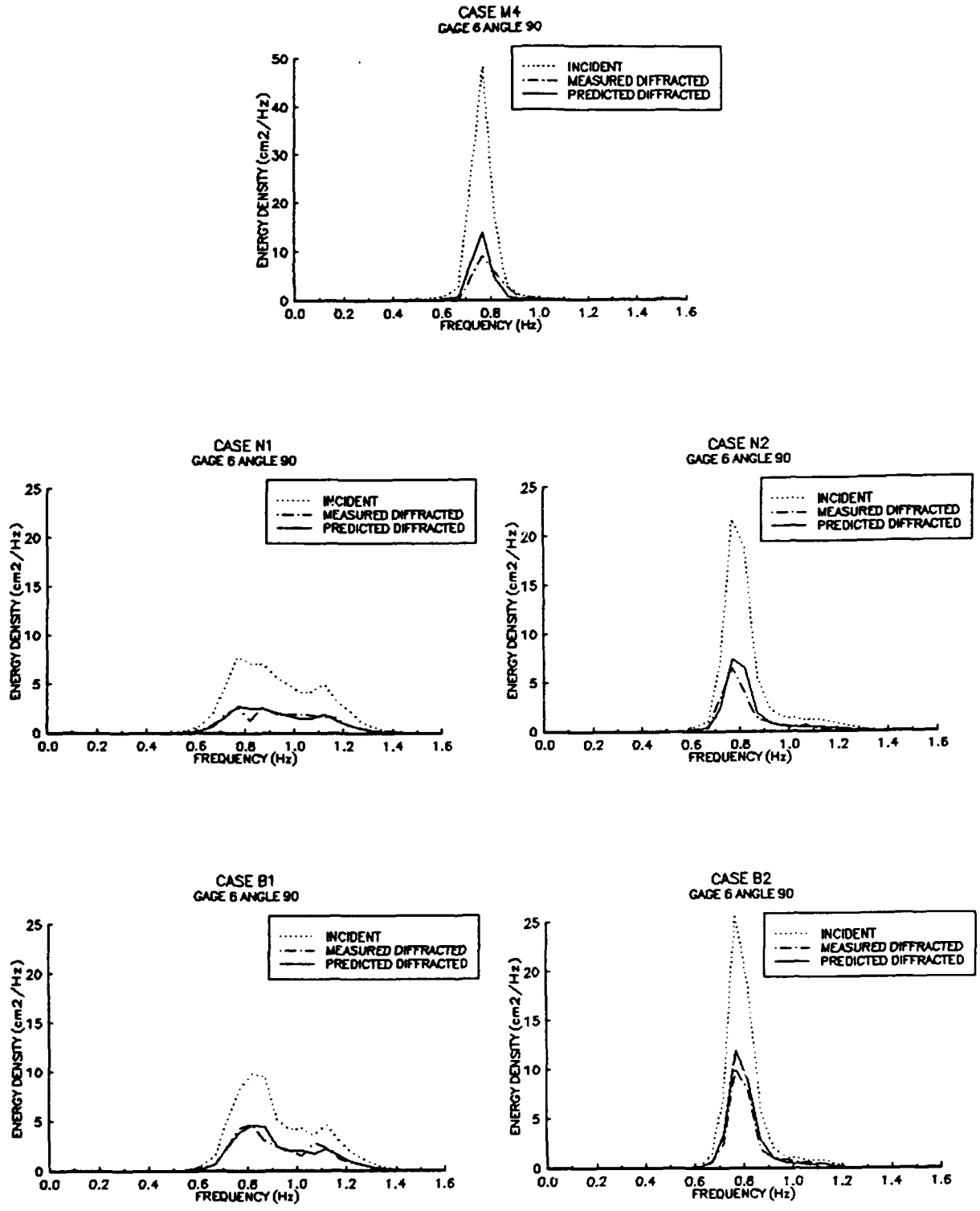

Figure 8. Frequency spectra - gage 6 angle 90 deg

monochromatic diffraction coefficient K_d used in Equation 7, which is the ratio of a diffracted monochromatic wave height to an incident monochromatic wave height. Spectral diffraction coefficients were tabulated for each incident wave condition and are shown in Appendix D. To be consistent with the customary presentation of diffraction diagrams, the spectral diffraction coefficients were contoured and are shown in Figures 9-13. Measured and predicted spectral diffraction coefficients are plotted together for comparison.

41. The diffracted spectra shown in Figures 2-8 show good agreement between the physical model test measurements and the numerical model predictions. For the incident wave conditions with a narrow directional spread, cases N1 and N2, the numerical model closely predicted both the magnitude of the energy in the diffracted spectrum and the distribution of the energy in frequency space. Although the measured and predicted diffracted spectra did not agree as well for the monochromatic case M4, or for the incident wave conditions with a broad directional spread, cases B1 and B2, there was still good agreement.

42. In general, the numerical model slightly underpredicts diffraction for cases N1 and N2 and moderately overpredicts diffraction for cases M4, B1, and B2. The rms difference between measured and predicted spectral diffraction coefficients was computed for each case and is shown in Table 5. The rms difference is defined as:

$$rms\ difference = \sqrt{\frac{\sum_{j=1}^{N} \left[(K_{dsp})_j - (K_{dsm})_j\right]^2}{N}} \qquad (11)$$

where

K_{dsp} = predicted spectral diffraction coefficient

K_{dsm} = measured spectral diffraction coefficient

N = number of spectral diffraction coefficients computed for each case; equals 27

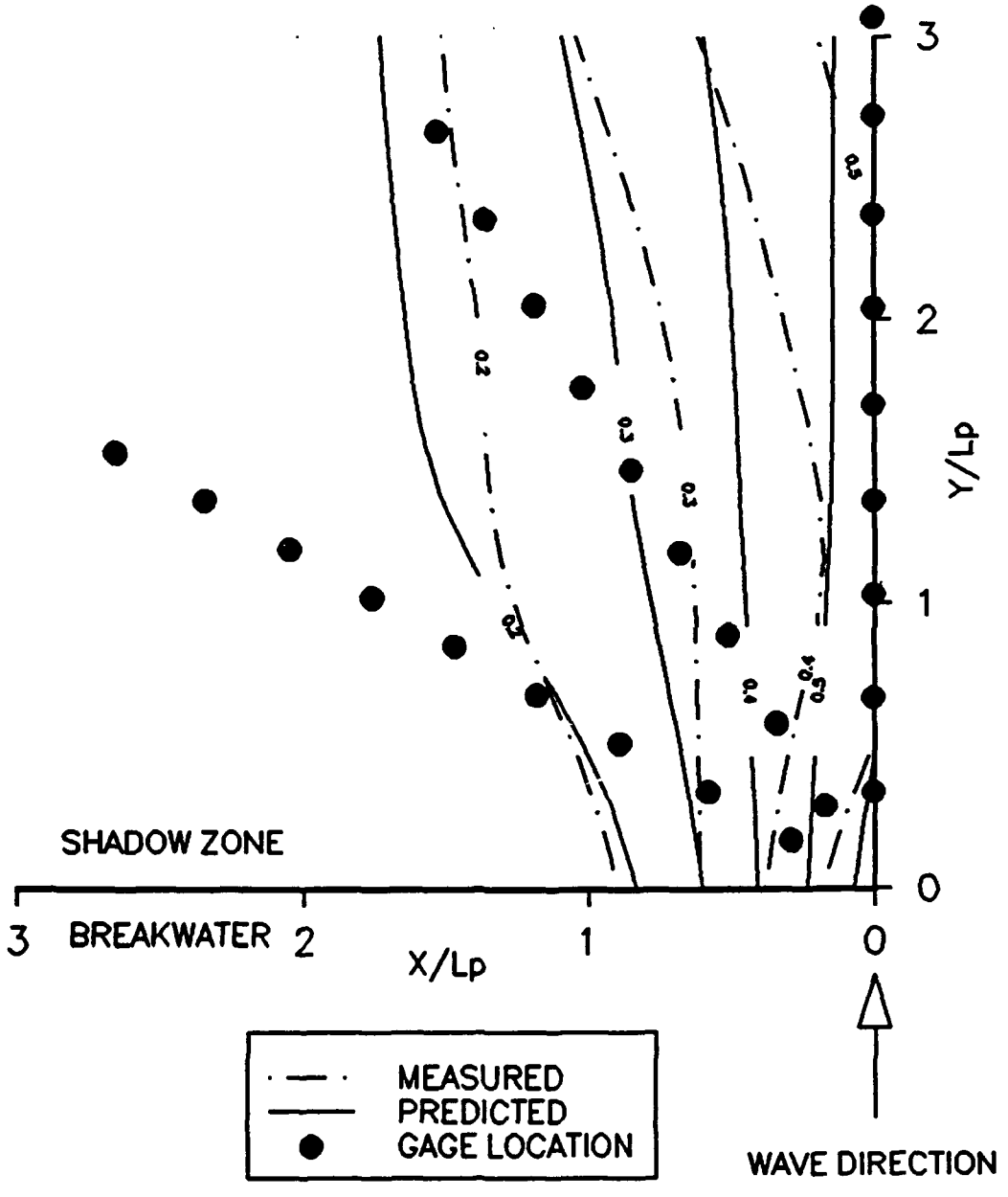

Figure 9. Spectral diffraction coefficients - case M4

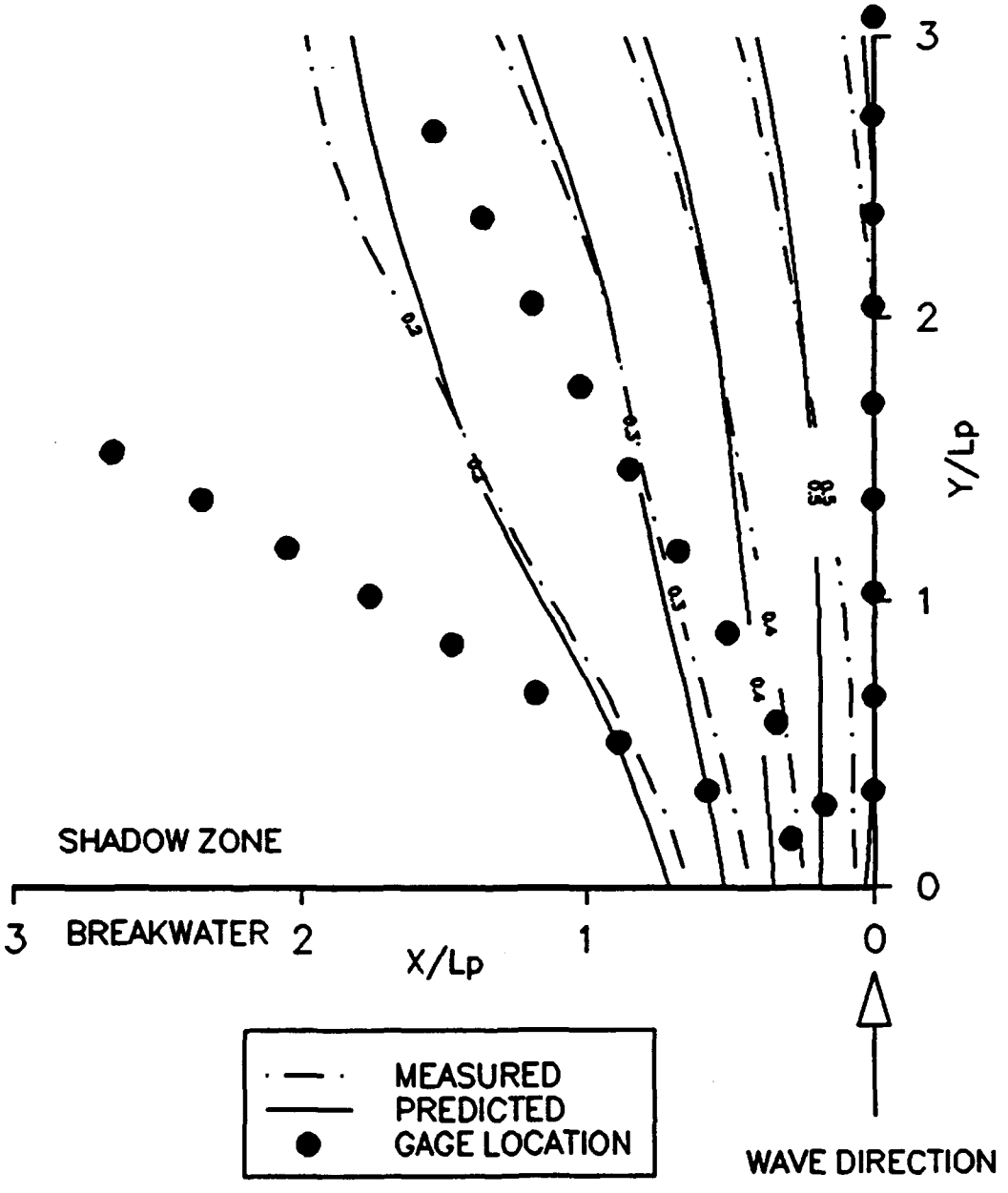

Figure 10. Spectral diffraction coefficients - case N1

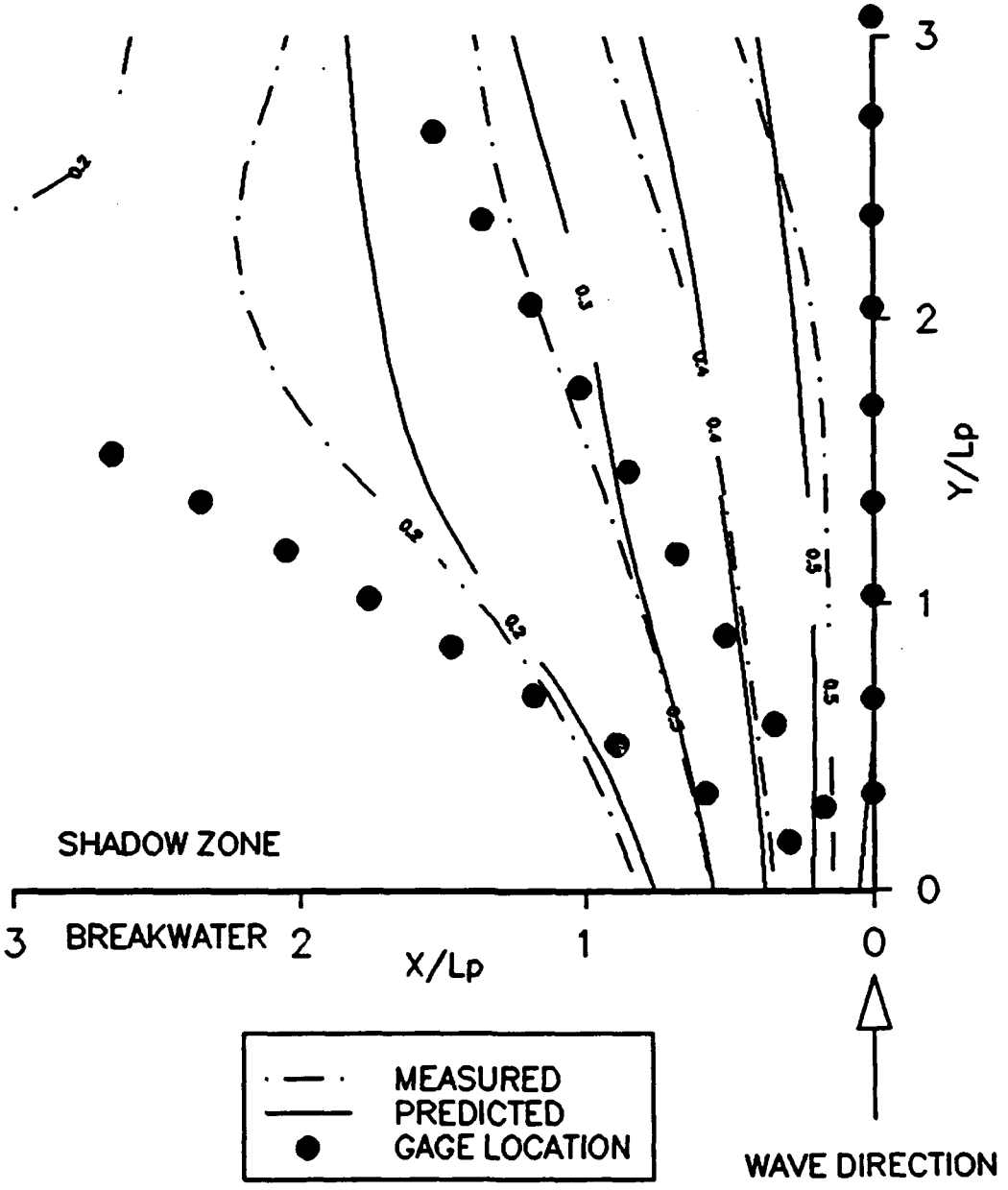

Figure 11. Spectral diffraction coefficients - case N2

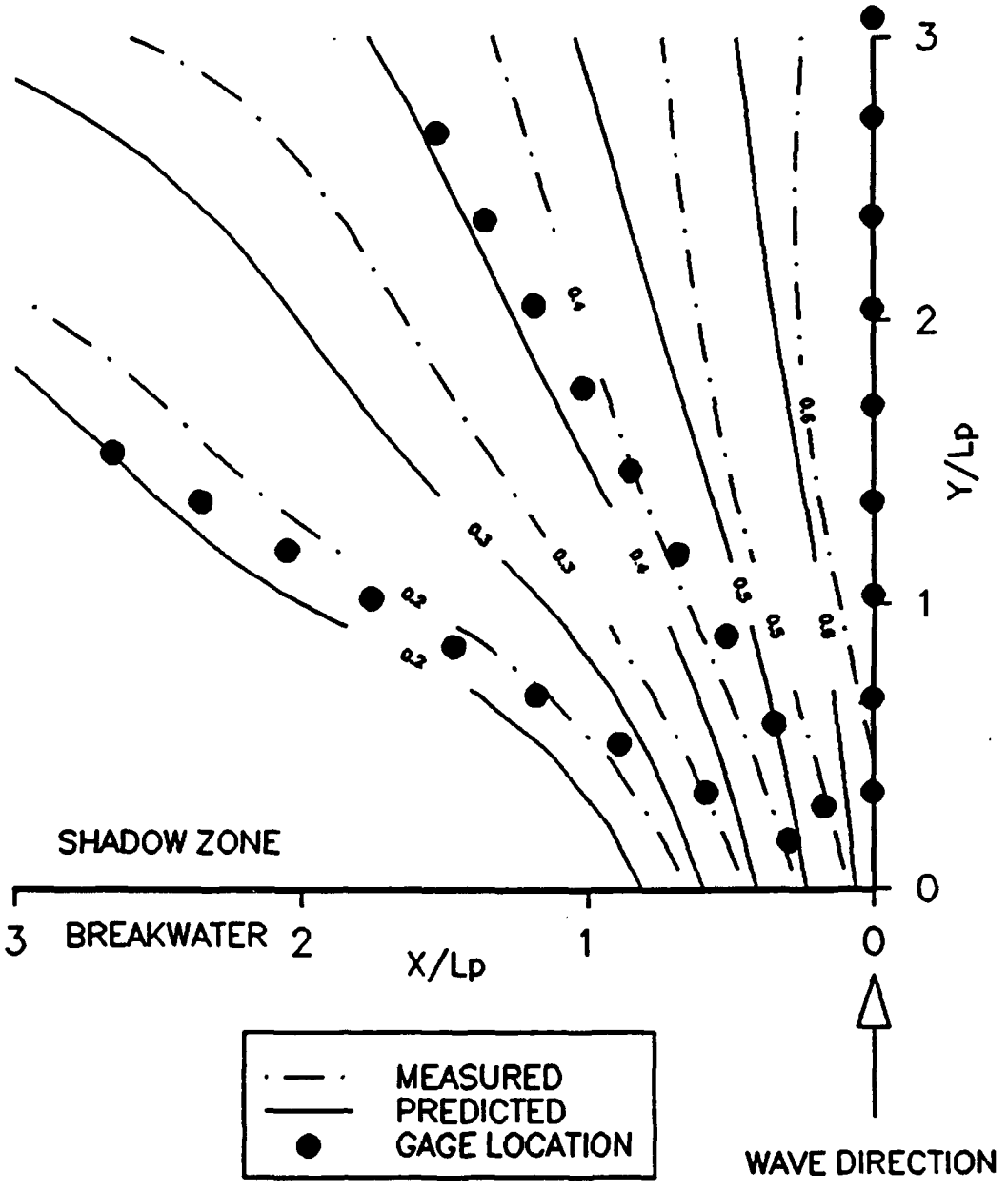

Figure 12. Spectral diffraction coefficients - case B1

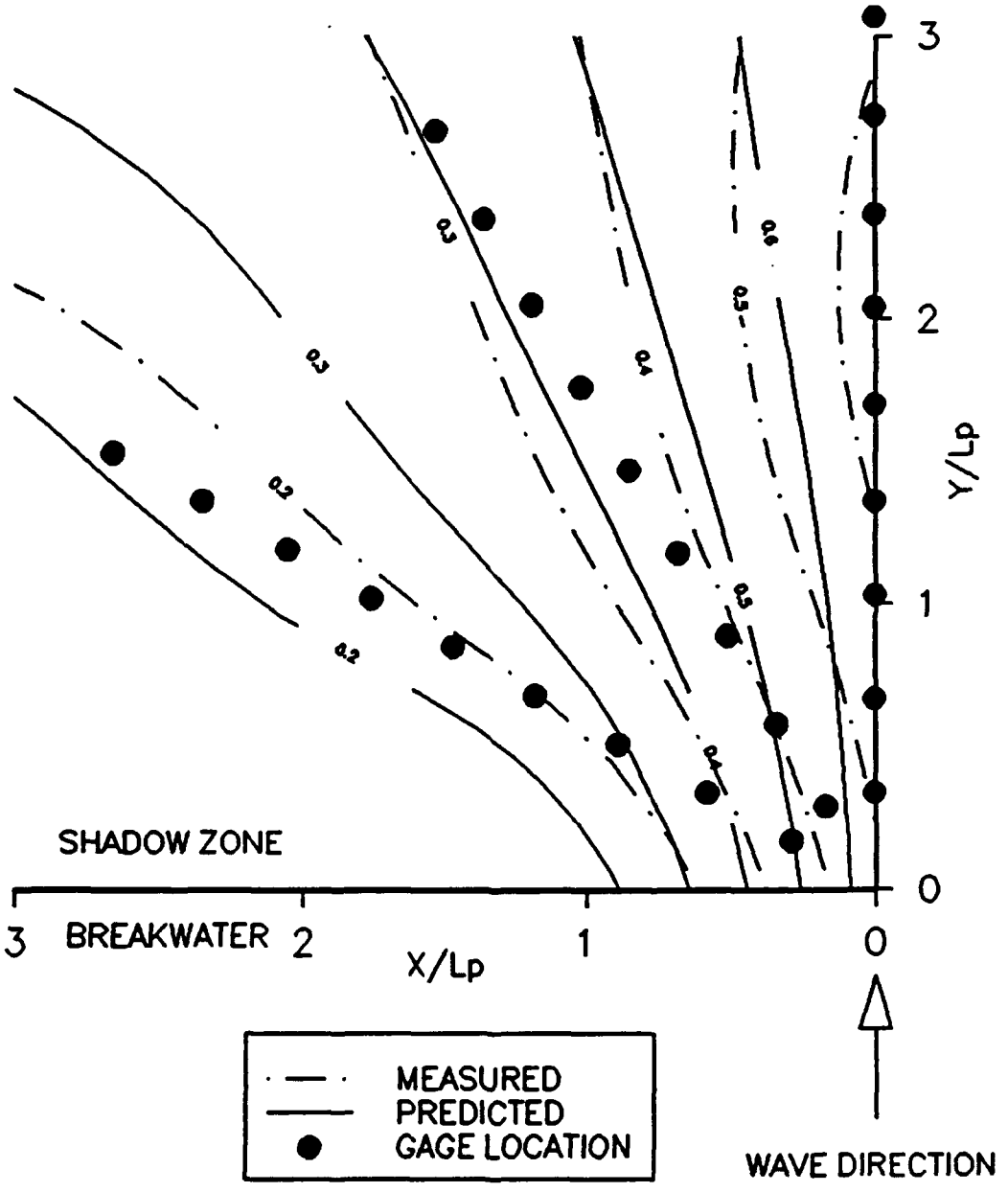

Figure 13. Spectral diffraction coefficients - case B2

Table 5

rms Difference Between Measured and Predicted Spectral Diffraction Coefficients

Case	rms Difference
M4	0.052
N1	0.025
N2	0.029
B1	0.042
B2	0.075

43. For case M4, the difference between the measured and predicted diffracted spectra may have been due to the difficulties associated with representing monochromatic waves with a spectrum. This affects the plots of the incident, measured diffracted, and predicted diffracted spectra, which would ideally plot as an infinite spike. The shape of the measured diffracted spectrum is also strongly dependent on the record length and the resolution bandwidth used in the SCFA analysis. The record length must be sufficiently long to obtain statistical representation of the time series, but not so long as to allow the wave field to become contaminated due to reflections. The resolution bandwidth is inversely proportional to the record length. For the 8 sec record length used in the SCFA analysis of case M4, the resolution bandwidth was 0.125 Hz, which may not have been sufficient to resolve the peak of the spectrum.

44. It is interesting to note that the rms difference for case M4 reduces to 0.021 if array angle 90 deg is excluded. The 90-deg angle is in a region of high gradients in wave heights, as wave energy passes along the crest from the unsheltered region to the sheltered region. For the incident waves with some degree of directional spreading, the gradient is smoothed over a wider region, and better agreement is obtained between the measured and predicted diffracted spectra.

45. For cases B1 and B2, the discretized incident spectra used in the numerical model may have been the reason that the predicted diffracted energy was greater than the measured diffracted energy. As previously discussed, there were problems in resolving the measured directional spread for those

cases. Using the calculated spreading function rather than the measured may have introduced energy into portions of the incident spectrum that were not actually generated in the physical model, specifically, in the directional bands beyond the physical limits of the DSWG. This could have resulted in a prediction of higher diffracted energy in the lee of the breakwater.

46. Since the plywood breakwater was cantilevered from the floor, it is possible that it was not perfectly rigid, and may have absorbed some incident wave energy. This would result in the measured diffracted energy being lower than predicted. However, as there was good agreement between the measured and diffracted spectra for cases N1 and N2, the amount of incident wave energy absorbed by the breakwater is believed to be minimal.

47. Figures 9-13 show the measured and predicted diffraction coefficients for each case. As was observed in Figures 2-8 and in Table 5, the best agreement was obtained for cases N1 and N2. This is seen in Figures 10 and 11. Figure 9 shows the spectral diffraction coefficient along the 90-deg array angle is approximately 0.5. It is known that the diffraction coefficient in the unsheltered region close to that array angle is close to 1.0. This illustrates the large gradient present in this area, as previously discussed.

PART VI: CONCLUSIONS

48. The numerical model written for this study closely predicts the diffraction of directional wave spectra incident upon a semi-infinite breakwater. Measured and predicted diffracted spectra were plotted for comparison at several locations in the lee of the breakwater within three nominal wavelengths of the breakwater tip. Good to excellent agreement was obtained for the incident spectra with a narrow directional spread, cases N1 and N2. For the incident spectra with a broad directional spread, cases B1 and B2, the numerical model predicted moderately higher diffracted spectra than were measured. The numerical model also predicted higher diffracted spectra than were measured for case M4, but this difference was small away from the region of high gradients in wave height.

49. Measured and predicted spectral diffraction coefficients were also plotted and compared. Cases N1 and N2 had the best agreement, with rms differences between measured and predicted spectral diffraction coefficients of 0.025 and 0.029, respectively. Cases B1 and B2 had rms differences of 0.042 and 0.075, respectively. Case M4 had an rms difference of 0.052 for all gages, but this reduced to 0.021 in the shadow zone away from the region of high gradients in wave height.

PART VII: RECOMMENDATIONS FOR FUTURE WORK

50. The numerical model developed for this report was not a flexible, general-use directional diffraction model, but was instead designed to obtain results which could be compared with model test results, to verify the methodology. Now that the validity of the methodology has been verified, it would be useful to expand the numerical model to make it more general. The following additions are recommended:

a. Allow user selection of incident frequency spectra; such as TMA, JONSWAP, Pierson and Moskowitz, and Bretschneider-Mitsuyasu. The functional form of these spectra could be coded, and the program could compute the spectral ordinates.

b. Allow user selection of incident directional spreading functions; such as wrapped normal, and Mitsuyasu. These should include the option for frequency dependence. As with the frequency spectra, the functional forms of these spreading functions could be coded, and the program could compute the ordinates.

c. Format the existing program to read standardized output formats of existing wave growth and transformation models, e.g., STWAVE and SHALWV.

d. Determine the sensitivity of varying the number of frequency and directional band width used in the discretization of the incident directional spectrum. Allow user definition of the upper and lower cutoffs for frequency and direction, band widths, and number of bands. Provide the user with guidance based on the sensitivity analysis.

e. Allow user selection of locations where information on diffracted wave heights is desired.

f. Allow user selection of output, to include tabulated and plotted incident and diffracted spectra, and contoured spectral diffraction coefficients.

g. Add capability to superpose diffracted waves from multiple breakwaters for arbitrary breakwater orientation.

51. The model could be adapted from its present form to accommodate these features. Items a., b, and c. constitute minor modifications to the model which would produce significant benefits. Item d. constitutes a moderate effort for the sensitivity analysis. Item e. constitutes a minor change in coding, but could significantly increase computer run time. This time can be minimized by the user by selecting fewer points for preliminary runs. Item f. constitutes minor changes in coding, but would be dependent on

graphics software selected. Item g. would involve consideration of wave phase and wave interactions, which is within the capability of existing theory, and would be a significant enhancement.

REFERENCES

Borgman, L. E. 1990. "Irregular Ocean Waves: Kinematics and Forces," In Ocean Engineering Science The Sea, Vol. 9, Part A (Edited by LeMehaute, B., and Hanes, D. M.), John Wiley and Sons, New York, 1-1301.

Bouws, E., Gunther, H., Rosenthal, W., and Vincent, C. 1985. "Similarity of the Wind Wave Spectrum in Finite Depth Water," J. Geophys. Research, 90(C1).

Bretschneider, C. L. 1968 (Feb). "Significant Waves and Wave Spectrum," Ocean Industry.

Briggs, M. J. 1988. "Unidirectional Spectral Wave Generation and Analysis in Wave Basins, Volume 1: Main Text and Appendix A," Technical Report CERC 88-11, Coastal Engineering Research Center, US Army Engineer Waterways Experiment Station, Vicksburg, MS.

Briggs, M. J., Grace, P. J. and Jensen, R. E. 1989. "Directional Spectral Wave Transformation in the Nearshore Region, Report 1, Directional Spectral Performance Characteristics," Technical Report CERC-89-14, US Army Engineer Waterways Experiment Station, Coastal Engineering Research Center, Vicksburg, MS.

Briggs, M. J., Thompson, E. F., and Vincent, C. L. 1991. "Wave Diffraction Around a Breakwater," submitted to ASCE Journal of Waterway, Port, Coastal and Ocean Engineering.

Chen, H. S. 1987. "Combined Reflection and Diffraction by a Vertical Wedge," Technical Paper 80-2, US Army Engineer Waterways Experiment Station, Coastal Engineering Research Center, Vicksburg, MS.

Goda, Y. 1985. Random Seas and Design of Maritime Structures, University of Tokyo Press, Tokyo, Japan.

Goda, Y., Takayama, T., and Suzuki, Y. 1978. "Diffraction Diagrams for Directional Random Waves," Proceedings of the 16th Conference on Coastal Engineering, Hamburg, West Germany.

Hughes, Steven A. 1984. "The TMA Shallow-Water Spectrum Description and Applications," Technical Report CERC 84-7, Coastal Engineering Research Center, US Army Engineer Waterways Experiment Station, Vicksburg, MS.

Irie, I. 1975. "Examination of Wave Deformation With Field Observation Data, Coastal Engineering in Japan," JSCE, Vol. 18.

Kaihatu, J. M. and Chen, H. S. 1988. "Combined Diffraction and Reflection by a Vertical Wedge: PCDFRAC User's Manual," Technical Report CERC-88-97, US Army Engineer Waterways Experiment Station, Coastal Engineering Research Center, Vicksburg, MS.

Leenknecht, D. A., Szuwalski, A., Sherlock, A. R., and George, M. E. 1990. Automated Coastal Engineering System, User's Guide and Technical Reference, US Army Engineer Waterways Experiment Station, Coastal Engineering Research Center, Vicksburg, MS.

Mitsuyasu, H. 1968. "On the Growth of the Spectrum of Wind-Generated Waves (I)," Rept. Res. Inst. for Applied Mech., Kyushu Univ., Vol. XVI, No. 55.

Mobarek, I. E., and Wiegel, R. L. 1966. "Diffraction of Wind Generated Water Waves," Proceedings of the 10th Conference on Coastal Engineering, Tokyo, Japan.

Nagai, K. 1972. "Diffraction of the Irregular Sea Due to Breakwaters," Coastal Engineering in Japan, JSCE, Vol 15.

Penney, W. G. and Price, A. T. 1944. "Diffraction of Sea Waves by Breakwaters," Technical History No. 26, Sec. 3-D, Directorate of Miscellaneous Weapons Development.

Sand, S. E., Kirkegaard, J., Larsen, J., and Rodenhuis, G. S. 1983. "Numerical and Physical Modeling of Directional Diffraction of Waves," International Conference on Coastal and Port Engineering in Developing Countries, Columbo, 20-26 March.

Shore Proection Manual. 1984. 4th ed., 2 vols, US Army Engineer Waterways Experiment Station, Coastal Engineering Research Center, US Government Printing Office, Washington, DC.

Sommerfeld, A. 1896. "Mathematische Theorie der Diffraction," Math. Ann., 47.

Stoker, J. J. 1957. "Water Waves," Interscience Publishers, Inc., New York.

Takayama, T., and Kamiyama, Y. 1977. "Diffraction of Sea waves by Rigid or Cushion Type Breakwaters," Report of the Port and Harbor Research Institute, Vol 16, No. 3.

Wiegel, R. L. 1962 (Jan). "Diffraction of Waves by a Semi-Infinite Breakwater," Journal of the Hydraulics Division, ASCE Vol. 88, No. HY1.

APPENDIX A: TARGET INCIDENT SPECTRA

Target Model Directional Spectrum

Case M4

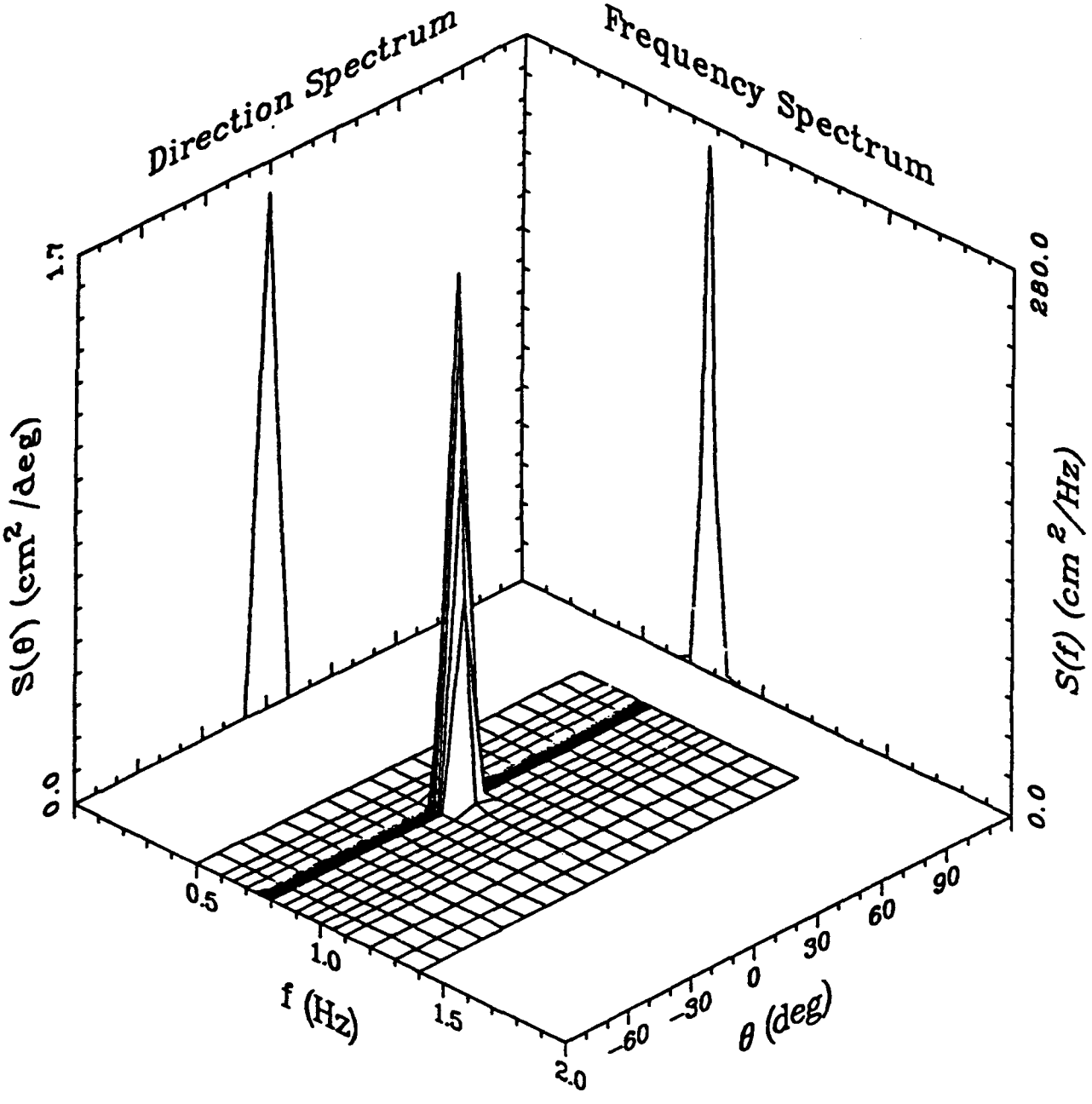

Target Model Directional Spectrum

Case N1

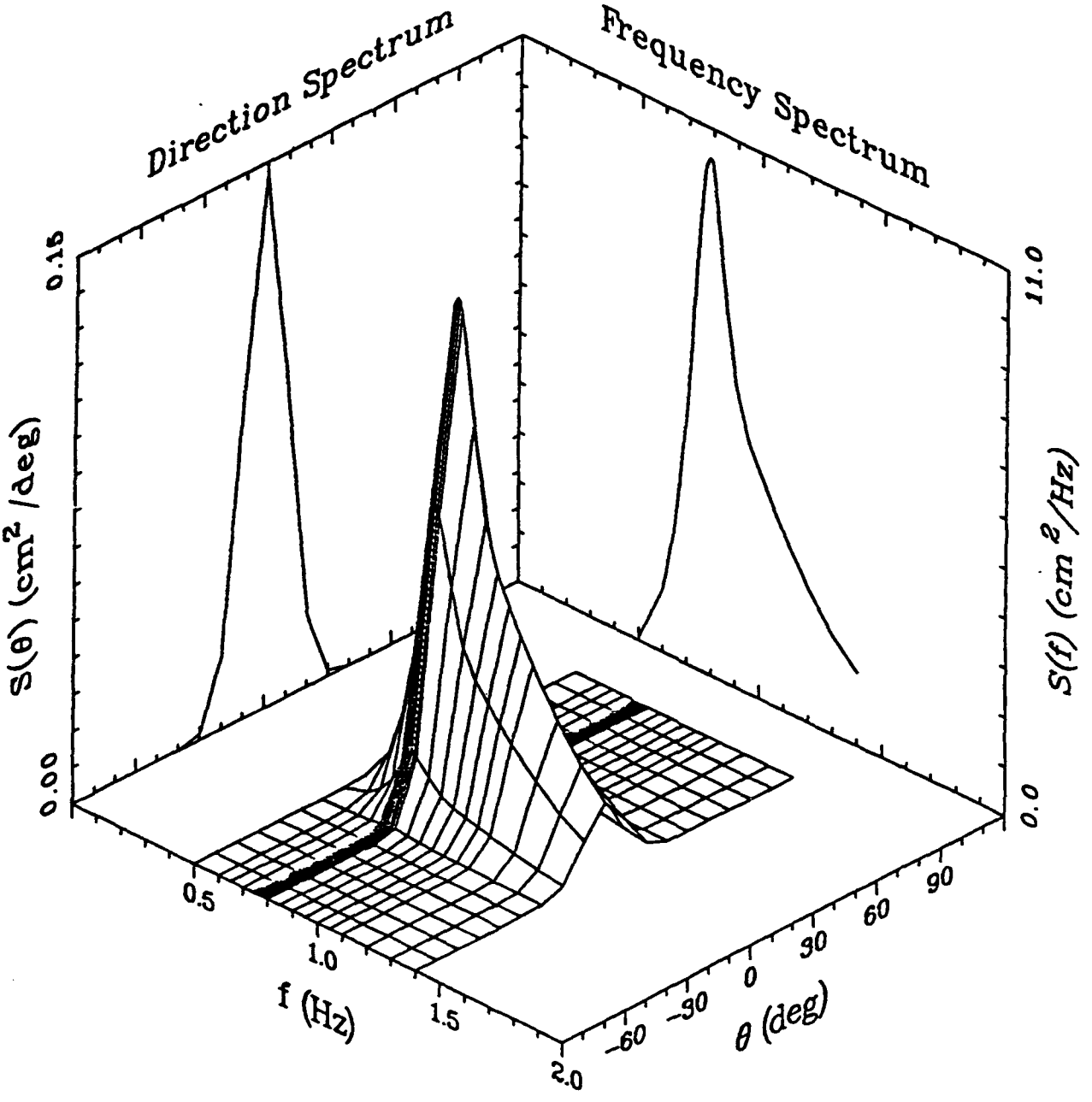

Target Model Directional Spectrum

Case N2

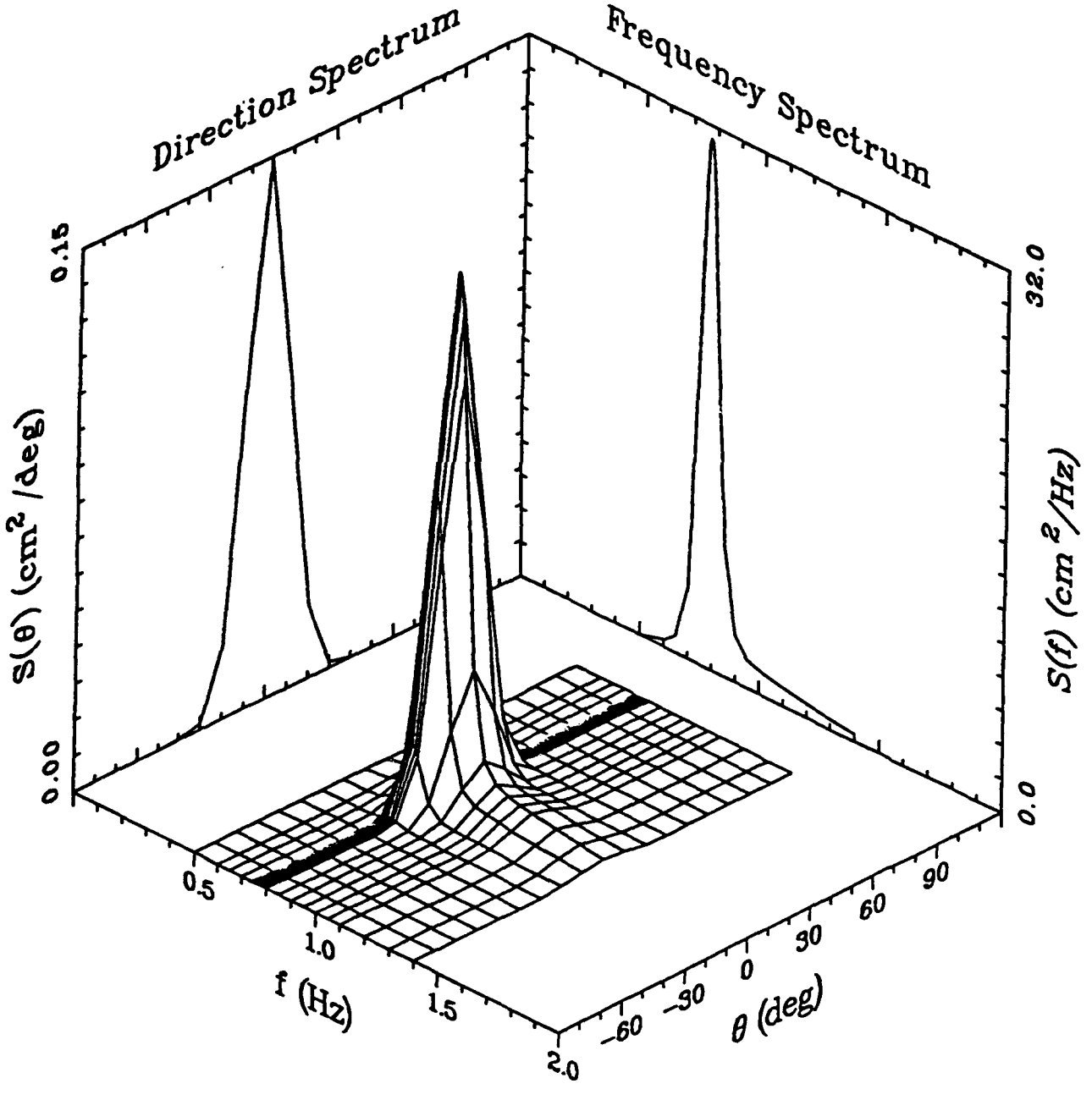

Target Model Directional Spectrum

Case B1

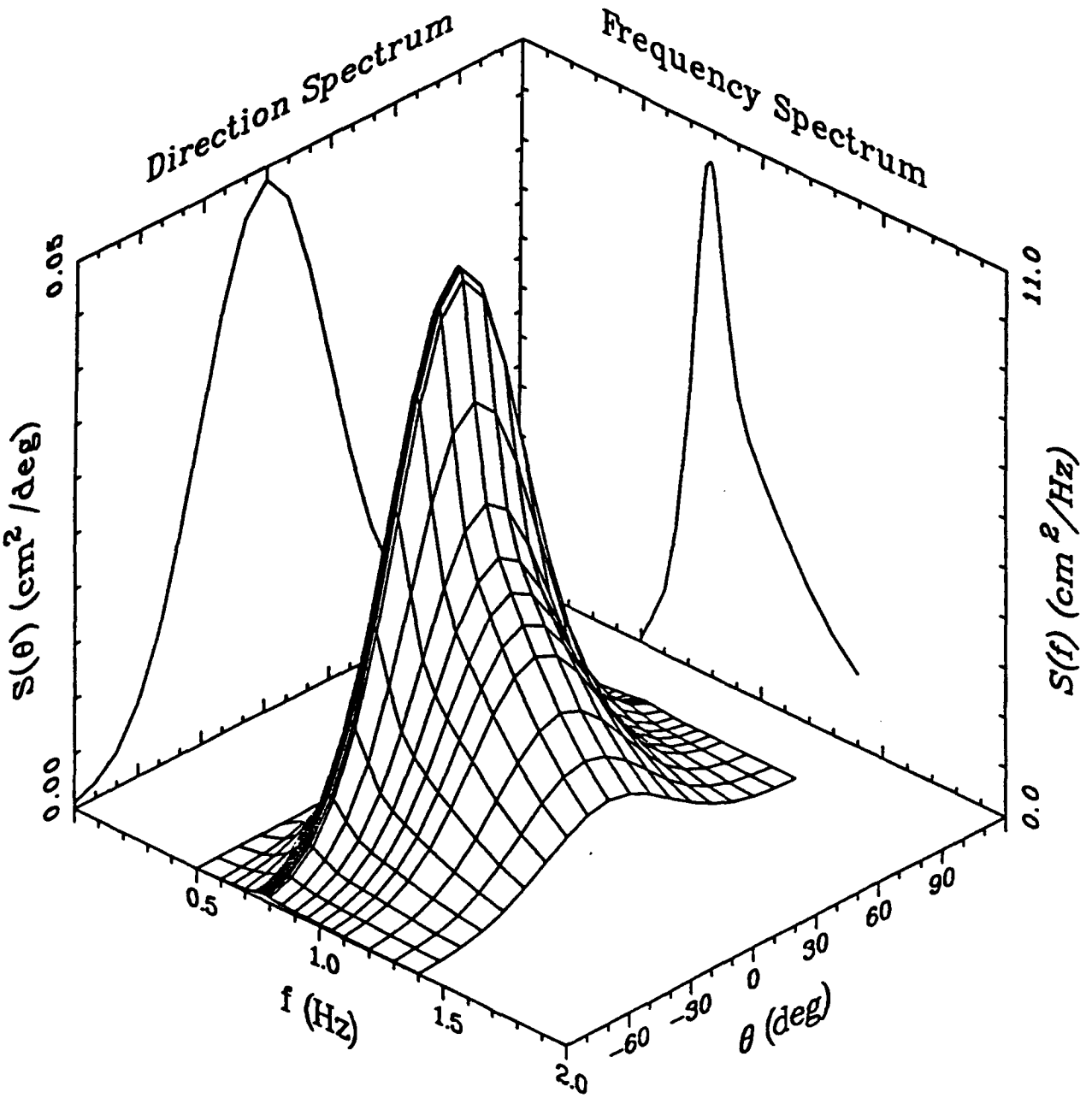

Target Model Directional Spectrum

Case B2

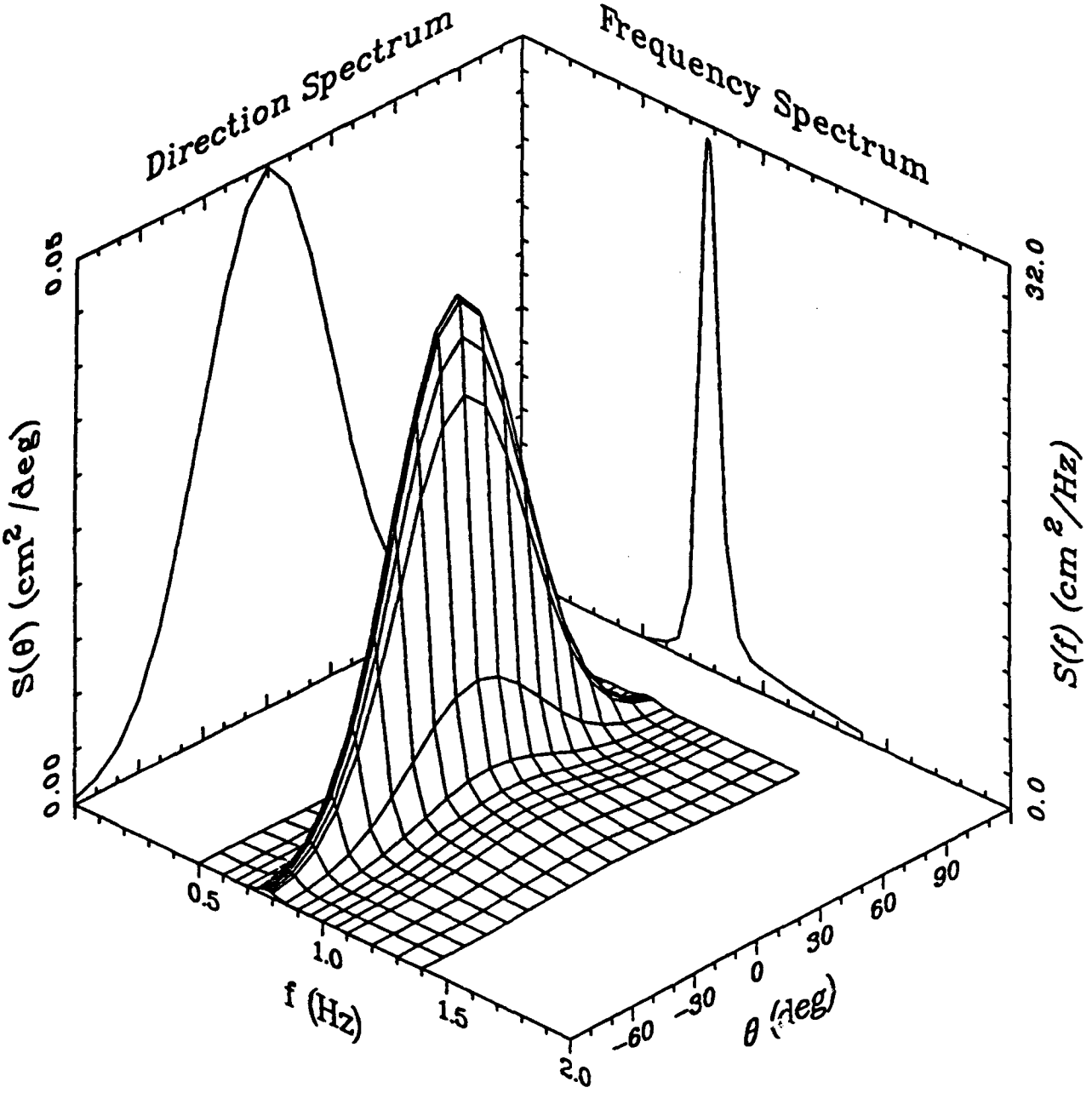

APPENDIX B: DISCRETIZED INCIDENT SPECTRA

Measured Model Directional Spectrum

Case M4

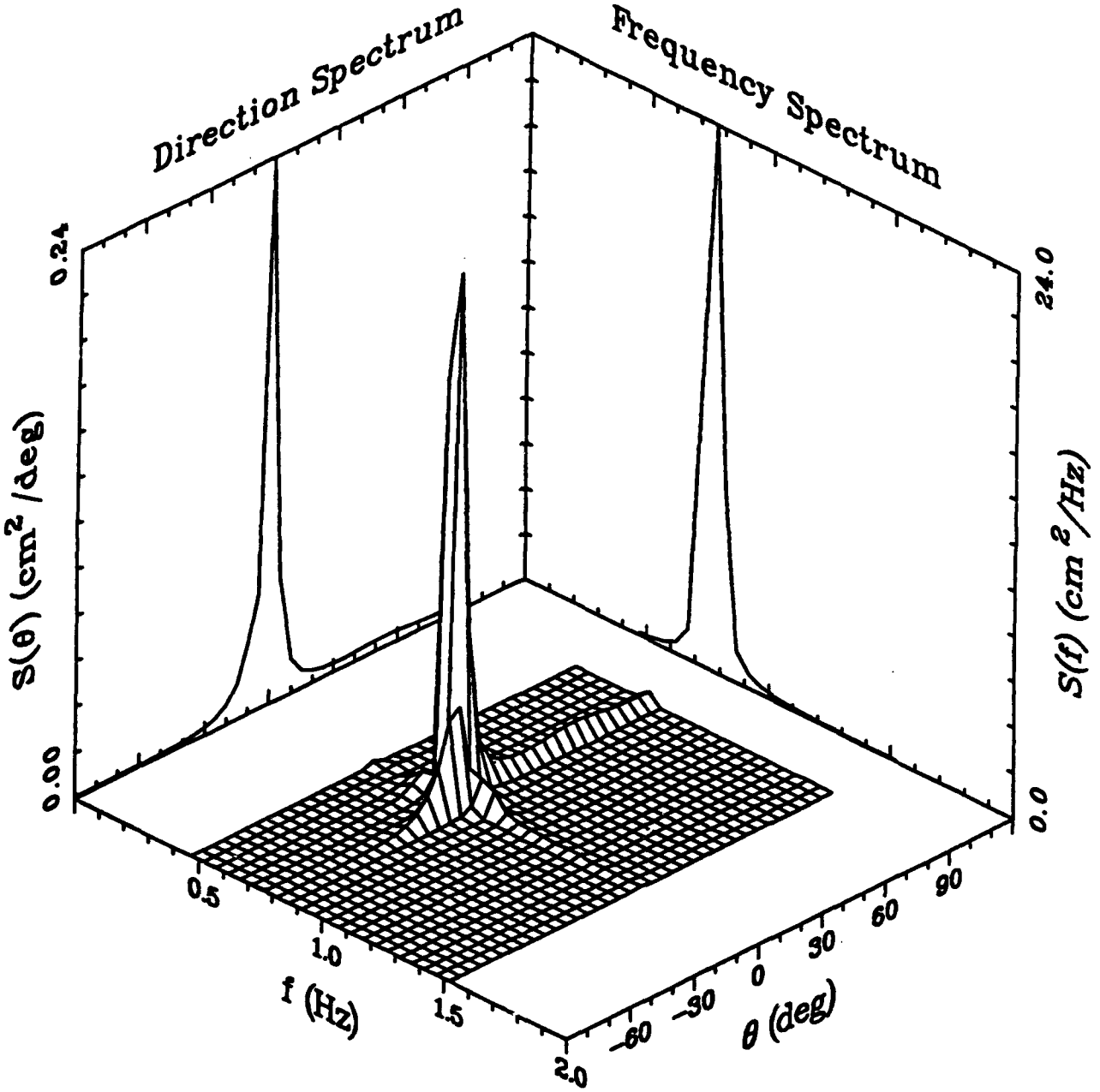

Measured Model Directional Spectrum

Case N1

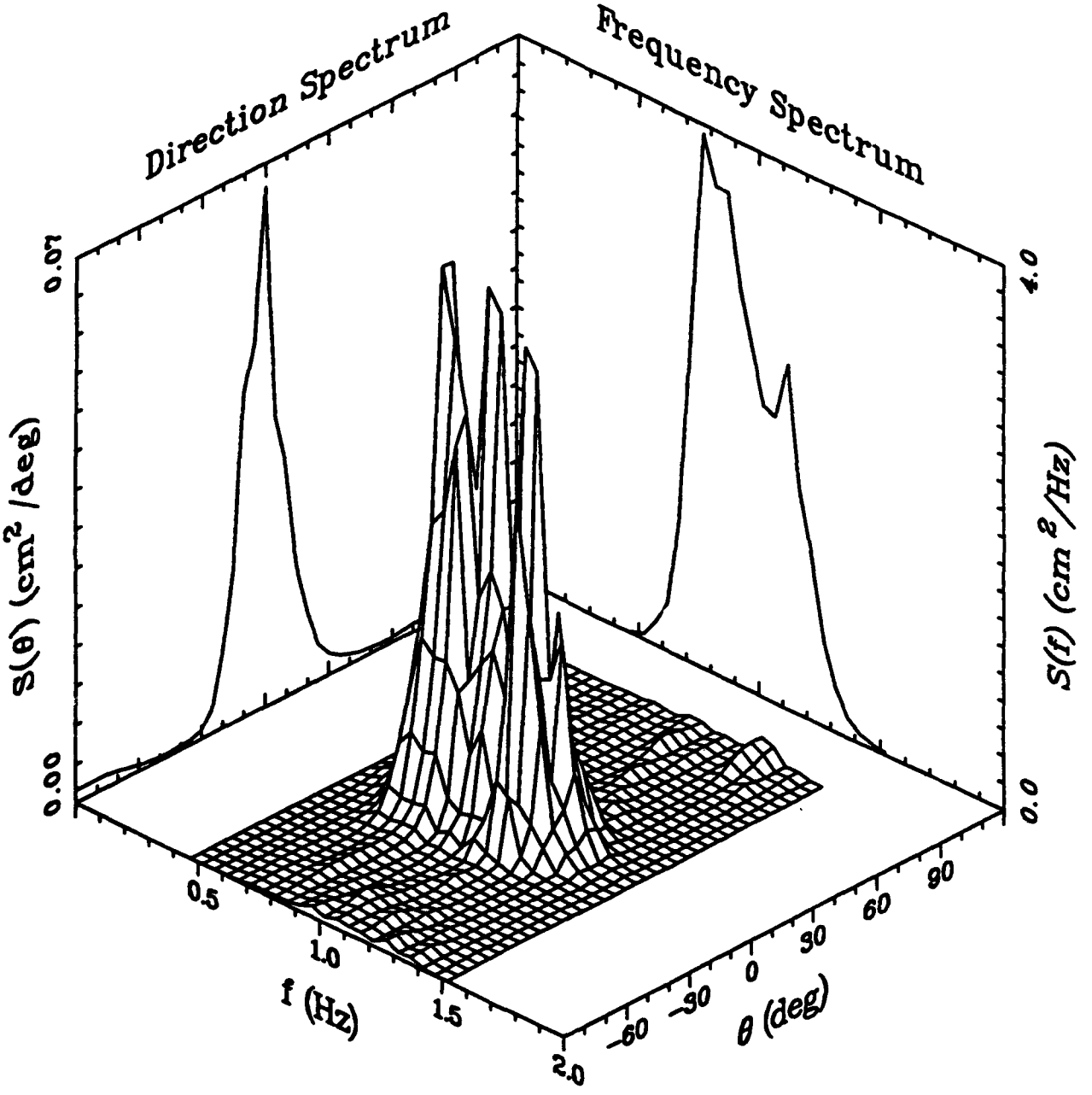

Measured Model Directional Spectrum

Case N2

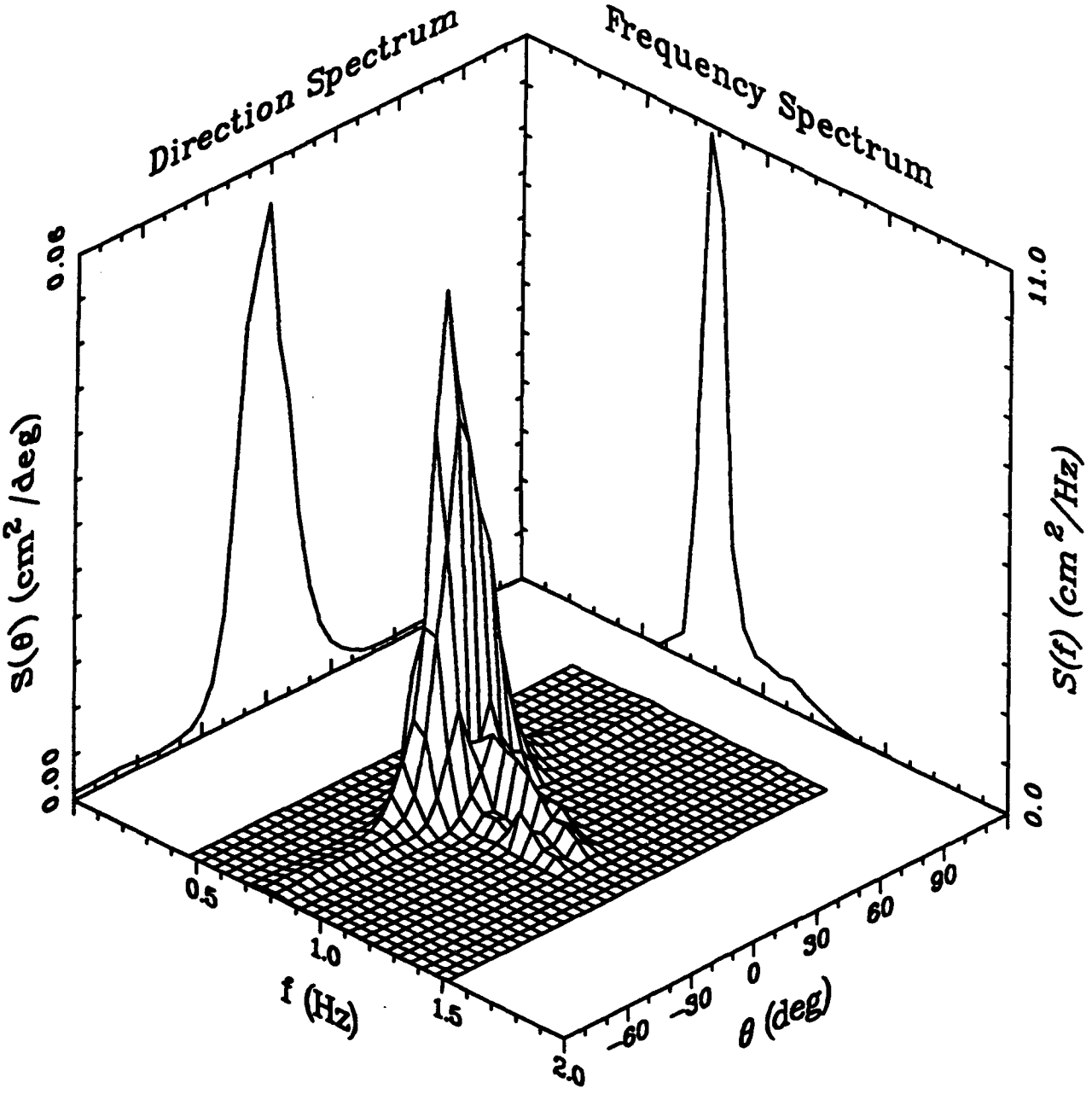

Measured Model Directional Spectrum

Case B1

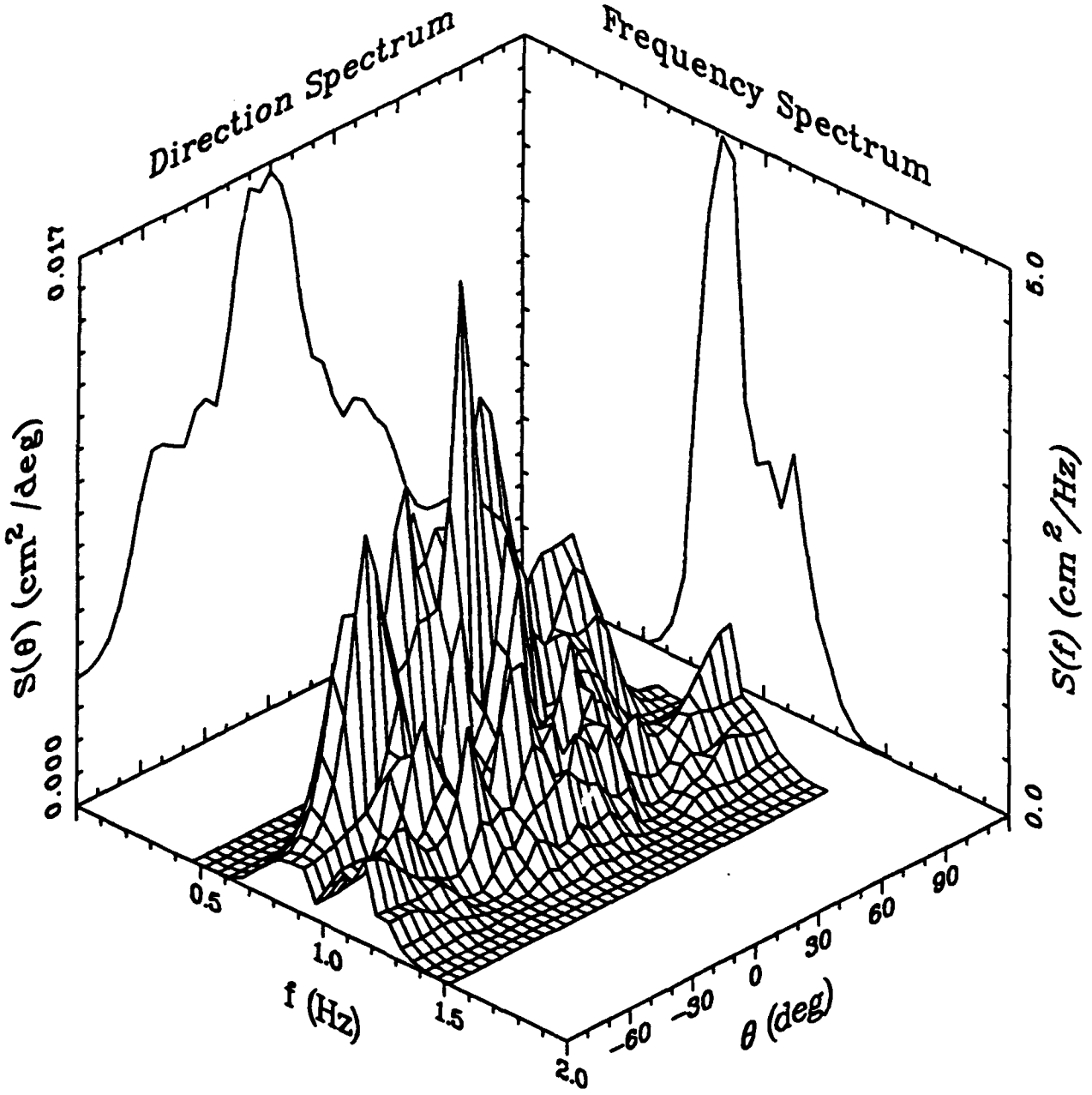

Measured Model Directional Spectrum

Case B2

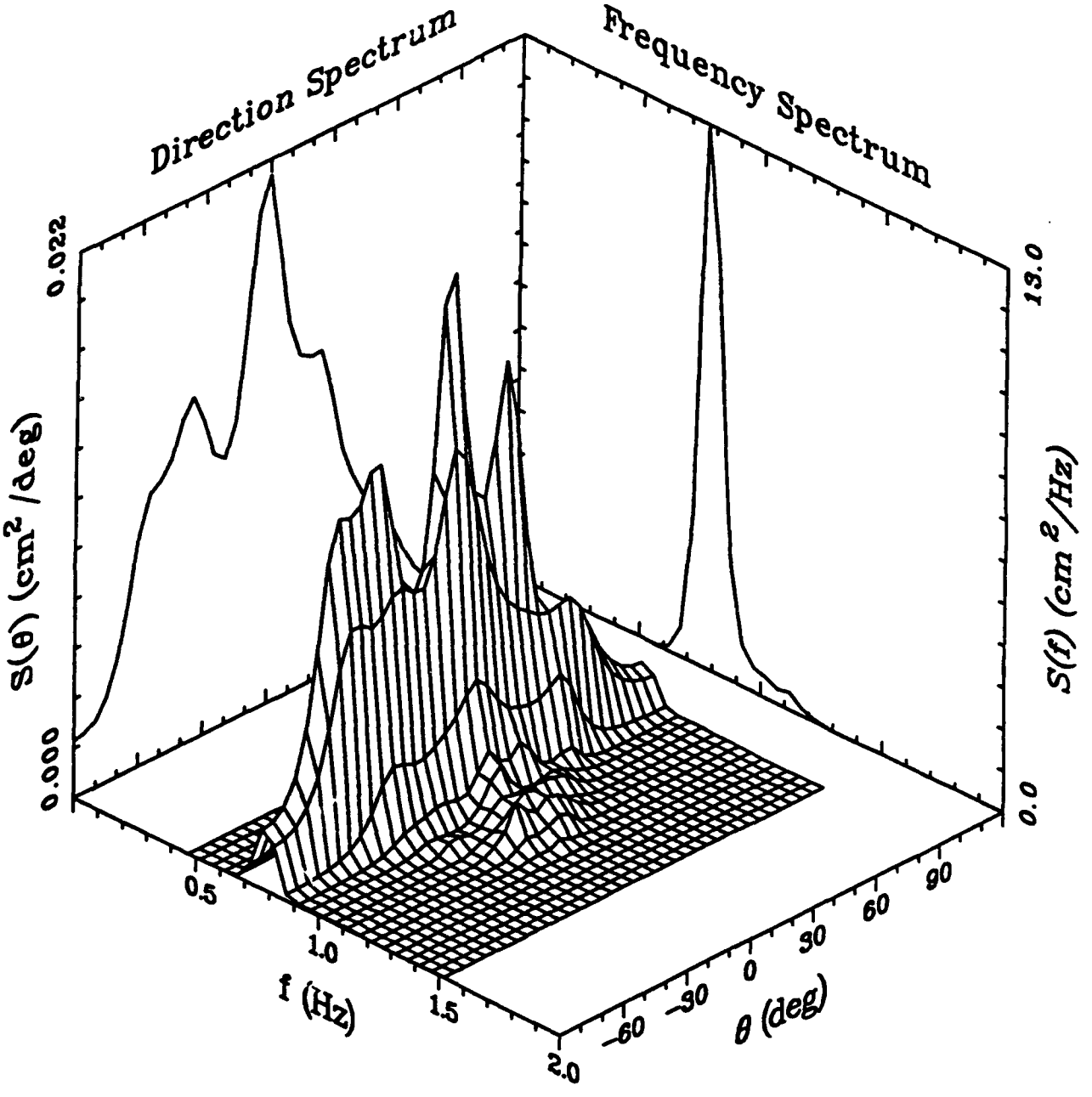

APPENDIX C: INCIDENT DIRECTIONAL SPECTRAL ENERGY DENSITY

CASE M4

INCIDENT DIRECTIONAL
SPECTRAL ENERGY DENSITY
S(F,THETA) IN cm^2/Hz/rad

WAVE DIRECTION (DEG CCW FROM POSITIVE X-AXIS)	FREQUENCY (Hz)										
	0.47	0.52	0.57	0.62	0.67	0.72	0.77	0.82	0.87	0.92	0.97
0	0.0	0.0	0.0	0.0	0.0	0.0	0.0	0.0	0.0	0.0	0.0
5	0.0	0.0	0.0	0.0	0.0	0.0	0.0	0.0	0.0	0.0	0.0
10	0.0	0.0	0.0	0.0	0.0	0.0	0.0	0.0	0.0	0.0	0.0
15	0.0	0.0	0.0	0.0	0.0	0.0	0.0	0.0	0.0	0.0	0.0
20	0.0	0.0	0.0	0.0	0.0	0.0	0.0	0.0	0.0	0.0	0.0
25	0.0	0.0	0.0	0.0	0.0	0.0	0.0	0.0	0.0	0.0	0.0
30	0.0	0.0	0.0	0.0	0.0	0.0	0.0	0.0	0.0	0.0	0.0
35	0.0	0.0	0.0	0.0	0.0	0.0	0.0	0.0	0.0	0.0	0.0
40	0.0	0.0	0.0	0.0	0.0	0.0	0.0	0.0	0.0	0.0	0.0
45	0.0	0.0	0.0	0.0	0.0	0.0	0.0	0.0	0.0	0.0	0.0
50	0.0	0.0	0.0	0.0	0.0	0.0	0.0	0.0	0.0	0.0	0.0
55	0.0	0.0	0.0	0.0	0.0	0.0	0.0	0.0	0.0	0.0	0.0
60	0.0	0.0	0.0	0.0	0.0	0.0	0.0	0.0	0.0	0.0	0.0
65	0.0	0.0	0.0	0.0	0.0	0.0	0.0	0.0	0.0	0.0	0.0
70	0.0	0.0	0.0	0.0	0.0	0.0	0.0	0.0	0.0	0.0	0.0
75	0.0	0.0	0.0	0.0	0.0	0.0	0.0	0.0	0.0	0.0	0.0
80	0.0	0.0	0.0	0.0	0.0	0.0	0.0	0.0	0.0	0.0	0.0
85	0.0	0.0	0.0	0.0	0.0	0.0	0.0	0.0	0.0	0.0	0.0
90	2.7	3.9	6.2	11.4	30.1	277.1	545.4	185.0	31.5	13.1	7.2
95	0.0	0.0	0.0	0.0	0.0	0.0	0.0	0.0	0.0	0.0	0.0
100	0.0	0.0	0.0	0.0	0.0	0.0	0.0	0.0	0.0	0.0	0.0
105	0.0	0.0	0.0	0.0	0.0	0.0	0.0	0.0	0.0	0.0	0.0
110	0.0	0.0	0.0	0.0	0.0	0.0	0.0	0.0	0.0	0.0	0.0
115	0.0	0.0	0.0	0.0	0.0	0.0	0.0	0.0	0.0	0.0	0.0
120	0.0	0.0	0.0	0.0	0.0	0.0	0.0	0.0	0.0	0.0	0.0
125	0.0	0.0	0.0	0.0	0.0	0.0	0.0	0.0	0.0	0.0	0.0
130	0.0	0.0	0.0	0.0	0.0	0.0	0.0	0.0	0.0	0.0	0.0
135	0.0	0.0	0.0	0.0	0.0	0.0	0.0	0.0	0.0	0.0	0.0
140	0.0	0.0	0.0	0.0	0.0	0.0	0.0	0.0	0.0	0.0	0.0
145	0.0	0.0	0.0	0.0	0.0	0.0	0.0	0.0	0.0	0.0	0.0
150	0.0	0.0	0.0	0.0	0.0	0.0	0.0	0.0	0.0	0.0	0.0
155	0.0	0.0	0.0	0.0	0.0	0.0	0.0	0.0	0.0	0.0	0.0
160	0.0	0.0	0.0	0.0	0.0	0.0	0.0	0.0	0.0	0.0	0.0
165	0.0	0.0	0.0	0.0	0.0	0.0	0.0	0.0	0.0	0.0	0.0
170	0.0	0.0	0.0	0.0	0.0	0.0	0.0	0.0	0.0	0.0	0.0
175	0.0	0.0	0.0	0.0	0.0	0.0	0.0	0.0	0.0	0.0	0.0
180	0.0	0.0	0.0	0.0	0.0	0.0	0.0	0.0	0.0	0.0	0.0

CASE M4

INCIDENT DIRECTIONAL
SPECTRAL ENERGY DENSITY
S(F,THETA) IN cm^2/Hz/rad

WAVE DIRECTION (DEG CCW FROM POSITIVE X-AXIS)	FREQUENCY (Hz)										
	1.02	1.07	1.12	1.17	1.22	1.27	1.32	1.37	1.42	1.47	1.52
0	0.0	0.0	0.0	0.0	0.0	0.0	0.0	0.0	0.0	0.0	0.0
5	0.0	0.0	0.0	0.0	0.0	0.0	0.0	0.0	0.0	0.0	0.0
10	0.0	0.0	0.0	0.0	0.0	0.0	0.0	0.0	0.0	0.0	0.0
15	0.0	0.0	0.0	0.0	0.0	0.0	0.0	0.0	0.0	0.0	0.0
20	0.0	0.0	0.0	0.0	0.0	0.0	0.0	0.0	0.0	0.0	0.0
25	0.0	0.0	0.0	0.0	0.0	0.0	0.0	0.0	0.0	0.0	0.0
30	0.0	0.0	0.0	0.0	0.0	0.0	0.0	0.0	0.0	0.0	0.0
35	0.0	0.0	0.0	0.0	0.0	0.0	0.0	0.0	0.0	0.0	0.0
40	0.0	0.0	0.0	0.0	0.0	0.0	0.0	0.0	0.0	0.0	0.0
45	0.0	0.0	0.0	0.0	0.0	0.0	0.0	0.0	0.0	0.0	0.0
50	0.0	0.0	0.0	0.0	0.0	0.0	0.0	0.0	0.0	0.0	0.0
55	0.0	0.0	0.0	0.0	0.0	0.0	0.0	0.0	0.0	0.0	0.0
60	0.0	0.0	0.0	0.0	0.0	0.0	0.0	0.0	0.0	0.0	0.0
65	0.0	0.0	0.0	0.0	0.0	0.0	0.0	0.0	0.0	0.0	0.0
70	0.0	0.0	0.0	0.0	0.0	0.0	0.0	0.0	0.0	0.0	0.0
75	0.0	0.0	0.0	0.0	0.0	0.0	0.0	0.0	0.0	0.0	0.0
80	0.0	0.0	0.0	0.0	0.0	0.0	0.0	0.0	0.0	0.0	0.0
85	0.0	0.0	0.0	0.0	0.0	0.0	0.0	0.0	0.0	0.0	0.0
90	4.6	3.3	2.6	1.9	1.6	1.4	1.2	1.1	1.1	1.4	1.6
95	0.0	0.0	0.0	0.0	0.0	0.0	0.0	0.0	0.0	0.0	0.0
100	0.0	0.0	0.0	0.0	0.0	0.0	0.0	0.0	0.0	0.0	0.0
105	0.0	0.0	0.0	0.0	0.0	0.0	0.0	0.0	0.0	0.0	0.0
110	0.0	0.0	0.0	0.0	0.0	0.0	0.0	0.0	0.0	0.0	0.0
115	0.0	0.0	0.0	0.0	0.0	0.0	0.0	0.0	0.0	0.0	0.0
120	0.0	0.0	0.0	0.0	0.0	0.0	0.0	0.0	0.0	0.0	0.0
125	0.0	0.0	0.0	0.0	0.0	0.0	0.0	0.0	0.0	0.0	0.0
130	0.0	0.0	0.0	0.0	0.0	0.0	0.0	0.0	0.0	0.0	0.0
135	0.0	0.0	0.0	0.0	0.0	0.0	0.0	0.0	0.0	0.0	0.0
140	0.0	0.0	0.0	0.0	0.0	0.0	0.0	0.0	0.0	0.0	0.0
145	0.0	0.0	0.0	0.0	0.0	0.0	0.0	0.0	0.0	0.0	0.0
150	0.0	0.0	0.0	0.0	0.0	0.0	0.0	0.0	0.0	0.0	0.0
155	0.0	0.0	0.0	0.0	0.0	0.0	0.0	0.0	0.0	0.0	0.0
160	0.0	0.0	0.0	0.0	0.0	0.0	0.0	0.0	0.0	0.0	0.0
165	0.0	0.0	0.0	0.0	0.0	0.0	0.0	0.0	0.0	0.0	0.0
170	0.0	0.0	0.0	0.0	0.0	0.0	0.0	0.0	0.0	0.0	0.0
175	0.0	0.0	0.0	0.0	0.0	0.0	0.0	0.0	0.0	0.0	0.0
180	0.0	0.0	0.0	0.0	0.0	0.0	0.0	0.0	0.0	0.0	0.0

CASE N1

INCIDENT DIRECTIONAL SPECTRAL ENERGY DENSITY S(F,THETA) IN cm^2/Hz/rad

WAVE DIRECTION (DEG CCW FROM POSITIVE X-AXIS)	FREQUENCY (Hz)										
	0.47	0.52	0.57	0.62	0.67	0.72	0.77	0.82	0.87	0.92	0.97
0	0.0	0.0	0.0	0.0	0.0	0.0	0.0	0.0	0.0	0.0	0.0
5	0.0	0.0	0.0	0.0	0.0	0.0	0.0	0.0	0.0	0.0	0.0
10	0.0	0.0	0.0	0.0	0.0	0.0	0.0	0.0	0.0	0.0	0.0
15	0.0	0.0	0.0	0.0	0.0	0.0	0.0	0.0	0.0	0.0	0.0
20	0.0	0.0	0.0	0.0	0.0	0.0	0.0	0.0	0.0	0.0	0.0
25	0.0	0.0	0.0	0.0	0.0	0.0	0.0	0.0	0.0	0.0	0.0
30	0.0	0.0	0.0	0.0	0.0	0.0	0.0	0.0	0.0	0.0	0.0
35	0.0	0.0	0.0	0.0	0.0	0.0	0.0	0.0	0.0	0.0	0.0
40	0.0	0.0	0.0	0.0	0.0	0.0	0.0	0.0	0.0	0.0	0.0
45	0.0	0.0	0.0	0.0	0.0	0.0	0.0	0.0	0.0	0.0	0.0
50	0.0	0.0	0.0	0.0	0.0	0.0	0.0	0.0	0.0	0.0	0.0
55	0.0	0.0	0.0	0.0	0.0	0.0	0.0	0.0	0.0	0.0	0.0
60	0.0	0.0	0.0	0.0	0.1	0.1	0.2	0.2	0.2	0.2	0.1
65	0.0	0.0	0.0	0.1	0.2	0.5	0.8	0.7	0.7	0.6	0.5
70	0.0	0.0	0.1	0.2	0.6	1.5	2.4	2.2	2.2	1.8	1.6
75	0.0	0.1	0.2	0.5	1.5	3.6	5.8	5.3	5.3	4.4	3.8
80	0.0	0.1	0.5	1.0	2.8	6.8	10.9	9.9	9.9	8.2	7.0
85	0.0	0.1	0.7	1.4	4.0	9.9	15.9	14.4	14.5	11.9	10.2
90	0.0	0.2	0.8	1.6	4.5	11.2	18.0	16.4	16.4	13.5	11.6
95	0.0	0.1	0.7	1.4	4.0	9.9	15.9	14.4	14.5	11.9	10.2
100	0.0	0.1	0.5	1.0	2.8	6.8	10.9	9.9	9.9	8.2	7.0
105	0.0	0.1	0.2	0.5	1.5	3.6	5.8	5.3	5.3	4.4	3.8
110	0.0	0.0	0.1	0.2	0.6	1.5	2.4	2.2	2.2	1.8	1.6
115	0.0	0.0	0.0	0.1	0.2	0.5	0.8	0.7	0.7	0.6	0.5
120	0.0	0.0	0.0	0.0	0.1	0.1	0.2	0.2	0.2	0.2	0.1
125	0.0	0.0	0.0	0.0	0.0	0.0	0.0	0.0	0.0	0.0	0.0
130	0.0	0.0	0.0	0.0	0.0	0.0	0.0	0.0	0.0	0.0	0.0
135	0.0	0.0	0.0	0.0	0.0	0.0	0.0	0.0	0.0	0.0	0.0
140	0.0	0.0	0.0	0.0	0.0	0.0	0.0	0.0	0.0	0.0	0.0
145	0.0	0.0	0.0	0.0	0.0	0.0	0.0	0.0	0.0	0.0	0.0
150	0.0	0.0	0.0	0.0	0.0	0.0	0.0	0.0	0.0	0.0	0.0
155	0.0	0.0	0.0	0.0	0.0	0.0	0.0	0.0	0.0	0.0	0.0
160	0.0	0.0	0.0	0.0	0.0	0.0	0.0	0.0	0.0	0.0	0.0
165	0.0	0.0	0.0	0.0	0.0	0.0	0.0	0.0	0.0	0.0	0.0
170	0.0	0.0	0.0	0.0	0.0	0.0	0.0	0.0	0.0	0.0	0.0
175	0.0	0.0	0.0	0.0	0.0	0.0	0.0	0.0	0.0	0.0	0.0
180	0.0	0.0	0.0	0.0	0.0	0.0	0.0	0.0	0.0	0.0	0.0

CASE N1

INCIDENT DIRECTIONAL SPECTRAL ENERGY DENSITY S(F,THETA) IN cm^2/Hz/rad

WAVE DIRECTION (DEG CCW FROM POSITIVE X-AXIS)	FREQUENCY (Hz)										
	1.02	1.07	1.12	1.17	1.22	1.27	1.32	1.37	1.42	1.47	1.52
0	0.0	0.0	0.0	0.0	0.0	0.0	0.0	0.0	0.0	0.0	0.0
5	0.0	0.0	0.0	0.0	0.0	0.0	0.0	0.0	0.0	0.0	0.0
10	0.0	0.0	0.0	0.0	0.0	0.0	0.0	0.0	0.0	0.0	0.0
15	0.0	0.0	0.0	0.0	0.0	0.0	0.0	0.0	0.0	0.0	0.0
20	0.0	0.0	0.0	0.0	0.0	0.0	0.0	0.0	0.0	0.0	0.0
25	0.0	0.0	0.0	0.0	0.0	0.0	0.0	0.0	0.0	0.0	0.0
30	0.0	0.0	0.0	0.0	0.0	0.0	0.0	0.0	0.0	0.0	0.0
35	0.0	0.0	0.0	0.0	0.0	0.0	0.0	0.0	0.0	0.0	0.0
40	0.0	0.0	0.0	0.0	0.0	0.0	0.0	0.0	0.0	0.0	0.0
45	0.0	0.0	0.0	0.0	0.0	0.0	0.0	0.0	0.0	0.0	0.0
50	0.0	0.0	0.0	0.0	0.0	0.0	0.0	0.0	0.0	0.0	0.0
55	0.0	0.0	0.0	0.0	0.0	0.0	0.0	0.0	0.0	0.0	0.0
60	0.1	0.1	0.1	0.1	0.1	0.0	0.0	0.0	0.0	0.0	0.0
65	0.4	0.4	0.5	0.3	0.2	0.1	0.1	0.0	0.0	0.0	0.0
70	1.3	1.3	1.6	1.0	0.7	0.4	0.2	0.1	0.0	0.0	0.0
75	3.2	3.1	3.7	2.4	1.8	0.9	0.4	0.2	0.1	0.0	0.0
80	5.9	5.8	7.0	4.6	3.3	1.7	0.8	0.4	0.2	0.1	0.1
85	8.6	8.4	10.2	6.6	4.8	2.5	1.2	0.5	0.3	0.1	0.1
90	9.7	9.6	11.5	7.5	5.4	2.8	1.4	0.6	0.3	0.1	0.1
95	8.6	8.4	10.2	6.6	4.8	2.5	1.2	0.5	0.3	0.1	0.1
100	5.9	5.8	7.0	4.6	3.3	1.7	0.8	0.4	0.2	0.1	0.1
105	3.2	3.1	3.7	2.4	1.8	0.9	0.4	0.2	0.1	0.0	0.0
110	1.3	1.3	1.6	1.0	0.7	0.4	0.2	0.1	0.0	0.0	0.0
115	0.4	0.4	0.5	0.3	0.2	0.1	0.1	0.0	0.0	0.0	0.0
120	0.1	0.1	0.1	0.1	0.1	0.0	0.0	0.0	0.0	0.0	0.0
125	0.0	0.0	0.0	0.0	0.0	0.0	0.0	0.0	0.0	0.0	0.0
130	0.0	0.0	0.0	0.0	0.0	0.0	0.0	0.0	0.0	0.0	0.0
135	0.0	0.0	0.0	0.0	0.0	0.0	0.0	0.0	0.0	0.0	0.0
140	0.0	0.0	0.0	0.0	0.0	0.0	0.0	0.0	0.0	0.0	0.0
145	0.0	0.0	0.0	0.0	0.0	0.0	0.0	0.0	0.0	0.0	0.0
150	0.0	0.0	0.0	0.0	0.0	0.0	0.0	0.0	0.0	0.0	0.0
155	0.0	0.0	0.0	0.0	0.0	0.0	0.0	0.0	0.0	0.0	0.0
160	0.0	0.0	0.0	0.0	0.0	0.0	0.0	0.0	0.0	0.0	0.0
165	0.0	0.0	0.0	0.0	0.0	0.0	0.0	0.0	0.0	0.0	0.0
170	0.0	0.0	0.0	0.0	0.0	0.0	0.0	0.0	0.0	0.0	0.0
175	0.0	0.0	0.0	0.0	0.0	0.0	0.0	0.0	0.0	0.0	0.0
180	0.0	0.0	0.0	0.0	0.0	0.0	0.0	0.0	0.0	0.0	0.0

CASE N2

INCIDENT DIRECTIONAL
SPECTRAL ENERGY DENSITY
S(F,THETA) IN cm^2/Hz/rad

WAVE DIRECTION (DEG CCW FROM POSITIVE X-AXIS)	FREQUENCY (Hz)										
	0.47	0.52	0.57	0.62	0.67	0.72	0.77	0.82	0.87	0.92	0.97
0	0.0	0.0	0.0	0.0	0.0	0.0	0.0	0.0	0.0	0.0	0.0
5	0.0	0.0	0.0	0.0	0.0	0.0	0.0	0.0	0.0	0.0	0.0
10	0.0	0.0	0.0	0.0	0.0	0.0	0.0	0.0	0.0	0.0	0.0
15	0.0	0.0	0.0	0.0	0.0	0.0	0.0	0.0	0.0	0.0	0.0
20	0.0	0.0	0.0	0.0	0.0	0.0	0.0	0.0	0.0	0.0	0.0
25	0.0	0.0	0.0	0.0	0.0	0.0	0.0	0.0	0.0	0.0	0.0
30	0.0	0.0	0.0	0.0	0.0	0.0	0.0	0.0	0.0	0.0	0.0
35	0.0	0.0	0.0	0.0	0.0	0.0	0.0	0.0	0.0	0.0	0.0
40	0.0	0.0	0.0	0.0	0.0	0.0	0.0	0.0	0.0	0.0	0.0
45	0.0	0.0	0.0	0.0	0.0	0.0	0.0	0.0	0.0	0.0	0.0
50	0.0	0.0	0.0	0.0	0.0	0.0	0.0	0.0	0.0	0.0	0.0
55	0.0	0.0	0.0	0.0	0.0	0.0	0.1	0.1	0.0	0.0	0.0
60	0.0	0.0	0.0	0.0	0.0	0.2	0.6	0.5	0.1	0.1	0.0
65	0.0	0.0	0.0	0.1	0.1	0.7	2.2	1.9	0.6	0.2	0.1
70	0.0	0.0	0.0	0.2	0.3	2.2	6.7	5.8	1.7	0.7	0.5
75	0.0	0.0	0.0	0.4	0.8	5.4	16.1	14.0	4.1	1.8	1.1
80	0.0	0.0	0.1	0.7	1.4	10.0	30.1	26.1	7.7	3.3	2.0
85	0.0	0.0	0.1	1.1	2.0	14.6	43.7	38.0	11.2	4.8	3.0
90	0.0	0.0	0.1	1.2	2.3	16.6	49.6	43.0	12.7	5.4	3.4
95	0.0	0.0	0.1	1.1	2.0	14.6	43.7	38.0	11.2	4.8	3.0
100	0.0	0.0	0.1	0.7	1.4	10.0	30.1	26.1	7.7	3.3	2.0
105	0.0	0.0	0.0	0.4	0.8	5.4	16.1	14.0	4.1	1.8	1.1
110	0.0	0.0	0.0	0.2	0.3	2.2	6.7	5.8	1.7	0.7	0.5
115	0.0	0.0	0.0	0.1	0.1	0.7	2.2	1.9	0.6	0.2	0.1
120	0.0	0.0	0.0	0.0	0.0	0.2	0.6	0.5	0.1	0.1	0.0
125	0.0	0.0	0.0	0.0	0.0	0.0	0.1	0.1	0.0	0.0	0.0
130	0.0	0.0	0.0	0.0	0.0	0.0	0.0	0.0	0.0	0.0	0.0
135	0.0	0.0	0.0	0.0	0.0	0.0	0.0	0.0	0.0	0.0	0.0
140	0.0	0.0	0.0	0.0	0.0	0.0	0.0	0.0	0.0	0.0	0.0
145	0.0	0.0	0.0	0.0	0.0	0.0	0.0	0.0	0.0	0.0	0.0
150	0.0	0.0	0.0	0.0	0.0	0.0	0.0	0.0	0.0	0.0	0.0
155	0.0	0.0	0.0	0.0	0.0	0.0	0.0	0.0	0.0	0.0	0.0
160	0.0	0.0	0.0	0.0	0.0	0.0	0.0	0.0	0.0	0.0	0.0
165	0.0	0.0	0.0	0.0	0.0	0.0	0.0	0.0	0.0	0.0	0.0
170	0.0	0.0	0.0	0.0	0.0	0.0	0.0	0.0	0.0	0.0	0.0
175	0.0	0.0	0.0	0.0	0.0	0.0	0.0	0.0	0.0	0.0	0.0
180	0.0	0.0	0.0	0.0	0.0	0.0	0.0	0.0	0.0	0.0	0.0

CASE N2

INCIDENT DIRECTIONAL
SPECTRAL ENERGY DENSITY
S(F,THETA) IN cm^2/Hz/rad

WAVE DIRECTION (DEG CCW FROM POSITIVE X-AXIS)	FREQUENCY (Hz)										
	1.02	1.07	1.12	1.17	1.22	1.27	1.32	1.37	1.42	1.47	1.52
0	0.0	0.0	0.0	0.0	0.0	0.0	0.0	0.0	0.0	0.0	0.0
5	0.0	0.0	0.0	0.0	0.0	0.0	0.0	0.0	0.0	0.0	0.0
10	0.0	0.0	0.0	0.0	0.0	0.0	0.0	0.0	0.0	0.0	0.0
15	0.0	0.0	0.0	0.0	0.0	0.0	0.0	0.0	0.0	0.0	0.0
20	0.0	0.0	0.0	0.0	0.0	0.0	0.0	0.0	0.0	0.0	0.0
25	0.0	0.0	0.0	0.0	0.0	0.0	0.0	0.0	0.0	0.0	0.0
30	0.0	0.0	0.0	0.0	0.0	0.0	0.0	0.0	0.0	0.0	0.0
35	0.0	0.0	0.0	0.0	0.0	0.0	0.0	0.0	0.0	0.0	0.0
40	0.0	0.0	0.0	0.0	0.0	0.0	0.0	0.0	0.0	0.0	0.0
45	0.0	0.0	0.0	0.0	0.0	0.0	0.0	0.0	0.0	0.0	0.0
50	0.0	0.0	0.0	0.0	0.0	0.0	0.0	0.0	0.0	0.0	0.0
55	0.0	0.0	0.0	0.0	0.0	0.0	0.0	0.0	0.0	0.0	0.0
60	0.0	0.0	0.0	0.0	0.0	0.0	0.0	0.0	0.0	0.0	0.0
65	0.1	0.1	0.1	0.1	0.1	0.0	0.0	0.0	0.0	0.0	0.0
70	0.4	0.4	0.4	0.3	0.2	0.1	0.1	0.0	0.0	0.0	0.0
75	1.0	0.8	0.9	0.7	0.5	0.3	0.1	0.0	0.0	0.0	0.0
80	1.9	1.6	1.7	1.2	0.9	0.5	0.2	0.1	0.0	0.1	0.1
85	2.7	2.3	2.4	1.8	1.2	0.8	0.3	0.1	0.0	0.1	0.1
90	3.1	2.6	2.8	2.0	1.4	0.9	0.4	0.1	0.0	0.1	0.1
95	2.7	2.3	2.4	1.8	1.2	0.8	0.3	0.1	0.0	0.1	0.1
100	1.9	1.6	1.7	1.2	0.9	0.5	0.2	0.1	0.0	0.1	0.1
105	1.0	0.8	0.9	0.7	0.5	0.3	0.1	0.0	0.0	0.0	0.0
110	0.4	0.4	0.4	0.3	0.2	0.1	0.1	0.0	0.0	0.0	0.0
115	0.1	0.1	0.1	0.1	0.1	0.0	0.0	0.0	0.0	0.0	0.0
120	0.0	0.0	0.0	0.0	0.0	0.0	0.0	0.0	0.0	0.0	0.0
125	0.0	0.0	0.0	0.0	0.0	0.0	0.0	0.0	0.0	0.0	0.0
130	0.0	0.0	0.0	0.0	0.0	0.0	0.0	0.0	0.0	0.0	0.0
135	0.0	0.0	0.0	0.0	0.0	0.0	0.0	0.0	0.0	0.0	0.0
140	0.0	0.0	0.0	0.0	0.0	0.0	0.0	0.0	0.0	0.0	0.0
145	0.0	0.0	0.0	0.0	0.0	0.0	0.0	0.0	0.0	0.0	0.0
150	0.0	0.0	0.0	0.0	0.0	0.0	0.0	0.0	0.0	0.0	0.0
155	0.0	0.0	0.0	0.0	0.0	0.0	0.0	0.0	0.0	0.0	0.0
160	0.0	0.0	0.0	0.0	0.0	0.0	0.0	0.0	0.0	0.0	0.0
165	0.0	0.0	0.0	0.0	0.0	0.0	0.0	0.0	0.0	0.0	0.0
170	0.0	0.0	0.0	0.0	0.0	0.0	0.0	0.0	0.0	0.0	0.0
175	0.0	0.0	0.0	0.0	0.0	0.0	0.0	0.0	0.0	0.0	0.0
180	0.0	0.0	0.0	0.0	0.0	0.0	0.0	0.0	0.0	0.0	0.0

CASE B1

INCIDENT DIRECTIONAL SPECTRAL ENERGY DENSITY S(F,THETA) IN cm^2/Hz/rad

WAVE DIRECTION (DEG CCW FROM POSITIVE X-AXIS)	FREQUENCY (Hz)										
	0.47	0.52	0.57	0.62	0.67	0.72	0.77	0.82	0.87	0.92	0.97
0	0.0	0.0	0.0	0.0	0.0	0.0	0.1	0.1	0.1	0.0	0.0
5	0.0	0.0	0.0	0.0	0.0	0.1	0.1	0.1	0.1	0.1	0.1
10	0.0	0.0	0.0	0.0	0.0	0.1	0.2	0.2	0.2	0.1	0.1
15	0.0	0.0	0.0	0.0	0.1	0.2	0.3	0.3	0.3	0.2	0.1
20	0.0	0.0	0.0	0.0	0.1	0.3	0.4	0.5	0.5	0.3	0.2
25	0.0	0.0	0.0	0.0	0.1	0.4	0.6	0.7	0.7	0.4	0.3
30	0.0	0.0	0.0	0.1	0.2	0.5	0.9	1.0	1.0	0.5	0.4
35	0.0	0.0	0.0	0.1	0.2	0.7	1.2	1.4	1.4	0.7	0.6
40	0.0	0.0	0.0	0.1	0.3	1.0	1.6	1.9	1.8	1.0	0.8
45	0.0	0.0	0.0	0.1	0.4	1.3	2.1	2.4	2.4	1.3	1.0
50	0.0	0.0	0.1	0.2	0.5	1.7	2.6	3.1	3.0	1.6	1.3
55	0.0	0.0	0.1	0.2	0.6	2.0	3.2	3.8	3.7	2.0	1.6
60	0.0	0.0	0.1	0.3	0.7	2.4	3.9	4.6	4.4	2.4	1.9
65	0.0	0.0	0.1	0.3	0.8	2.8	4.5	5.3	5.1	2.8	2.3
70	0.0	0.0	0.1	0.4	0.9	3.2	5.1	6.0	5.8	3.2	2.6
75	0.0	0.0	0.1	0.4	1.0	3.5	5.6	6.6	6.4	3.5	2.8
80	0.0	0.0	0.1	0.4	1.1	3.8	6.0	7.1	6.9	3.8	3.0
85	0.0	0.0	0.1	0.4	1.2	4.0	6.3	7.4	7.2	3.9	3.2
90	0.0	0.0	0.1	0.4	1.2	4.0	6.4	7.5	7.3	4.0	3.2
95	0.0	0.0	0.1	0.4	1.2	4.0	6.3	7.4	7.2	3.9	3.2
100	0.0	0.0	0.1	0.4	1.1	3.8	6.0	7.1	6.9	3.8	3.0
105	0.0	0.0	0.1	0.4	1.0	3.5	5.6	6.6	6.4	3.5	2.8
110	0.0	0.0	0.1	0.4	0.9	3.2	5.1	6.0	5.8	3.2	2.6
115	0.0	0.0	0.1	0.3	0.8	2.8	4.5	5.3	5.1	2.8	2.3
120	0.0	0.0	0.1	0.3	0.7	2.4	3.9	4.6	4.4	2.4	1.9
125	0.0	0.0	0.1	0.2	0.6	2.0	3.2	3.8	3.7	2.0	1.6
130	0.0	0.0	0.1	0.2	0.5	1.7	2.6	3.1	3.0	1.6	1.3
135	0.0	0.0	0.0	0.1	0.4	1.3	2.1	2.4	2.4	1.3	1.0
140	0.0	0.0	0.0	0.1	0.3	1.0	1.6	1.9	1.8	1.0	0.8
145	0.0	0.0	0.0	0.1	0.2	0.7	1.2	1.4	1.4	0.7	0.6
150	0.0	0.0	0.0	0.1	0.2	0.5	0.9	1.0	1.0	0.5	0.4
155	0.0	0.0	0.0	0.0	0.1	0.4	0.6	0.7	0.7	0.4	0.3
160	0.0	0.0	0.0	0.0	0.1	0.3	0.4	0.5	0.5	0.3	0.2
165	0.0	0.0	0.0	0.0	0.1	0.2	0.3	0.3	0.3	0.2	0.1
170	0.0	0.0	0.0	0.0	0.0	0.1	0.2	0.2	0.2	0.1	0.1
175	0.0	0.0	0.0	0.0	0.0	0.1	0.1	0.1	0.1	0.1	0.1
180	0.0	0.0	0.0	0.0	0.0	0.0	0.1	0.1	0.1	0.0	0.0

CASE B1

INCIDENT DIRECTIONAL SPECTRAL ENERGY DENSITY S(F,THETA) IN cm^2/Hz/rad

WAVE DIRECTION (DEG CCW FROM POSITIVE X-AXIS)	FREQUENCY (Hz)										
	1.02	1.07	1.12	1.17	1.22	1.27	1.32	1.37	1.42	1.47	1.52
0	0.0	0.0	0.0	0.0	0.0	0.0	0.0	0.0	0.0	0.0	0.0
5	0.1	0.0	0.1	0.0	0.0	0.0	0.0	0.0	0.0	0.0	0.0
10	0.1	0.1	0.1	0.1	0.0	0.0	0.0	0.0	0.0	0.0	0.0
15	0.1	0.1	0.2	0.1	0.1	0.0	0.0	0.0	0.0	0.0	0.0
20	0.2	0.2	0.2	0.2	0.1	0.1	0.0	0.0	0.0	0.0	0.0
25	0.3	0.3	0.3	0.2	0.1	0.1	0.0	0.0	0.0	0.0	0.0
30	0.4	0.4	0.5	0.3	0.2	0.1	0.1	0.0	0.0	0.0	0.0
35	0.6	0.5	0.7	0.4	0.3	0.2	0.1	0.0	0.0	0.0	0.0
40	0.8	0.7	0.9	0.6	0.4	0.2	0.1	0.0	0.0	0.0	0.0
45	1.1	0.9	1.1	0.8	0.5	0.3	0.1	0.1	0.0	0.0	0.0
50	1.4	1.1	1.4	1.0	0.6	0.4	0.2	0.1	0.0	0.0	0.0
55	1.7	1.4	1.8	1.2	0.7	0.5	0.2	0.1	0.0	0.0	0.0
60	2.0	1.6	2.1	1.4	0.9	0.5	0.3	0.1	0.0	0.0	0.0
65	2.3	1.9	2.5	1.6	1.0	0.6	0.3	0.1	0.0	0.0	0.0
70	2.6	2.2	2.8	1.9	1.1	0.7	0.3	0.1	0.0	0.0	0.0
75	2.9	2.4	3.1	2.1	1.2	0.8	0.4	0.1	0.0	0.0	0.0
80	3.1	2.6	3.3	2.2	1.3	0.8	0.4	0.2	0.0	0.0	0.0
85	3.2	2.7	3.5	2.3	1.4	0.9	0.4	0.2	0.0	0.0	0.0
90	3.3	2.7	3.5	2.3	1.4	0.9	0.4	0.2	0.0	0.0	0.0
95	3.2	2.7	3.5	2.3	1.4	0.9	0.4	0.2	0.0	0.0	0.0
100	3.1	2.6	3.3	2.2	1.3	0.8	0.4	0.2	0.0	0.0	0.0
105	2.9	2.4	3.1	2.1	1.2	0.8	0.4	0.1	0.0	0.0	0.0
110	2.6	2.2	2.8	1.9	1.1	0.7	0.3	0.1	0.0	0.0	0.0
115	2.3	1.9	2.5	1.6	1.0	0.6	0.3	0.1	0.0	0.0	0.0
120	2.0	1.6	2.1	1.4	0.9	0.5	0.3	0.1	0.0	0.0	0.0
125	1.7	1.4	1.8	1.2	0.7	0.5	0.2	0.1	0.0	0.0	0.0
130	1.4	1.1	1.4	1.0	0.6	0.4	0.2	0.1	0.0	0.0	0.0
135	1.1	0.9	1.1	0.8	0.5	0.3	0.1	0.1	0.0	0.0	0.0
140	0.8	0.7	0.9	0.6	0.4	0.2	0.1	0.0	0.0	0.0	0.0
145	0.6	0.5	0.7	0.4	0.3	0.2	0.1	0.0	0.0	0.0	0.0
150	0.4	0.4	0.5	0.3	0.2	0.1	0.1	0.0	0.0	0.0	0.0
155	0.3	0.3	0.3	0.2	0.1	0.1	0.0	0.0	0.0	0.0	0.0
160	0.2	0.2	0.2	0.2	0.1	0.1	0.0	0.0	0.0	0.0	0.0
165	0.1	0.1	0.2	0.1	0.1	0.0	0.0	0.0	0.0	0.0	0.0
170	0.1	0.1	0.1	0.1	0.0	0.0	0.0	0.0	0.0	0.0	0.0
175	0.1	0.0	0.1	0.0	0.0	0.0	0.0	0.0	0.0	0.0	0.0
180	0.0	0.0	0.0	0.0	0.0	0.0	0.0	0.0	0.0	0.0	0.0

CASE B2

INCIDENT DIRECTIONAL
SPECTRAL ENERGY DENSITY
S(F,THETA) IN cm^2/Hz/rad

WAVE DIRECTION (DEG CCW FROM POSITIVE X-AXIS)	FREQUENCY (Hz)										
	0.47	0.52	0.57	0.62	0.67	0.72	0.77	0.82	0.87	0.92	0.97
0	0.0	0.0	0.0	0.0	0.0	0.1	0.2	0.2	0.1	0.0	0.0
5	0.0	0.0	0.0	0.0	0.0	0.1	0.4	0.3	0.1	0.0	0.0
10	0.0	0.0	0.0	0.0	0.0	0.2	0.6	0.4	0.1	0.0	0.0
15	0.0	0.0	0.0	0.0	0.0	0.2	0.9	0.6	0.2	0.1	0.0
20	0.0	0.0	0.0	0.0	0.1	0.4	1.3	1.0	0.3	0.1	0.1
25	0.0	0.0	0.0	0.0	0.1	0.5	1.9	1.4	0.4	0.1	0.1
30	0.0	0.0	0.0	0.0	0.1	0.7	2.7	2.0	0.6	0.2	0.1
35	0.0	0.0	0.0	0.0	0.2	1.0	3.7	2.7	0.9	0.3	0.2
40	0.0	0.0	0.0	0.0	0.3	1.4	4.9	3.6	1.1	0.4	0.2
45	0.0	0.0	0.0	0.1	0.3	1.8	6.4	4.7	1.5	0.5	0.3
50	0.0	0.0	0.0	0.1	0.4	2.2	8.1	5.9	1.9	0.6	0.4
55	0.0	0.0	0.0	0.1	0.5	2.8	9.9	7.3	2.3	0.8	0.5
60	0.0	0.0	0.0	0.1	0.6	3.3	11.9	8.8	2.8	0.9	0.5
65	0.0	0.0	0.0	0.1	0.8	3.9	13.9	10.2	3.2	1.1	0.6
70	0.0	0.0	0.0	0.1	0.9	4.4	15.7	11.6	3.7	1.2	0.7
75	0.0	0.0	0.0	0.1	0.9	4.8	17.3	12.8	4.0	1.4	0.8
80	0.0	0.0	0.0	0.1	1.0	5.2	18.6	13.7	4.3	1.5	0.8
85	0.0	0.0	0.0	0.2	1.1	5.4	19.3	14.3	4.5	1.5	0.9
90	0.0	0.0	0.0	0.2	1.1	5.5	19.6	14.5	4.6	1.5	0.9
95	0.0	0.0	0.0	0.2	1.1	5.4	19.3	14.3	4.5	1.5	0.9
100	0.0	0.0	0.0	0.1	1.0	5.2	18.6	13.7	4.3	1.5	0.8
105	0.0	0.0	0.0	0.1	0.9	4.8	17.3	12.8	4.0	1.4	0.8
110	0.0	0.0	0.0	0.1	0.9	4.4	15.7	11.6	3.7	1.2	0.7
115	0.0	0.0	0.0	0.1	0.8	3.9	13.9	10.2	3.2	1.1	0.6
120	0.0	0.0	0.0	0.1	0.6	3.3	11.9	8.8	2.8	0.9	0.5
125	0.0	0.0	0.0	0.1	0.5	2.8	9.9	7.3	2.3	0.8	0.5
130	0.0	0.0	0.0	0.1	0.4	2.2	8.1	5.9	1.9	0.6	0.4
135	0.0	0.0	0.0	0.1	0.3	1.8	6.4	4.7	1.5	0.5	0.3
140	0.0	0.0	0.0	0.0	0.3	1.4	4.9	3.6	1.1	0.4	0.2
145	0.0	0.0	0.0	0.0	0.2	1.0	3.7	2.7	0.9	0.3	0.2
150	0.0	0.0	0.0	0.0	0.1	0.7	2.7	2.0	0.6	0.2	0.1
155	0.0	0.0	0.0	0.0	0.1	0.5	1.9	1.4	0.4	0.1	0.1
160	0.0	0.0	0.0	0.0	0.1	0.4	1.3	1.0	0.3	0.1	0.1
165	0.0	0.0	0.0	0.0	0.0	0.2	0.9	0.6	0.2	0.1	0.0
170	0.0	0.0	0.0	0.0	0.0	0.2	0.6	0.4	0.1	0.0	0.0
175	0.0	0.0	0.0	0.0	0.0	0.1	0.4	0.3	0.1	0.0	0.0
180	0.0	0.0	0.0	0.0	0.0	0.1	0.2	0.2	0.1	0.0	0.0

CASE B2

INCIDENT DIRECTIONAL
SPECTRAL ENERGY DENSITY
S(F,THETA) IN cm^2/Hz/rad

WAVE DIRECTION (DEG CCW FROM POSITIVE X-AXIS)	FREQUENCY (Hz)										
	1.02	1.07	1.12	1.17	1.22	1.27	1.32	1.37	1.42	1.47	1.52
0	0.0	0.0	0.0	0.0	0.0	0.0	0.0	0.0	0.0	0.0	0.0
5	0.0	0.0	0.0	0.0	0.0	0.0	0.0	0.0	0.0	0.0	0.0
10	0.0	0.0	0.0	0.0	0.0	0.0	0.0	0.0	0.0	0.0	0.0
15	0.0	0.0	0.0	0.0	0.0	0.0	0.0	0.0	0.0	0.0	0.0
20	0.1	0.0	0.0	0.0	0.0	0.0	0.0	0.0	0.0	0.0	0.0
25	0.1	0.1	0.1	0.0	0.0	0.0	0.0	0.0	0.0	0.0	0.0
30	0.1	0.1	0.1	0.0	0.0	0.0	0.0	0.0	0.0	0.0	0.0
35	0.1	0.1	0.1	0.1	0.0	0.0	0.0	0.0	0.0	0.0	0.0
40	0.2	0.1	0.2	0.1	0.0	0.0	0.0	0.0	0.0	0.0	0.0
45	0.3	0.2	0.2	0.1	0.0	0.0	0.0	0.0	0.0	0.0	0.0
50	0.3	0.2	0.3	0.1	0.0	0.0	0.0	0.0	0.0	0.0	0.0
55	0.4	0.3	0.3	0.1	0.0	0.0	0.0	0.0	0.0	0.0	0.0
60	0.5	0.3	0.4	0.2	0.0	0.0	0.0	0.0	0.0	0.0	0.0
65	0.5	0.4	0.4	0.2	0.1	0.0	0.0	0.0	0.0	0.0	0.0
70	0.6	0.4	0.5	0.2	0.1	0.0	0.0	0.0	0.0	0.0	0.0
75	0.7	0.5	0.6	0.2	0.1	0.0	0.0	0.0	0.0	0.0	0.0
80	0.7	0.5	0.6	0.3	0.1	0.0	0.0	0.0	0.0	0.0	0.0
85	0.8	0.5	0.6	0.3	0.1	0.0	0.0	0.0	0.0	0.0	0.0
90	0.8	0.5	0.6	0.3	0.1	0.0	0.0	0.0	0.0	0.0	0.0
95	0.8	0.5	0.6	0.3	0.1	0.0	0.0	0.0	0.0	0.0	0.0
100	0.7	0.5	0.6	0.3	0.1	0.0	0.0	0.0	0.0	0.0	0.0
105	0.7	0.5	0.6	0.2	0.1	0.0	0.0	0.0	0.0	0.0	0.0
110	0.6	0.4	0.5	0.2	0.1	0.0	0.0	0.0	0.0	0.0	0.0
115	0.5	0.4	0.4	0.2	0.1	0.0	0.0	0.0	0.0	0.0	0.0
120	0.5	0.3	0.4	0.2	0.0	0.0	0.0	0.0	0.0	0.0	0.0
125	0.4	0.3	0.3	0.1	0.0	0.0	0.0	0.0	0.0	0.0	0.0
130	0.3	0.2	0.3	0.1	0.0	0.0	0.0	0.0	0.0	0.0	0.0
135	0.3	0.2	0.2	0.1	0.0	0.0	0.0	0.0	0.0	0.0	0.0
140	0.2	0.1	0.2	0.1	0.0	0.0	0.0	0.0	0.0	0.0	0.0
145	0.1	0.1	0.1	0.1	0.0	0.0	0.0	0.0	0.0	0.0	0.0
150	0.1	0.1	0.1	0.0	0.0	0.0	0.0	0.0	0.0	0.0	0.0
155	0.1	0.1	0.1	0.0	0.0	0.0	0.0	0.0	0.0	0.0	0.0
160	0.1	0.0	0.0	0.0	0.0	0.0	0.0	0.0	0.0	0.0	0.0
165	0.0	0.0	0.0	0.0	0.0	0.0	0.0	0.0	0.0	0.0	0.0
170	0.0	0.0	0.0	0.0	0.0	0.0	0.0	0.0	0.0	0.0	0.0
175	0.0	0.0	0.0	0.0	0.0	0.0	0.0	0.0	0.0	0.0	0.0
180	0.0	0.0	0.0	0.0	0.0	0.0	0.0	0.0	0.0	0.0	0.0

APPENDIX D: SPECTRAL DIFFRACTION COEFFICIENTS

CASE M4

ARRAY ANGLE DEG	GAGE NO.	|X/Lp|	|Y/Lp|	SPECTRAL DIFFRACTION COEFFICIENTS	
				MEASURED	PREDICTED
30	1	0.29	0.17	0.34	0.38
30	2	0.58	0.34	0.29	0.29
30	3	0.89	0.51	0.24	0.24
30	4	1.18	0.68	0.21	0.21
30	5	1.47	0.85	0.17	0.19
30	6	1.76	1.02	0.17	0.17
30	7	2.05	1.19	0.16	0.16
30	8	2.35	1.36	0.16	0.15
30	9	2.66	1.53	0.15	0.14
60	1	0.17	0.29	0.41	0.46
60	2	0.34	0.58	0.36	0.38
60	3	0.51	0.89	0.30	0.33
60	4	0.68	1.18	0.27	0.30
60	5	0.85	1.47	0.24	0.27
60	6	1.02	1.76	0.22	0.25
60	7	1.19	2.05	0.21	0.24
60	8	1.36	2.35	0.19	0.22
60	9	1.53	2.66	0.17	0.21
90	1	0.00	0.34	0.55	0.61
90	2	0.00	0.67	0.51	0.58
90	3	0.00	1.03	0.44	0.56
90	4	0.00	1.36	0.41	0.55
90	5	0.00	1.70	0.43	0.55
90	6	0.00	2.04	0.49	0.54
90	7	0.00	2.37	0.52	0.54
90	8	0.00	2.72	0.58	0.54
90	9	0.00	3.07	0.55	0.53

CASE N1

ARRAY ANGLE DEG	GAGE NO.	|X/Lp|	|Y/Lp|	SPECTRAL DIFFRACTION COEFFICIENTS	
				MEASURED	PREDICTED
30	1	0.29	0.17	0.30	0.35
30	2	0.58	0.34	0.24	0.26
30	3	0.89	0.51	0.20	0.22
30	4	1.18	0.68	0.18	0.19
30	5	1.47	0.85	0.17	0.17
30	6	1.76	1.02	0.17	0.16
30	7	2.05	1.19	0.14	0.15
30	8	2.35	1.36	0.15	0.14
30	9	2.66	1.53	0.14	0.13
60	1	0.17	0.29	0.38	0.44
60	2	0.34	0.58	0.34	0.36
60	3	0.51	0.89	0.29	0.31
60	4	0.68	1.18	0.27	0.28
60	5	0.85	1.47	0.25	0.26
60	6	1.02	1.76	0.25	0.25
60	7	1.19	2.05	0.23	0.23
60	8	1.36	2.35	0.24	0.22
60	9	1.53	2.66	0.22	0.21
90	1	0.00	0.34	0.54	0.60
90	2	0.00	0.67	0.54	0.58
90	3	0.00	1.03	0.54	0.58
90	4	0.00	1.36	0.57	0.59
90	5	0.00	1.70	0.57	0.59
90	6	0.00	2.04	0.60	0.59
90	7	0.00	2.37	0.61	0.60
90	8	0.00	2.72	0.63	0.61
90	9	0.00	3.07	0.63	0.61

CASE N2

ARRAY ANGLE DEG	GAGE NO.	|X/Lp|	|Y/Lp|	SPECTRAL DIFFRACTION COEFFICIENTS	
				MEASURED	PREDICTED
30	1	0.29	0.17	0.33	0.38
30	2	0.58	0.34	0.29	0.28
30	3	0.89	0.51	0.25	0.24
30	4	1.18	0.68	0.21	0.21
30	5	1.47	0.85	0.18	0.19
30	6	1.76	1.02	0.21	0.17
30	7	2.05	1.19	0.17	0.16
30	8	2.35	1.36	0.18	0.15
30	9	2.66	1.53	0.17	0.14
60	1	0.17	0.29	0.42	0.46
60	2	0.34	0.58	0.38	0.38
60	3	0.51	0.89	0.34	0.33
60	4	0.68	1.18	0.32	0.30
60	5	0.85	1.47	0.30	0.28
60	6	1.02	1.76	0.29	0.26
60	7	1.19	2.05	0.29	0.25
60	8	1.36	2.35	0.27	0.23
60	9	1.53	2.66	0.25	0.22
90	1	0.00	0.34	0.58	0.61
90	2	0.00	0.67	0.59	0.59
90	3	0.00	1.03	0.55	0.58
90	4	0.00	1.36	0.54	0.58
90	5	0.00	1.70	0.55	0.59
90	6	0.00	2.04	0.55	0.59
90	7	0.00	2.37	0.55	0.59
90	8	0.00	2.72	0.62	0.60
90	9	0.00	3.07	0.60	0.60

CASE B1

ARRAY ANGLE DEG	GAGE NO.	|X/Lp|	|Y/Lp|	SPECTRAL DIFFRACTION COEFFICIENTS	
				MEASURED	PREDICTED
30	1	0.29	0.17	0.33	0.40
30	2	0.58	0.34	0.27	0.32
30	3	0.89	0.51	0.23	0.28
30	4	1.18	0.68	0.21	0.25
30	5	1.47	0.85	0.21	0.24
30	6	1.76	1.02	0.19	0.23
30	7	2.05	1.19	0.18	0.22
30	8	2.35	1.36	0.18	0.21
30	9	2.66	1.53	0.17	0.20
60	1	0.17	0.29	0.42	0.49
60	2	0.34	0.58	0.40	0.44
60	3	0.51	0.89	0.37	0.43
60	4	0.68	1.18	0.38	0.42
60	5	0.85	1.47	0.37	0.41
60	6	1.02	1.76	0.37	0.41
60	7	1.19	2.05	0.36	0.41
60	8	1.36	2.35	0.37	0.41
60	9	1.53	2.66	0.36	0.41
90	1	0.00	0.34	0.59	0.65
90	2	0.00	0.67	0.63	0.66
90	3	0.00	1.03	0.65	0.67
90	4	0.00	1.36	0.66	0.68
90	5	0.00	1.70	0.66	0.68
90	6	0.00	2.04	0.68	0.69
90	7	0.00	2.37	0.68	0.69
90	8	0.00	2.72	0.66	0.69
90	9	0.00	3.07	0.65	0.69

CASE B2

ARRAY ANGLE DEG	GAGE NO.	|X/Lp|	|Y/Lp|	SPECTRAL DIFFRACTION COEFFICIENTS	
				MEASURED	PREDICTED
30	1	0.29	0.17	0.32	0.42
30	2	0.58	0.34	0.28	0.34
30	3	0.89	0.51	0.25	0.29
30	4	1.18	0.68	0.23	0.27
30	5	1.47	0.85	0.20	0.25
30	6	1.76	1.02	0.21	0.24
30	7	2.05	1.19	0.19	0.23
30	8	2.35	1.36	0.18	0.22
30	9	2.66	1.53	0.18	0.21
60	1	0.17	0.29	0.41	0.51
60	2	0.34	0.58	0.40	0.45
60	3	0.51	0.89	0.36	0.43
60	4	0.68	1.18	0.33	0.42
60	5	0.85	1.47	0.33	0.42
60	6	1.02	1.76	0.32	0.41
60	7	1.19	2.05	0.32	0.41
60	8	1.36	2.35	0.32	0.41
60	9	1.53	2.66	0.31	0.41
90	1	0.00	0.34	0.53	0.65
90	2	0.00	0.67	0.58	0.65
90	3	0.00	1.03	0.57	0.66
90	4	0.00	1.36	0.60	0.67
90	5	0.00	1.70	0.63	0.68
90	6	0.00	2.04	0.64	0.68
90	7	0.00	2.37	0.60	0.69
90	8	0.00	2.72	0.62	0.69
90	9	0.00	3.07	0.59	0.69

APPENDIX E: COMPUTER PROGRAMS

```
      PROGRAM FILEMGMT

*     READS IN: MEASURED INCIDENT FREQUENCY SPECTRAL ENERGY DENSITIES
*               S(I)

*     FROM:     WaBbblCNUSPWcd.OUT
*               where:a='S' for spectral or 'M' for monochromatic
*                     bb=case number CASENO
*                      c=# of gages used in the MLM measurement analysis
*                      d=distance from linear array of wave gages to the
*                        Directional Spectral Wave Generator (DSWG)


*     READS IN: TARGET INCIDENT DIRECTIONAL SPREADING FUNCTION VALUES
*               D(J)

*     FROM:     SPREADee.OUT
*               where:ee=width of directional spread in degrees

*     WRITES:   INCIDENT DIRECTIONAL SPECTRAL ENERGY DENSITIES SMID(I,J)

*     TO:       SMIDbbf
*               where:f=1 or 2
*                     bb=as above

*     READS IN: MEASURED DIFFRACTED FREQUENCY SPECTRAL ENERGY DENSITIES
*               SMDF(I)

*     FROM:     WaBbbgC.SSP
*               where:a=as above
*                     bb=as above
*                     g=angle between linear array and breakwater
*                      =30, 60, or 90 degrees

*     WRITES:   MEASURED DIFFRACTED FREQUENCY SPECTRAL ENERGY DENSITIES
*               SMDF(I)

*     TO:       SMDFbbfh
*               where:bb=as above
*                     g=as above
*                     h=gage number GAGENO

      CHARACTER*13 SMIDINP,SMDFINP
      CHARACTER*11 SMIDLAB1,SMIDLAB2,SMIDLAB,SMDFLAB
      CHARACTER* 2 CASE

      DIMENSION FREQ(23),WAVEA(38),S(23),SMDF(23),SF(23),D(38)
      DIMENSION SMID(23,38)
      INTEGER GAGENO,ARRAYANG
      REAL*4 MO
```

```
*     READ IN MEASURED INCIDENT FREQUENCY SPECTRA
*     READ IN TARGET INCIDENT DIRECTIONAL SPREADING FUNCTION VALUES
*     CALCULATE INCIDENT DIRECTIONAL SPECTRAL ENERGY DENSITIES
*     CONSTRUCT INCIDENT DIRECTIONAL SPECTRUM

      OPEN (1,FILE='MIDSFILE.BAT',STATUS='OLD')

      DO 400 K=1,5

      READ(1,100)SMIDINP,SMIDLAB1,SMIDLAB2,SMIDLAB,CASE
100   FORMAT(A13,3A8,A2)

      OPEN (2,FILE=SMIDINP,STATUS='OLD')

*     READ IN MEASURED INCIDENT FREQUENCY SPECTRA IN ft^2/Hz

      IF(K.EQ.1)THEN
      READ(2,110)
110   FORMAT(36(/))
      READ(2,120)(FREQ(I),I=1,10)
120   FORMAT(2(/),T14,10F12.5)
      READ(2,130)(S(I),I=1,10)
130   FORMAT(4(/),T14,10F12.5)
      READ(2,120)(FREQ(I),I=11,20)
      READ(2,130)(S(I),I=11,20)
      READ(2,120)(FREQ(I),I=21,22)
      READ(2,140)(S(I),I=21,22)
140   FORMAT(4(/),T14,2F12.5)
      ELSE IF(K.EQ.4)THEN
      READ(2,150)
150   FORMAT(40(/))
      READ(2,120)(FREQ(I),I=1,10)
      READ(2,160)(S(I),I=1,10)
160   FORMAT(8(/),T14,10F12.5)
      READ(2,120)(FREQ(I),I=11,20)
      READ(2,160)(S(I),I=11,20)
      READ(2,120)(FREQ(I),I=21,22)
      READ(2,170)(S(I),I=21,22)
170   FORMAT(8(/),T14,2F12.5)
      ELSE
      READ(2,180)
180   FORMAT(42(/))
      READ(2,120)(FREQ(I),I=1,10)
      READ(2,190)(S(I),I=1,10)
190   FORMAT(10(/),T14,10F12.5)
      READ(2,120)(FREQ(I),I=11,20)
      READ(2,190)(S(I),I=11,20)
      READ(2,120)(FREQ(I),I=21,22)
      READ(2,200)(S(I),I=21,22)
200   FORMAT(10(/),T14,2F12.5)
      ENDIF
```

```
*     CALCULATE Hmo OF MLM FREQUENCY SPECTRUM FOR VERIFICATION

      SUMF=0.0

      DO 210 I=1,22
      SUMF=SUMF+S(I)*0.05
210   CONTINUE

      HMO=4*SQRT(SUMF)
      WRITE(5,*)'HMO FROM MLM FREQUENCY SPECTRUM                = ',HMO

*     READ IN TARGET INCIDENT DIRECTIONAL SPREADING FUNCTION VALUES
*     IN rad-1

      IF(K.EQ.1)THEN
      OPEN (3,FILE='SPREAD1.OUT',STATUS='OLD')
      ELSE IF(K.EQ.2 .OR. K.EQ.3)THEN
      OPEN (3,FILE='SPREAD10.OUT',STATUS='OLD')
      ELSE
      OPEN (3,FILE='SPREAD30.OUT',STATUS='OLD')
      ENDIF
      READ (3,220)
220   FORMAT(23(/))
      DO 240 J=19,1,-1
      JCOMPLIM=38-J
      READ (3,230)WAVEA(J),D(J)
230   FORMAT(T11,F4.1,T33,E12.6)
      WAVEA(J)=90-WAVEA(J)
      WAVEA(JCOMPLIM)=180-WAVEA(J)
      D(JCOMPLIM)=D(J)
240   CONTINUE
      CLOSE (3,STATUS='KEEP')

      WRITE(5,*)WAVEA(19)-90, D(19)

      CLOSE(2,STATUS='KEEP')

*     CALCULATE INCIDENT DIRECTIONAL SPECTRAL ENERGY DENSITIES.
*     CONSTRUCT INCIDENT DIRECTIONAL SPECTRUM.

      DO 260 I=1,22
      DO 250 J=1,37
      SMID(I,J)=S(I)*D(J)
250   CONTINUE
260   CONTINUE
```

```
*     CALCULATE Hmo OF INCIDENT DIRECTIONAL SPECTRUM FOR VERIFICATION

      PI=3.141592654
      DEGTORAD=PI/180.
      DTHETAD=5.0
      DTHETAR=DTHETAD*DEGTORAD

      DO 280 I=1,22
      SF(I)=0.0
      DO 270 J=1,37
      SF(I)=SF(I)+SMID(I,J)*DTHETAR
270   CONTINUE
280   CONTINUE

      MO=0.0
      DFREQ=0.05
      DO 290 I=1,22
      MO=MO+SF(I)*DFREQ
290   CONTINUE

      HMO=4*SQRT(MO)
      WRITE(5,*)'HMO FROM INCIDENT DIRECTIONAL SPECTRUM        = ',HMO
      WRITE(5,*)' '

*     CONVERT INCIDENT SPECTRAL ENERGY DENSITIES FROM
*     ft^2/(Hz*rad) TO cm^2/(Hz*rad)

      FT2TOCM2=12.**2 * 2.54**2

      DO 310 I=1,22
      DO 300 J=1,37
      SMID(I,J)=SMID(I,J)*FT2TOCM2
300   CONTINUE
310   CONTINUE
```

```
*     WRITE INCIDENT DIRECTIONAL SPECTRAL ENERGY DENSITIES

      OPEN(2,FILE=SMIDLAB1,STATUS='UNKNOWN')
      WRITE(2,320)CASE
320   FORMAT(T37,'CASE ',A2)
      WRITE(2,330)
330   FORMAT(/,T31,'INCIDENT DIRECTIONAL',/,T29,
     *'SPECTRAL ENERGY DENSITY',/T1,'WAVE DIRECTION',T28,
     *'S(F,THETA) IN cm^2/Hz/rad',/T1,'(DEG CCW FROM',/T1,
     *'POSITIVE X-AXIS)',T34,'FREQUENCY (Hz)')
      WRITE(2,340)(FREQ(I),I=1,11)
340   FORMAT(/T4,11F7.2)
      WRITE(2,*)' '
      WRITE(2,350)(WAVEA(J),(SMID(I,J),I=1,11),J=1,37)
350   FORMAT(T1,I3,11F7.1)

      CLOSE(2,STATUS='KEEP')

      OPEN(2,FILE=SMIDLAB2,STATUS='UNKNOWN')
      WRITE(2,320)CASE
      WRITE(2,330)
      WRITE(2,340)(FREQ(I),I=12,22)
      WRITE(2,*)' '
      WRITE(2,350)(WAVEA(J),(SMID(I,J),I=12,22),J=1,37)
      CLOSE(2,STATUS='KEEP')

      OPEN(2,FILE=SMIDLAB,STATUS='UNKNOWN')
      WRITE(2,320)CASE
      WRITE(2,330)
      WRITE(2,370)(FREQ(I),I=1,22)
370   FORMAT(/T4,22F7.2)
      WRITE(2,*)' '
      WRITE(2,380)(WAVEA(J),(SMID(I,J),I=1,22),J=1,37)
380   FORMAT(T1,I3,22F7.1)
      CLOSE(2,STATUS='KEEP')

400   CONTINUE

      CLOSE(1,STATUS='KEEP')
```

```
*
*     READ IN MEASURED DIFFRACTED FREQUENCY SPECTRAL ENERGY DENSITIES
*
      FREQ(1)=0.47
      DFREQ=0.05

      DO 500 I=1,21
      FREQ(I+1)=FREQ(I)+DFREQ
500   CONTINUE

      OPEN (1,FILE='MDFSFILE.BAT',STATUS='OLD')

      DO 800 K=1,15

      READ(1,510)SMDFINP,CASE,ARRAYANG
510   FORMAT(A13,T40,A2,T48,I2)

      OPEN(2,FILE=SMDFINP,STATUS='OLD')

      READ(2,520)
520   FORMAT(3(/))

      DO 700 L=1,9

      READ(1,530)SMDFLAB,X,Y
530   FORMAT(T14,A8,T51,2F10.2)
      READ(2,540)GAGENO
540   FORMAT(T3,I1)

      DO 550  I=1,22
      SMDF(I)=0.0
550   CONTINUE

      IF(K.LE.3)THEN
      READ(2,560)SMDF(5)
560   FORMAT(T66,E13.6)
      READ(2,570)SMDF(7),(SMDF(I),I=10,14,2)
570   FORMAT(4E13.6,/)
      SMDF(6) =-0.5 *(SMDF(5) +SMDF(7) )
      SMDF(8) =-SMDF(7)-0.33*(SMDF(7) +SMDF(10))
      SMDF(9) =-SMDF(7)-0.67*(SMDF(7) +SMDF(10))
      SMDF(11)=0.5 *(SMDF(10)+SMDF(12))
      SMDF(13)=0.5 *(SMDF(12)+SMDF(14))
      ELSE
      READ(2,580)(SMDF(I),I=1,3)
580   FORMAT(/T40,3E13.6)
      READ(2,590)(SMDF(I),I=4,21)
590   FORMAT(6E13.6)
      ENDIF
```

```
*     CONVERT MEASURED DIFFRACTED FREQUENCY SPECTRAL ENERGY DENSITIES
*     FROM FT^2/Hz TO cm^2/Hz

      DO 600 I=1,22
      SMDF(I)=SMDF(I)*FT2TOCM2
600   CONTINUE

*     WRITE MEASURED DIFFRACTED FREQUENCY SPECTRAL ENERGY DENSITIES

      OPEN(3,FILE=SMDFLAB,STATUS='UNKNOWN')
      WRITE(3,610)CASE,SMDFLAB
610   FORMAT(T1,'CASE ',A2,T30,'OUTPUT FILENAME = ',A12)
      WRITE(3,620)GAGENO,ARRAYANG,X,Y
620   FORMAT(/,'GAGE NUMBER ',I1,', ARRAY ANGLE = ',I2,' deg, X = ',
     *F5.2,' ft, Y = ',F6.2,' ft')
      WRITE(3,630)
630   FORMAT(//T17,'MEASURED DIFFRACTED',/T16,'FREQUENCY SPECTRA S(F)',
     *//T1,'FREQUENCY',T19,'ENERGY DENSITY',/T3,'(Hz)',T21,'(cm^2/Hz)'/)
      WRITE(3,640)(FREQ(I),SMDF(I),I=1,22)
640   FORMAT(T3,F4.2,T21,F9.6)

      CLOSE(3,STATUS='KEEP')

700   CONTINUE

      CLOSE(2,STATUS='KEEP')

800   CONTINUE

      CLOSE(1,STATUS='KEEP')

      END
```

```
      PROGRAM KDGEN

*     PCDFRAC AND DRWEDG AS MODIFIED BY MATTHEW WALSH JULY 1991

*     DIMENSION VARIABLES

      IMPLICIT REAL*4 (A-Z)
      INTEGER*2 I
      INTEGER GAGENO,ARRAYANG
      REAL*4 L,PI,TWOPI
      CHARACTER*11 KD1FILE,KD2FILE,KDFILE
      COMMON L,PI,TWOPI,PER(23),FREQ(23),WAVEA(38),FABS(23,38),FPHA

*     INITIALIZE VARIABLES

      PI=3.141592654
      TWOPI=2.*PI

*     BATCH OPERATION

      OPEN (1,FILE='KD.BAT',STATUS='OLD')

      DO 400 K=1,27

      READ (1,100)KD1FILE,KD2FILE,KDFILE,GAGENO,ARRAYANG,X,Y
100   FORMAT(3A12,1X,I1,1X,I2,T51,2F10.2)

      FREQ(1)=0.47
      DFREQ=0.05
      WAVEA(1)=0.0
      DTHETA=5.0

      DO 300 I=1,22

      PER(I)=1/FREQ(I)

      CALL PADES(PER(I),L)

      DO 200 J=1,37

      CALL DRWEDG (X,Y,L,WAVEA(J),FABS(I,J),FPHA)

      WAVEA(J+1)=WAVEA(J)+DTHETA

200   CONTINUE

      FREQ(I+1)=FREQ(I)+DFREQ

300   CONTINUE
```

```
      OPEN (2,FILE=KD1FILE,STATUS='UNKNOWN')
      WRITE(2,310)KD1FILE
310   FORMAT(T2,'OUTPUT FILENAME = ',A11)
      WRITE(2,320)GAGENO,ARRAYANG,X,Y
320   FORMAT(/,'GAGE NUMBER ',I1,', ARRAY ANGLE = ',I2,' deg, X = ',
     *F5.2,' ft, Y = ',F6.2,' ft')
      WRITE(2,330)
330   FORMAT(/,'WAVE ANGLE',T34,'AMPLIFICATION FACTORS',/,
     *'THETA (DEG',T39,'KD(F,THETA)',/,'CCW FROM',/,
     *'POSITIVE',/,'X-AXIS',T38,'FREQUENCY (Hz)')
      WRITE(2,340)(FREQ(I),I=1,11)
340   FORMAT(/T12,11F6.3)
      WRITE(2,*)' '
      WRITE(2,350)(WAVEA(J),(FABS(I,J),I=1,11),J=1,37)
350   FORMAT(T5,I3,T12,11F6.3)
      CLOSE(2,STATUS='KEEP')

      OPEN (2,FILE=KD2FILE,STATUS='UNKNOWN')
      WRITE(2,310)KD2FILE
      WRITE(2,320)GAGENO,ARRAYANG,X,Y
      WRITE(2,330)
      WRITE(2,340)(FREQ(I),I=12,22)
      WRITE(2,*)' '
      WRITE(2,350)(WAVEA(J),(FABS(I,J),I=12,22),J=1,37)
      CLOSE(2,STATUS='KEEP')

      OPEN (2,FILE=KDFILE,STATUS='UNKNOWN')
      WRITE(2,310)KDFILE
      WRITE(2,320)GAGENO,ARRAYANG,X,Y
      WRITE(2,330)
      WRITE (2,360)(FREQ(I),I=1,22)
360   FORMAT(/T12,22F6.3)
      WRITE(2,*)' '
      WRITE(2,370)(WAVEA(J),(FABS(I,J),I=1,22),J=1,37)
370   FORMAT(T5,I3,T12,22F6.3)
      CLOSE(2,STATUS='KEEP')

400   CONTINUE

      CLOSE(1,STATUS='KEEP')

      END
```

```
      PROGRAM DIRSPDIF

      REAL*4 MOIM,MODM,MODP,KDSPECM,KDSPECP
      INTEGER GAGENO,ARRAYANG
      CHARACTER*2  CASE
      CHARACTER*11 SMIDLAB,SMDFLAB,KDFILE,FSTABLE,SPECAMP
      COMMON MOIM,MODM,MODP,HMOIM,HMODM,HMODP,KDSPECM,KDSPECP
      COMMON SMID(23,38),FABS(23,38),SPDD(23,38),D(23,38),
     *       SI(23,38),SD(23,38)
      COMMON SMIF(23),SMDF(23),SPDF(23),S(23),FREQ(23)

      OPEN(1,FILE='MIDSFILE.BAT',STATUS='OLD')
      OPEN(2,FILE='MDFSFILE.BAT',STATUS='OLD')
      OPEN(4,FILE='FSTABLE.BAT',STATUS='OLD')
      OPEN(7,FILE='SPECAMP.BAT',STATUS='OLD')

      DO 500 K=1,5
*
*     INCIDENT SPECTRA
*
      READ(1,100)SMIDLAB,CASE
100   FORMAT(T31,A6,T38,A2)

      OPEN(6,FILE=SMIDLAB,STATUS='OLD')
      READ(6,110)(FREQ(I),I=1,22)
110   FORMAT(8(/),T4,22F7.3,/)
      READ(6,120)((SMID(I,J),I=1,22),J=1,37)
120   FORMAT(T4,22F7.1)

      CLOSE(6,STATUS='KEEP')

      CALL CONVERT(SMID,SMIF)

      CALL MOMENT(SMIF,MOIM)

*     WRITE HEADER FOR TABLE OF SPECTRAL AMPLIFICATION FACTORS
*     ********************
      READ(7,121)SPECAMP
121   FORMAT(A9)
      OPEN(8,FILE=SPECAMP,STATUS='UNKNOWN')
      WRITE(8,122)CASE
122   FORMAT(T33,'CASE ',A2,/T2,70('-'),/T56,'SPECTRAL',/T5,'ARRAY',
     *T50,'AMPLIFICATION FACTORS',/T5,'ANGLE',T17,'GAGE',T50,22('-'),
     */T6,'DEG',T17,'NO.',T28,'|X/Lp|',T40,'|Y/Lp|',T51,'MEASURED',T62,
     *'PREDICTED',/6(' ',10('-'),' '),/)
*     ********************
```

```
      OPEN(3,FILE='KD.BAT',STATUS='OLD')

      DO 400 L=1,3
*
*     MEASURED DIFFRACTED SPECTRA
*
      READ(2,125)ARRAYANG
125   FORMAT(T48,I2)

      DO 300 M=1,9

      READ(2,130)SMDFLAB
130   FORMAT(T14,A8)

      OPEN(6,FILE=SMDFLAB,STATUS='OLD')
      READ(6,140)
140   FORMAT(10(/))
      READ(6,150)(SMDF(I),I=1,22)
150   FORMAT(T21,F9.6)
      CLOSE(6,STATUS='KEEP')

      IF(M.EQ.6)THEN
      WRITE(5,*)ARRAYANG,SMDF(7)
      ENDIF

      CALL MOMENT(SMDF,MODM)
*
*     PREDICTED DIFFRACTED SPECTRA
*
      READ(3,160)KDFILE,GAGENO,X,Y
160   FORMAT(T26,A8,T38,I1,T51,2F10.2)

      OPEN(6,FILE=KDFILE,STATUS='OLD')
      READ(6,170)
170   FORMAT(11(/))
      READ(6,180)((FABS(I,J),I=1,22),J=1,37)
180   FORMAT(T12,22F6.3)
      CLOSE(6,STATUS='KEEP')

      CALL PREDDIFF(SMID,FABS,SPDD)

      CALL CONVERT(SPDD,SPDF)

      CALL MOMENT(SPDF,MODP)

*     COMPARISON OF MEASURED INCIDENT, MEASURED DIFFRACTED, AND
*     PREDICTED DIFFRACTED SPECTRA

      CALL SPECKD(MOIM,MODM,MODP,HMOIM,HMODM,HMODP,KDSPECM,KDSPECP)
```

```
*     WRITE OUTPUT TO FILE

      READ(4,190)FSTABLE
190   FORMAT(A12)

      OPEN (6,FILE=FSTABLE,STATUS='UNKNOWN')
      WRITE(6,200)CASE,FSTABLE
200   FORMAT(T1,'CASE ',A2,T30,'OUTPUT FILENAME = ',A11)
      WRITE (6,210)GAGENO,ARRAYANG,X,Y
210   FORMAT(/,'GAGE NUMBER ',I1,', ARRAY ANGLE = ',I2,' deg, X = ',
     *F5.2,' ft, Y = ',F6.2,' ft')
      WRITE (6,220)
220   FORMAT(//T24,'FREQUENCY SPECTRA S(F)',//T36,'DIFFRACTED',/T31,
     *20('-'),/T19,'INCIDENT',T31,'MEASURED',T42,'PREDICTED',/T19,
     *8('-'),T31,8('-'),T42,9('-'),/,'FREQUENCY',T29,'ENERGY DENSITY',
     */T9,'(Hz)',T32,'(cm^2/Hz)',/)
      WRITE (6,230)(FREQ(I),SMIF(I),SMDF(I),SPDF(I),I=1,22)
230   FORMAT(T1,4F12.2)
      WRITE(6,240)
240   FORMAT(T1,12('-'),T19,6('-'),T31,6('-'),T43,6('-'))
      WRITE(6,250)MOIM,MODM,MODP
250   FORMAT(T1,'mo',T13,3F12.4)
      WRITE(6,260)HMOIM,HMODM,HMODP
260   FORMAT(/T1,'Hmo',T13,3F12.4)
      WRITE(6,270)KDSPECM,KDSPECP
270   FORMAT(/T1,'SPECTRAL KD',T19,6('-'),T25,2F12.4)
      CLOSE(6,STATUS='KEEP')

*     CONVERT X AND Y TO METERS AND NORMALIZE BY THE WAVELENGTH
*     CORRESPONDING TO THE PEAK PERIOD

      FTTOMET=12.*2.54/100.
      X=X*FTTOMET
      Y=Y*FTTOMET
      WAVELENP=2.26
      XNORM=ABS(X/WAVELENP)
      YNORM=ABS(Y/WAVELENP)

      WRITE(8,275)ARRAYANG,GAGENO,XNORM,YNORM,KDSPECM,KDSPECP
275   FORMAT(T6,I2,T19,I1,T24,2F12.2,T48,2F12.2)
300   CONTINUE
400   CONTINUE
      CLOSE(3,STATUS='KEEP')
      CLOSE(8,STATUS='KEEP')
500   CONTINUE
      CLOSE(7,STATUS='KEEP')
      CLOSE(4,STATUS='KEEP')
      CLOSE(2,STATUS='KEEP')
      CLOSE(1,STATUS='KEEP')

      END
```

```
      SUBROUTINE CONVERT(D,S)

*     CONVERTS 3-D DIRECTIONAL SPECTRA TO 2-D FREQUENCY SPECTRA

      DIMENSION D(23,38),S(23)

      PI=3.141592654
      DEGTORAD=PI/180.
      DTHETAD=5.0
      DTHETAR=DTHETAD*DEGTORAD
*     DFREQ=0.05

      DO 200 I=1,22

      S(I)=0.0

      DO 100 J=1,37

*     SUM DIRECTIONAL SPECTRAL ENEREGY DENSITIES OVER THETA TO OBTAIN
*     THE FREQUENCY SPECTRUM

      S(I)=S(I)+D(I,J)*DTHETAR

100   CONTINUE

200   CONTINUE

      RETURN
      END


      SUBROUTINE MOMENT(S,MO)

*     CALCULATES ZEROETH-MOMENT OF A SPECTRUM

      REAL*4 MO
      DIMENSION S(23)

      MO=0.0
      DFREQ=0.05

      DO 100 I=1,22

      MO=MO+S(I)*DFREQ

100   CONTINUE

      RETURN
      END
```

```
      SUBROUTINE PREDDIFF(SI,FABS,SD)

*     CALCULATES PREDICTED DIFFRACTED SPECTRUM

      DIMENSION SI(23,38),FABS(23,38),SD(23,38)

*     APPLY AMPLIFICATION FACTORS TO THE INCIDENT DIRECTIONAL SPECTRAL
*     ENERGY DENSITY VALUES TO OBTAIN DIFFRACTED SPECTRAL ENERGY
*     DENSITIES

      DO 200 I=1,22

      DO 100 J=1,37

      SD(I,J)=SI(I,J)*FABS(I,J)**2

100   CONTINUE

200   CONTINUE

      RETURN
      END


      SUBROUTINE SPECKD(MOIM,MODM,MODP,HMOIM,HMODM,HMODP,KDSPECM,
     *KDSPECP)

*     CALCULATES SPECTRAL DIFFRACTION COEFFICIENT

      REAL*4 MOIM,MODM,MODP,KDSPECM,KDSPECP

      HMOIM=4*SQRT(MOIM)
      HMODM=4*SQRT(MODM)
      HMODP=4*SQRT(MODP)

      KDSPECM=HMODM/HMOIM
      KDSPECP=HMODP/HMOIM

      RETURN
      END
```

Waterways Experiment Station Cataloging-in-Publication Data

Walsh, Matthew T.

Diffraction of directional wave spectra around a semi-infinite breakwater / by Matthew T. Walsh ; prepared for Department of the Army, U.S. Army Corps of Engineers ; monitored by Coastal Engineering Research Center, US Army Engineer Waterways Experiment Station.

85 p. : ill. ; 28 cm. — (Miscellaneous paper ; CERC-92-5)

Includes bibliographic references.

1. Ocean waves — Mathematical models. 2. Breakwaters — Data processing. 3. Hydrodynamics — Computer programs. 4. Spectral energy distribution — Mathematical models. I. United States. Army. Corps of Engineers. II. Coastal Engineering Research Center (U.S.) III. U.S. Army Engineer Waterways Experiment Station. IV. Title. V. Series: Miscellaneous paper (U.S. Army Engineer Waterways Experiment Station) ; CERC-92-5.

TA7 W34m no.CERC-92-5